Rapid prediction of milk powder quality by hyperspectral imaging

Asma Khan

A thesis submitted in partial fulfilment of the requirements for the degree of Ph. D. in Chemical and Materials Engineering

The University of Auckland, 2020.

Abstract

Economically motivated rapid quality testing and assurance of milk powder is a well-known issue. This is a complex problem in the dairy industry that needs to be tackled with a range of techniques including rapid quality testing using sophisticated process analysers such as near-infrared spectroscopy (NIR) and hyperspectral imaging (HSI).

Instant whole milk powder (IWMP) is custom-made to exhibit good rehydration properties. Dispersibility and bulk density are among the important parameters to evaluate IWMP functional performance in dissolution, and potentially affected by variation in particle size distribution. Therefore, commercial-grade IWMP was divided into three discrete fractions of varying particle size. These three fractions were coarse ("C", having particles of 355µm or higher); medium ("M", having particles smaller than 355µm and larger than 180µm); and fine ("F", having particles smaller than 180µm). These milk powder fractions were remixed with specific known ratios to prepare seven types of reconstructed milk powder samples that had an extended range of dispersibility, bulk density and particle size distribution from the commercial-grade IWMP to be used in this research.

In this research, NIR spectrum (within 1000 – 2500 nm wavelength range) of reconstructed samples of IWMP was correlated to its dispersibility, bulk density and percent of fine particles with partial least squares (PLS) models. Different spectral data pre-treatment approaches such as Savitzky-Golay (SG) filtering, standard normal variate (SNV) transformation, multiplicative scatter correction (MSC), and their combinations were applied. Results showed that fine particle fraction was predicted with a coefficient

of prediction of 0.703 for spectral smoothing by SG. For dispersibility prediction, the combination of SG & MSC gave the highest prediction correlation coefficient of 0.973 and for bulk density prediction SG treated spectra proved to be the suitable data treatment method with a prediction correlation coefficient of 0.978.

Hyperspectral imaging (HSI) is an emerging technique in food quality analysis. Hyperspectral images over the 400 – 1000 nm wavelength range were recorded for the individual particle size fraction samples and reconstructed IWMP samples. Principal component analysis (PCA) discriminated HSI data of coarse, medium and fine particle fractions successfully across the first two principal components (PC_1 and PC_2). The partial least squares (PLS) discriminant analysis on full wavelengths successfully classified the three fractions of milk powder with a coefficient of prediction of 0.943. However, for efficient data analysis, five wavelengths were selected by the loading plot of three principal components (PC_1, PC_2 and PC_3) from PCA and eleven wavelengths were selected from weighted regression analysis (WRC) of the HSI data of three particle size fractions. Simplified models on reduced wavelengths gave better classification results in less computation time.

Average spectra of each particle size fraction were used to calculate the spectral similarity of pixels of hyperspectral images of reconstructed IWMP samples. Furthermore, based upon the similarity to coarse, medium, or fine particle fraction, their distribution in the reconstructed samples of IWMP was predicted. Partial least square (PLS) model performed well to predict the bulk density and dispersibility of reconstructed IWMP samples.

Keywords; *Instant whole milk powder, hyperspectral imaging, near-infrared spectroscopy, quality, particle size*

Dedication

This thesis is dedicated to my wonderful kids

Ahmed, Mahd and Haya.

Acknowledgements

First and foremost, I would like to thank **God Almighty** for giving me the opportunity, and ability to fulfil my dream. I could not imagine accomplishing this work without His blessings.

This journey could never have been possible without the support of my husband Salman Javed Khan. Your encouragement when times got rough, your endless support throughout this tenure and your patience have enabled me to achieve my goal.

My deepest gratitude is extended to my supervisor Prof. Brent Young for his guidance, encouragement, suggestions and appreciation. Apart from being a highly knowledgeable person, you are an extraordinary human being.

I convey my thanks to Dr. Tajammal Munir for helping me out, encouraging me and steering me in the right direction. I extend my sincerest acknowledgments to Dr. Wei Yu for his thoughtful discussions and suggestions for my work. I would also like to thank Melodie for proofreading my thesis.

Last but not least, I am indebted to my parents; their prayers were by my side in this voyage.

Table of Contents

List of Figures

List of Tables

Publications related to the current research

List of journal publications

1. Asma Khan, M.T. Munir, W. Yu, and B.R. Young, A Review towards hyperspectral imaging for real time quality control of food products with an illustrative case study of milk powder production. Journal of Food and Bioprocess Technology; (Published; https://doi.org/10.1007/s11947-020-02433-w).

2. Asma Khan, M.T. Munir, W. Yu, and B.R. Young, Using Hyperspectral imaging for predicting milk powder particle size fractions, dispersibility and bulk density. Journal of Food Analytical Methods; (Submitted).

3. Asma Khan, M.T. Munir, W. Yu, and B.R. Young, Near-infrared spectroscopy and data analysis for predicting milk powder quality attributes. International Journal of Dairy Technology; (Published; http://dx.doi.org/10.1111/1471-0307.12734).

4. Asma Khan, M.T. Munir, W. Yu, and B.R. Young, Wavelength selection for rapid identification of different particle size fractions of milk powder using hyperspectral imaging. Journal "Sensor" for their special issue "Non-destructive Sensors and Machine Learning for Food Safety & Quality Inspection"; (Published; https://doi.org/10.3390/s20164645)

List of conference articles

1. Asma Khan, M.T. Munir, W. Yu, and B.R. Young, Hyperspectral imaging for the discrimination of milk powder. Chemeca 2017. Melbourne, Australia.

THE UNIVERSITY OF AUCKLAND
Te Whare Wananga o Tamaki Makaurau
NEW ZEALAND
Email: postgradinfo@auckland.ac.nz

School of Graduate Studies
AskAuckland Central Alfred Nathan house
The University of Auckland
Tel: +64 9 373 7599 ext 81321

Co-Authorship Form

This form is to accompany the submission of any PhD that contains published or unpublished co-authored work. **Please include one copy of this form for each co-authored work**. Completed forms should be included in all copies of your thesis submitted for examination and library deposit (including digital deposit), following your thesis Acknowledgements. Co-authored works may be included in a thesis if the candidate has written all or the majority of the text and had their contribution confirmed by all co-authors as not less than 65%.

Please indicate the chapter/section/pages of this thesis that are extracted from a co-authored work and give the title and publication details or details of submission of the co-authored work. Chapter 2	
Nature of contribution by PhD candidate	Developed methodology, performed experiments, drafted manuscript, editing, publication correspondence
Extent of contribution by PhD candidate (%)	85

CO-AUTHORS

Name	Nature of Contribution
Tajammal Munir	Structure of manuscript, and Editing
Wei Yu	Supervision
Brent Young	Proof reading, Supervision and Editing

Certification by Co-Authors

The undersigned hereby certify that:

- the above statement correctly reflects the nature and extent of the PhD candidate's contribution to this work, and the nature of the contribution of each of the co-authors; and
- that the candidate wrote all or the majority of the text.

Name	Signature	Date
Tajammal Munir	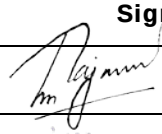	03.03.2020
Wei Yu		03.03.2020
Brent Young		03.03.2020

Last updated: 28 November 2017

THE UNIVERSITY OF AUCKLAND
Te Whare Wananga o Tamaki Makaurau
NEW ZEALAND
Email: postgradinfo@auckland.ac.nz

School of Graduate Studies
AskAuckland Central Alfred Nathan house
The University of Auckland
Tel: +64 9 373 7599 ext 81321

Co-Authorship Form

This form is to accompany the submission of any PhD that contains published or unpublished co-authored work. **Please include one copy of this form for each co-authored work**. Completed forms should be included in all copies of your thesis submitted for examination and library deposit (including digital deposit), following your thesis Acknowledgements. Co-authored works may be included in a thesis if the candidate has written all or the majority of the text and had their contribution confirmed by all co-authors as not less than 65%.

Please indicate the chapter/section/pages of this thesis that are extracted from a co-authored work and give the title and publication details or details of submission of the co-authored work.	
Chapter 3	
Nature of contribution by PhD candidate	Literature review, Discussion arguments of literature review, manuscript draft, editing, publication correspondance
Extent of contribution by PhD candidate (%)	75

CO-AUTHORS

Name	Nature of Contribution
Tajammal Munir	Discussion arguments of literature review, structure of manuscript, and Editing
Wei Yu	Supervision and Editing
Brent Young	Structure of manuscript, Proof reading, Supervision and Editing

Certification by Co-Authors

The undersigned hereby certify that:

- the above statement correctly reflects the nature and extent of the PhD candidate's contribution to this work, and the nature of the contribution of each of the co-authors; and
- that the candidate wrote all or the majority of the text.

Name	Signature	Date
Tajammal Munir	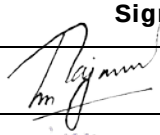	03.03.2020
Wei Yu		03.03.2020
Brent Young		03.03.2020

Last updated: 28 November 2017

THE UNIVERSITY OF AUCKLAND
Te Whare Wananga o Tamaki Makaurau
NEW ZEALAND
Email: postgradinfo@auckland.ac.nz

School of Graduate Studies
AskAuckland Central Alfred Nathan house
The University of Auckland
Tel: +64 9 373 7599 ext 81321

Co-Authorship Form

This form is to accompany the submission of any PhD that contains published or unpublished co-authored work. **Please include one copy of this form for each co-authored work**. Completed forms should be included in all copies of your thesis submitted for examination and library deposit (including digital deposit), following your thesis Acknowledgements. Co-authored works may be included in a thesis if the candidate has written all or the majority of the text and had their contribution confirmed by all co-authors as not less than 65%.

Please indicate the chapter/section/pages of this thesis that are extracted from a co-authored work and give the title and publication details or details of submission of the co-authored work. Chapter 4	
Nature of contribution by PhD candidate	Methodology, Experimental work, Data analysis, manuscript draft, editing, publication correspondance
Extent of contribution by PhD candidate (%)	85

CO-AUTHORS

Name	Nature of Contribution
Tajammal Munir	Guideline in data analysis,supervision, Editing
Wei Yu	Design of experiments and Supervision
Brent Young	Proof reading, Supervision and Editing

Certification by Co-Authors

The undersigned hereby certify that:

- the above statement correctly reflects the nature and extent of the PhD candidate's contribution to this work, and the nature of the contribution of each of the co-authors; and
- that the candidate wrote all or the majority of the text.

Name	Signature	Date
Tajammal Munir	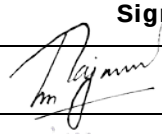	03.03.2020
Wei Yu		03.03.2020
Brent Young		03.03.2020

Last updated: 28 November 2017

THE UNIVERSITY OF AUCKLAND
Te Whare Wananga o Tamaki Makaurau
NEW ZEALAND
Email: postgradinfo@auckland.ac.nz

School of Graduate Studies
AskAuckland Central Alfred Nathan house
The University of Auckland
Tel: +64 9 373 7599 ext 81321

Co-Authorship Form

This form is to accompany the submission of any PhD that contains published or unpublished co-authored work. **Please include one copy of this form for each co-authored work**. Completed forms should be included in all copies of your thesis submitted for examination and library deposit (including digital deposit), following your thesis Acknowledgements. Co-authored works may be included in a thesis if the candidate has written all or the majority of the text and had their contribution confirmed by all co-authors as not less than 65%.

Please indicate the chapter/section/pages of this thesis that are extracted from a co-authored work and give the title and publication details or details of submission of the co-authored work. Chapter 5	
Nature of contribution by PhD candidate	Methodology, Experimental work, Data analysis, manuscript draft, editing, publication correspondance
Extent of contribution by PhD candidate (%)	90

CO-AUTHORS

Name	Nature of Contribution
Tajammal Munir	Supervision
Wei Yu	Supervision
Brent Young	Proof reading, Supervision and Editing

Certification by Co-Authors

The undersigned hereby certify that:

- the above statement correctly reflects the nature and extent of the PhD candidate's contribution to this work, and the nature of the contribution of each of the co-authors; and
- that the candidate wrote all or the majority of the text.

Name	Signature	Date
Tajammal Munir	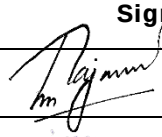	03.03.2020
Wei Yu		03.03.2020
Brent Young		03.03.2020

Last updated: 28 November 2017

Chapter 1. Introduction

1.1. Preface

This chapter presents a basic introduction and the background to major topics related to this research. The goal of this chapter is to provide a glimpse of the significance of the milk powder industry to the New Zealand economy, to present an overview of the production process, and the routine quality monitoring practices. Alternative quality monitoring techniques such as near-infrared spectroscopy and hyperspectral imaging proposed in this research study are also introduced in this chapter.

1.2. Dairy (powder) sector of New Zealand

Liquid milk has been known and valued for its nutritional benefits for centuries. The history of milk powder production starts from the early years of the 13th century when sundried paste from raw milk was carried by soldiers in war. However, the first commercial production started in 1834 in Russia (Blyth 1896).

New Zealand is one of the top ten largest liquid milk producing countries in the world. New Zealand's dairy exports comprised more than 25% of the total exports of New Zealand and directly added 3.1% of to its GDP (Destremau and Siddharth 2018). The export revenue generated from the different dairy products of New Zealand is presented in Figure 1.1. New Zealand exports different dairy products such as whole milk powder (WMP), skimmed milk powder (SMP), buttermilk powder (BMP), infant formula milk, butter, and cheese to more than 140 countries in the world. Therefore, the dairy sector is the most internationally connected industry in New Zealand in terms of products and its services. Whole milk powder (WMP) exports contribute more than 30% of the total dairy

export of New Zealand and meet 50% of the total milk powder demand worldwide (OECD 2019).

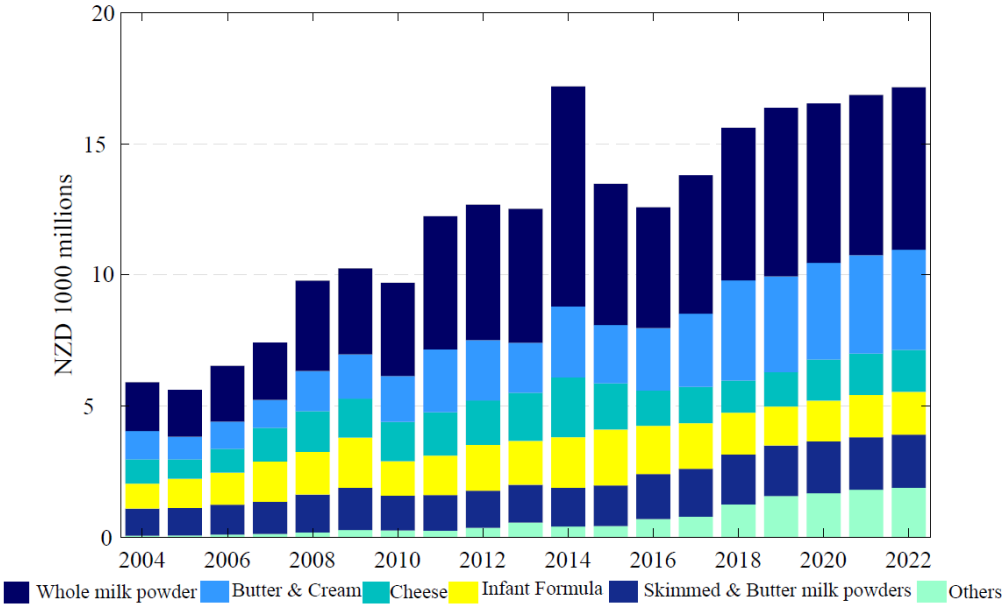

Figure 1.1. Export value of the New Zealand dairy industry

(For year ended 2004-2019, 2020-2022 forecast) (Islam 2019)

New Zealand is the world's largest producer of whole milk powder and 90% of the produced WMP is exported. Figure 1.2 presents the WMP export amount of New Zealand in thousands of tonnes. In 2004, New Zealand was exporting ~ 660,000 tonnes of WMP and until 2008 this remained approximately similar at around 700,000 tonnes. In the next six years from 2008 through to 2014, WMP export increased to more than doubled, from 677,000 tonnes to 1,460,000 tonnes. Chinese infant formula's melamine contamination scandal in 2008 and a false botulism indication in a single batch of one of the largest WMP manufacturers in New Zealand in 2013 had significant economic implications on the global WMP market. After 2013, New Zealand's WMP exports had slightly declined until the year 2017. However, by last year (2019) it has reached a new high with an increased export of 35,538 tonnes from year 2017. It is worth mentioning that the New Zealand dairy industry has continued to grow and innovate, consolidating the improvements in quality measurement and control. Furthermore, these incidents made

the consumer more conscious of the quality and safety of the product as well. The consumers are willing to pay a high price for better quality and functionality of the product.

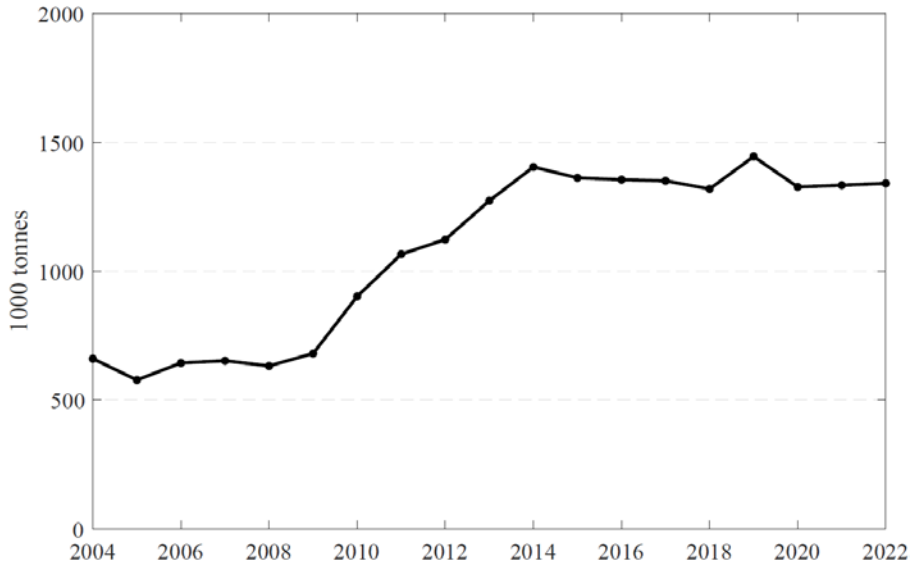

Figure 1.2. New Zealand's WMP exports

(For year ended 2004-2019, 2020-2022 forecast) (Islam 2019)

1.3. Research Background

Milk shelf life can be increased by evaporating water from liquid milk, its transportation becomes easier due to reduced volume, and its storage properties improve because of less moisture content (Kelly et al. 2003). A variety of milk powders are being produced such as whole milk powder, skim milk powder, infant formula, etc. These varieties of milk powders are produced according to various customer demands and different food engineering applications such as confectionaries, milk chocolates, dairy beverages, cheeses, yogurts, and other applications. This research is conducted on instant whole milk powder (IWMP), commercially modified to give quick rehydration characteristics.

1.3.1 **An overview of the milk powder manufacturing process: Instant whole milk powder process description**

A typical instant whole milk powder production process is shown in Figure 1.3. This production process is adapted from Kelly et al. (2003) and presented holistically as process operation and parameters are strongly related to the desired product specifications. However, a detailed and comprehensive virtual tool is developed by Tertiary Education Commission (TEC) New Zealand, to present all the essential unit operation and processes of an actual dairy powder manufacturing plant (TEC 2012). It can be helpful to understand from the milk chemistry and milk collection through powder production with process flow diagrams (PFDs) and process instrumentation diagrams (PIDs) as well.

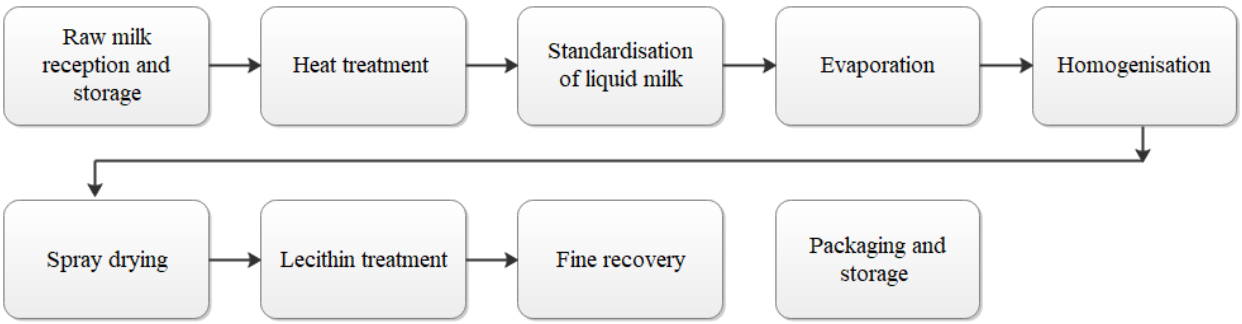

Figure 1.3. Stages of instant whole milk powder production

i. Heat treatment

After the receipt of raw milk at the production site, it is stored in bulk vessels. This liquid milk is heated for a specified time (from several seconds to a few minutes to a certain temperature ranging from 75 – 120 °C). This heating step is essential to decrease microbial activity within the liquid milk and ensure product safety. However, proteins are sensitive towards heat treatment and whey proteins can be denatured if exposed to high temperatures for a prolonged time (Hussain et al. 2012). Hence, the quality of milk

powder can be compromised. Therefore, there is a trade-off between the temperature for heating and residence time which is key to the quality of the final product.

ii. Standardisation

The fat component of liquid milk is separated using a centrifugal cream separator. A portion of cream is added back to standardise the liquid milk for maintaining 26 – 30 % fat in the whole milk powder (WMP) irrespective of the seasonal and nutritional variations of the raw milk received initially (Skanderby et al. 2009).

iii. Evaporation

This preheated milk is forwarded to evaporators to reduce the water content. Whole milk (liquid) usually has a total milk solids content of around 13 %. It is concentrated to 45 – 52 % solid contents by simply evaporating the water under vacuum. Evaporation stage also impacts the properties of the milk powder produced. Milk powder particle structure is developed as water is removed. The pattern of airflow and its flow rate influence the particle size of the milk powder (Schuck 2011). Denaturing of protein can also occur during evaporation, which has a negative impact on the reconstitution ability of the milk powder. Therefore, the temperature in the evaporator is often below 72 $^{\circ}$C (Ye et al. 2005). Secondly, evaporation is linked with the process intensification and contribute to lowering energy costs if multi-effect evaporators are used rather than single effect evaporators (Singh 2007).

iv. Drying

The concentrated milk (having solids contents > 45%) is sent to a homogeniser to disintegrate large fat globules into small ones and a homogeneous emulsion is obtained. Therefore, texture similarity is expected in the powder formed after the drying step. The function of the dryer is to further reduce water content. Commonly, spray dryers in the

dairy industry use hot air (~200 °C) for drying (Vignolles et al. 2009). Concentrated milk stream is introduced in droplet form and once these droplets come into contact with hot air, the remaining water is evaporated leaving the solid contents of milk in powder form. These milk particles could have 5 – 6 % moisture content remaining while leaving the dryer. Therefore, a secondary drying can be achieved via fluidised bed blown with heated air and the moisture content is reduced to 2 – 4 % in the final product. Drying is a crucial stage to obtain a high-quality product. Particle size, bulk density and free fat molecules in the milk particles are related with the type and operating speed of the pressurised atomiser used for injecting concentrated milk (Kim et al. 2003). The temperature in the spray dryer is linked with the physical properties and chemical components of the milk powder (Kim et al. 2009). These processes are conventional and carried out at a large scale in a production plant under strict hygiene conditions.

v. Lecithin treatment

An additional lecithin treatment is subjected to improve the instant property in the milk powder product. Instant property refers to the quick dissolving behaviour of milk powder when reconstituted with water (Tuohy 1989). It is achieved by spraying soy lecithin and butter oil solutions over the milk powder particles before being sent to the fluidised bed for drying and cooling.

vi. Fines recovery system

Fine particles are screened from the fluidised bed and collected and recycled to the spray dryer. These fine particles come in contact with the concentrated milk liquid (coming from the evaporator) and provide nuclei for large and porous milk agglomerates (Ye et al. 2005). This step improves the milk powder quality and reduces product loss. The milk powder product, after the fluidised bed stage, is sent to packaging and storage to protect it from moisture, light, heat and oxygen.

1.3.2 **Milk powder quality**

Determining and maintaining milk powder quality are usually complicated tasks due to the multi-array nature of quality (Karoui 2017). Quality tests are vital for ensuring hygiene of the product, regulatory standards, and customer requirements. Milk powders are tested for their physical, chemical and biological nature to determine functional performance, and consumer acceptance. Different parameters of the milk powder are determined by physical characterisation (particle size and shape, density, particle size distribution, etc,), chemical analysis (nutrients amount, presence of adulterants, etc.), functional testing (dispersibility, solubility, flowability, etc.), and sensory analysis (colour, texture, flavour, etc.) (Resch and Daubert 2002). These quality tests are recognised by regulatory authorities of the International Organization of Standardization (ISO), International Dairy Foundation (IDF) or countries' internal regulations such as EU commission. The majority of these tests are done post-production, providing low optimisation margins to the process. Nonetheless, the traditional dairy industry is evolving by gradually adapting a proactive approach and optimisation throughout the value chain of the product (Niamh Burke 2018). Rapid in-situ ‘analyse - predict if reject - prevent’ is a developing interest for the future dairy sector.

The quality of IWMP is related to its quick reconstitution performance. Dispersibility is one of the important rehydration characteristics of IWMP as instant milk powder is custom made to achieve quick rehydration when reconstituted with water. One can refer to dispersibility as how easily powder lumps and agglomerates fall apart when reconstituted with water (Crowley et al. 2015). Thus, a well-dispersible powder product will be a preferred choice as it represents good rehydration (a functional property). Usually, it is determined offline as per the International Dairy Federation (IDF) standard guidelines or the New Zealand Dairy Board (NZDB) dispersibility method (Munir et al.

2017). One can struggle to directly relate this to the operational parameters of IWMP production. However, bulk density, size of particles and particularly the presence of the fine particles of the milk powder are among the crucial factors that affect the rehydration ability of IWMP (Ji et al. 2016). Large, porous, open agglomerates that have good flowability and low bulk density present quick dissolution when reconstituted to liquid (Lee et al. 2014). It is necessary to monitor the dispersibility of the IWMP produced as the retail value of the product is related to the quality and functional performance of the product directly.

Bulk density is a measure of the exact volume occupied by a certain mass of the milk powder. Reference guidelines for bulk density measurements of milk powders are provided by International dairy federation (IDF) standard IDF (2005). It directly influences packaging and transportation costs and also the flow properties and wetting ability during reconstitution. Therefore, milk powder with a narrow range of expected bulk density is desirable to produce at the production plant. Product downgrade at a manufacturing plant in New Zealand was estimated ~25 % due to not complying with the desired bulk density (Williams 2017).

Bulk density is also related to the size of particles in the milk powder and the agglomeration conditions in the spray dryer (Oldfield and Singh 2005). Therefore, rapid monitoring of dispersibility, bulk density and particle size distribution of the milk powder could help to quickly identify a reject product, if produced, and an appropriate corrective measure could be adopted to minimise product loss.

i. Challenges in the current approach and proposed solution

Existing offline and manual quality monitoring approach of the milk powder is sufficient to identify out-of-specification product. However, tests are subjective and time-

consuming and carry the risk that any incorrectly identified out-of-specification product results in product loss, downgrade and economic loss. A skilled workforce is also necessary to perform these tests. Furthermore, these existing methods are practically impossible to implement in the at-line or on-line settings during production.

In the last two decades, spectroscopic analysis has been popular among researchers to monitor the quality of the food products almost in real-time (Manley 2014). Spectroscopic techniques are non-invasive and non-destructive by nature; rapid to perform; environment-friendly, as no pollutant or waste is generated; no sample preparation or pre-treatment required; and robust (Geladi and Manley 2010). Now-a-days, suitable analysers based upon spectroscopy are replacing the manual quality tests and are adaptable to at-line and/or online measurements in an industrial environment (Pasquini 2018).

Spectroscopic techniques have the advantage of determining several physiochemical properties and compositional analyses from the same spectrum of the sample. This enables improvement to the overall quality control scheme, which usually requires high numbers of routine sampling for various property measurements (Yoon et al. 2010). This single sample spectrum avoids sampling variation for different quality attributes, and it can provide diverse quality information from different prediction models saving time and effort.

1.3.3 **Spectroscopic analysis**

Light is an electromagnetic spectrum of different wavelengths. Spectroscopy can be described as the analysis of light variation when it interacts with the matter. This variation of light occurs if the analysed substances vary in molecular or atomic arrangement and/or there are differences in their physical appearance (i.e. shape, size, colour, etc.).

Spectroscopy is an experimental technique widely used in physics, chemistry and astronomy to investigate compositional analysis, physical characteristics and electronic structure from the atomic scale to the macro-level (Pavia et al. 2008). Several spectroscopic techniques are based upon their characteristic wavelength ranges. Infrared (IR) (780-10000 nm) and mid-infrared (MIR) (1400-3000 nm) range spectroscopic techniques have been frequently reported for chemical/compositional analysis, while near-infrared (NIR) (780-1400 nm), ultraviolet-visible (UV-vis) (300-700 nm) spectroscopy are mostly reported for the physical and functional analysis of food products (Karoui et al. 2010, Spyros and Dais 2009, Yang and Ying 2011). Reflectance, fluorescence, Raman shift and/or Fourier transformation are spectrum generation and detection methodologies associated with these spectroscopic techniques.

The selection of an appropriate spectroscopic technique is subjective to its application. For example, Moros et al. (2010) referred to IR spectroscopy (5000 nm and above wavelengths) as a suitable technique for atomic structure analysis of agri-products, including food materials. For the analysis of the physical structure and chemical constituents of various food products, Li-Chan et al. (2010) referred to 400-2500 nm as an effective wavelength range to explore while Ozaki et al. (2006) presented NIR spectroscopy (1000-2500 nm) as a smart tool for food's qualitative assessment.

Near-infrared (NIR) spectroscopy and visible to near-infrared range hyperspectral imaging (HSI) are proposed for determining the physical properties (particle size distribution and bulk density) and rehydration performance (in terms of dispersibility) of instant whole milk powder in this research. Supporting evidence from the literature is given in the relevant sections below, and in the respective chapters as well.

ii. Near-infrared (NIR) spectroscopy

Near-infrared (NIR) spectroscopy is the type of vibrational spectroscopy performed in the wavelength range of 750 to 2500 nm. Near-infrared equipment basically consists of three components; light source, monochromator or polychromator (that is used to split the radiation into one or multiple directions before it reaches the sample) and a detector (used to sense the radiation leaving the sample and analyse it). The spectrum (λ) produced in NIR spectroscopy can be measured in terms of reflection, transmission or absorption depending upon the sample. Samples that vary in composition or physically different (size variation, porosity variation, etc) from each other can be differentiated with NIR spectroscopy (Manley et al. 2008). However, an appropriate chemometric data analysis tool (such as discriminant analysis, regression analysis and/or neural network) is coupled with NIR spectroscopy to correlate the spectral data of the samples qualitatively or quantitatively (Shikata et al. 2017).

The fundamental concepts of spectroscopy have been well understood for over a century. However, the application of NIR for quality determination of food and agri-products was not exercised until after the 1970s (Norris 1996). With the development in instrument hardware (Yu et al. 2013) and advanced chemometric tools (Brown 2017) in past two decades, NIR spectroscopy has been successfully applied from analyses at the microscopic level (such as bacterial or fungal detection) to the macroscopic (bulk properties) analysis of products of various natures.

Near-infra spectroscopy is used in a diverse range of applications, from chemical and biological analysis of substances to physical and functional characterisation of materials (Manley 2014, Nakakimura et al. 2012). For example, NIR has been used for quantitative analysis of active pharmaceutical ingredients (API) in medicines, determining particle

sizing, and for measures of compression strength and bulk density of powders for tablets production in the pharmaceutical industry (Swarbrick 2014). Near-infrared spectroscopy is also used to monitor soil contamination (heavy metals) (Shi et al. 2014), to estimate the carbon content in soil (Gholizadeh et al. 2013) and to predict the physical, chemical, and biological properties of the soil (Soriano-Disla et al. 2014). The processing and reaction monitoring of polymers are also performed by NIR devices online (Heigl et al. 2007, Watari 2014). For wood and paper processing, NIR has facilitated the chemical and waste recovery (Jin and Xu 2011, Trung et al. 2015).

Near-infrared spectroscopic analysers are popular in food product quality monitoring due to their robustness, non-invasive nature of sensors, fast acquisition speed, and low operating cost (Karoui et al. 2010). Many researchers have published successful applications of NIR spectroscopy towards meat (Prieto et al. 2017), cereals (Dowell et al. 1998), fruits (Li et al. 2016, Xie et al. 2016), vegetables (Itoh et al. 2010), coffee (Alessandrini et al. 2008, Ribeiro et al. 2011), honey (Zábrodská and Vorlová 2015), beverages (Wang et al. 2017), milk (Poonia et al. 2017), and cheese (Woodcock et al. 2008) quality assessment. Near-infrared spectroscopy provided qualitative information for these products in terms of estimating adulteration, unwanted substances, biological contamination, maturity, and freshness. Moreover, reported studies provided NIR spectroscopy applications to authenticate and classify food products (Lohumi et al. 2015). NIR spectroscopy has also been used as a non-conventional technique for at-line estimation of particle size, density, porosity and flowability of wheat flour and ground spices (Kaddour and Cuq 2009, Pasikatan et al. 2001). Although sensory analysis is another complex domain of food quality assessment, there are a few research studies that also predict the sensory flavours of coffee drink (Ribeiro et al. 2011), liquid milk (Wolf et al. 2013) and cheese (Downey et al. 2005) by near-infrared spectroscopic analysis.

Near-infrared spectroscopy is a comparatively mature technique with multidisciplinary applications. Comprehensive methods and procedures have been defined by regulatory authorities for the implementation of NIR spectroscopy (EMA 2009). Therefore, for different applications, a huge number of chemometric procedures are reported in the literature to analyse the NIR data produced. One approach may appear to work fine for some applications, while it may fail in others (Pasquini 2018). Therefore, knowledge and understanding of the field of interest will be helpful to choose an appropriate data analysis technique.

Near-infrared spectroscopy has been mainly employed in the dairy industry for examining raw milk chemical and biological constituents (Melfsen et al. 2012, Núñez-Sánchez et al. 2016). Near-infrared spectroscopy has been reported as a feasible method for: determining milk powder constituents such as proteins and fats (Di et al. 2008, Wu et al. 2007, Wu et al. 2008), identification of adulterants in milk powder (Balabin and Smirnov 2011), and predicting the brand classification and protein concentration to quantify milk powder (Chen et al. 2018). Holroyd et al. (2013) have suggested NIR instrumentation for at-line and in-line moisture prediction in milk powder at one of the production facilities in New Zealand. However, no studies were found relating milk powders' spectral characteristics with powder particle size analysis, bulk density and functional property (dispersibility).

iii. Hyperspectral imaging (HSI)

Hyperspectral imaging (HSI) is a hybrid (imaging and spectroscopy) technology that generates a spatial map of spectral variations of a sample. It combines spectroscopy with imaging to measure both spectral (λ) and spatial (x - y) information from the sample. The fundamental working principle behind the HSI is the "Result of the projected

electromagnetic waves (light) on a matter is the reflection, scattering, and transmission of light"(Chelladurai and Jayas 2014). The portion of the light that penetrates into the surface of a sample is absorbed and the rest of the electromagnetic waves either scatter or transmit through the sample. The emission or absorption intensity of the electromagnetic waves through a sample is subjective to the physical and chemical nature of the material. The emitted light from a sample is recorded and converted into a spectrum and further used to extract the characteristic information about the sample. This spectral data, when received with the relevant spatial position in a sample, is called a hyperspectral image.

Hyperspectral imaging system consists of these main components: an illumination (light) source, a camera to record spectral and spatial data, a spectrograph to convert reflected/transmitted light into signal, a stage to place the sample (it can be stationary or attached to a conveyer to move the sample), and a computer to view, process and store hyperspectral images.

Hyperspectral images, known as hypercube, can be represented as three-dimensional blocks of data, comprised of two spatial and one wavelength dimension, as described in Figure 1.4. Each hyperspectral image is a diversified combination of adjoining wavebands and spatial $(x - y)$ positions of the sampled matter. As a result, every pixel shown in the hyperspectral image contains a bundle of information in terms of the wavelength absorbed/transmitted. The spectrum related to every pixel serves as a fingerprint. It holds information about the chemical and physical properties of the sample (Huang et al. 2014).

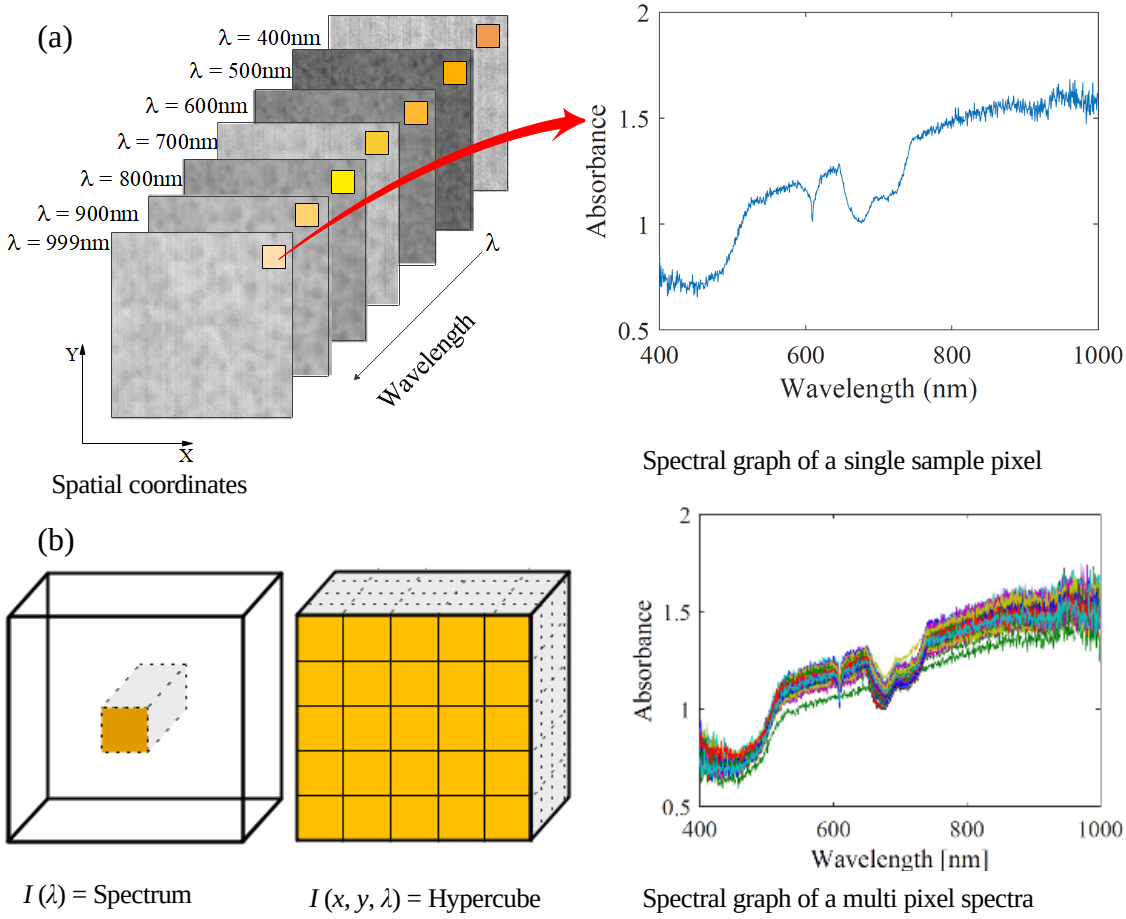

Figure 1.4. (a) HSI images of milk powder[1] as a function of wavelength, (b) Structure of data cube and multi-pixel spectral plot

Hyperspectral imaging contains a wide range of data and for some cases, the analysis of this "big data" could be complicated (M. ElMasry and Nakauchi 2016). However, with the selection of appropriate regression and correlation tools, one can minimise this problem to a workable solution. Evidence from the literature suggests if one can reduce spectra to a few wavelengths, it is helpful to reduce the amount of data needed to process and its processing time as well (Li et al. 2009, Renzullo et al. 2006). This is known as multi-spectrum imaging (MSI). However, a lot of information can be overlooked if multi-spectral imaging is adopted directly in a process. Extensive and robust multivariate data

[1] These spatial images of milk powder at different wavelengths (as shown in Figure 1.4 (a)) and single and multi-pixels spectral plots of milk powder (as shown in Figure 1.4 (a & b)) are from the current research.

analysis methods by HSI can ultimately lead to multi-spectrum imaging as an ultimate goal (Feng and Sun 2012). In general, principal component analysis (PCA), partial least squares analysis (PLS), discriminant analysis and specific weights analysis could be the potential methods to produce correct and useful information (Dufour 2011). Furthermore, a multivariate data analysis section is included in each chapter to discuss and relate it with respective objectives.

Machine vision based on red-green-blue (RGB) (three wavebands of colour vision systems) has been applied to evaluate the external characteristics in the food and dairy industry (Subramanian et al. 2016). But normal machine vision systems are not able to capture broad spectral information related to internal characteristics. Hence, they have limited ability to conduct quantitative analysis (Chelladurai and Jayas 2014). Contrary to machine vision, HSI consists of 20 to several hundred narrow wavebands (Li et al. 2012). It is capable of replacing human visual inspection so that it can incorporate spatial features (such as colour, appearance, etc.) with the advantage of exploring spectral characteristics as well.

Hyperspectral imaging is believed to monitor multi-constituent information and is flexible about extracting spectral information in various applications of food safety and quality monitoring (Baiano 2017, Liu et al. 2017, Ravikanth et al. 2017). Hyperspectral imaging has been used for meat quality prediction by assessing tenderness, colour, freshness and microbial spoilage (Feng et al. 2018, Wu and Sun 2013); for fruits and vegetables to determine surface defects, degree of ripening, sugar & moisture contents and identifying processing injuries (Abasi et al. 2019, Ariana and Lu 2008, ElMasry et al. 2007); and for natural cereals, by classifying different varieties based upon their appearance, size, and constituents (Geladi and Manley 2010, Williams et al. 2012). There

are studies that suggest HSI techniques to detect adulteration and determine the fat and protein content in milk powder (Huang et al. 2016b, Huang et al. 2014b). Munir et al. (2018) used HSI to discriminate milk powders produced by different drying facilities at three different production plants which exhibited variation in their dissolving behaviour. These stated evidences as well as other evidence found in published literature has established an understanding that HSI can be a potential analyser for rapid monitoring of the milk powder properties.

1.4. Novelty of the research

It has been discussed earlier that status-quo of milk powder bulk density and dispersibility measurements are off-line. Particle size analysis is also done post-production by sieving or laser diffraction. In this study, the potential of hyperspectral imaging (HSI), and near-infrared (NIR) spectroscopic techniques are evaluated to predict different particle size fractions in the milk powder sample and estimate its bulk density and dispersibility. It is worth highlighting that no research study has been found in the published domain that used NIR spectral information of milk powder to predict the particle size fractions, bulk density and dispersibility. Although, HSI has been used by Munir et al. (2018) to classify milk powders with accepted and non-accepted dissolution behaviours. However, these milk powder samples were manufactured by different drying units and were produced at different locations. The author has extended their work approach by assuming that variation in particle size is one of the reasons for failed rehydration behaviours of milk powder samples. Therefore, spectral information (produced by HSI) of milk powder samples is related to the size of particles in the samples, which is an addition to existing information available in the literature. Bulk density and dispersibility of the milk powder samples are also predicted from HSI data of the samples. Moreover, the number of

wavelengths is also reduced for determining particle size fraction in milk powders samples. This is also novel compared to current knowledge in this field.

1.5. Research questions and hypotheses

In this study, near-infrared (NIR) spectroscopy and hyperspectral imaging (HSI) techniques are proposed to predict different particle size fractions in the milk powder sample and estimate bulk density and dispersibility. From the current information available in the literature, the following research questions were developed to investigate and study in this research:

- How does NIR spectroscopy differentiate the variation in particle size in the milk powder sample?
- How does NIR spectroscopy predict the quality of milk powder samples in terms of fine particles in the sample, bulk density, and dispersibility?
- How does HSI differentiate the milk powders with different size particles?
- How can the distribution of different particle size fractions be predicted?
- How are the bulk density and dispersibility obtained from HSI data cube?

The necessary hypotheses to address these research questions are the following:

I. Milk powder bulk density and dispersibility are sensitive to particle size variation.

II. Milk powder particles varying in size possess spectral variation.

III. Pre-processed spectra can be correlated with quality attributes by regression and/or discriminant analysis.

IV. Data analysis can be simplified by reducing the number of wavelengths.

1.6. Thesis structure

To address the above-stated research questions, investigative studies were performed, and the details have been organised in the thesis as shown in Figure 1.5. A brief introduction to the thesis chapters is given below:

Chapter 1 discusses the importance of the dairy industry towards the New Zealand economy. It introduces the generic production process of instant whole milk powder and reviews the status quo of quality measurements. Research questions are identified from the existing literature and current practices and as possible solutions, NIR spectroscopy and HSI techniques are introduced.

Chapter 2 details a method where commercial-grade milk powder (having narrow functional and physical property range) is fractioned into three groups based upon varying particle size. These milk powder fractions were recombined in various proportions to prepare milk powder samples with an extended range of functional and physical properties. This chapter discusses the option of using NIR spectroscopy for the milk powder samples. The impact of different pre-processing spectral techniques such as standard normal variance, multiplicative spectral correction and Savitsky-Golay filters have been analysed. Predictive PLS models are also included and used to estimate the quality of the milk powder samples from the ratio of fine particles present within a sample and dispersibility of the milk powder samples.

Chapter 3 reviews the application of hyperspectral imaging across various food products either at a lab or commercial scale. It identifies knowledge gaps that can hinder the successful implementation of hyperspectral imaging in real-time applications. It also presents an illustration for the dairy powder industry to propose HSI as a quality monitoring tool.

Chapter 4 discusses the option of using hyperspectral imaging for estimation of milk powder physical properties (particle size analysis and bulk density) and rehydration performance in terms of dispersibility. Milk powder samples were prepared as per methods used in Chapter 2. Milk powder size fractions are differentiated when principal component analysis (PCA) been performed to their respective HSI data sets. These hyperspectral data sets are further used in the prediction of particle size fractions' distributions in the recombined milk powder samples. Dispersibility and bulk density of the recombined milk powder samples are predicted by PLS regression models based upon respective HSI data.

Chapter 5 identifies important wavelengths of HSI data by principal component analysis (PCA) and weighted regression coefficients (WRC) analysis. These sets of reduced wavelengths are used to develop simplified partial least square discriminant analysis (PLS-DA) of three different particle size fractions of milk powder.

Chapter 6 offers concluding remarks on the experimental methods for hyperspectral imaging and multivariate data analysis models for HSI data of milk powder based on the results obtained from this study. It also provides some recommendations for future work.

1.7. Summary

Rapid monitoring of quality and relevant parameters proficient to manipulate milk powder quality is an important task. Instant milk powder is tested for dispersibility for its functional performance and bulk density for its packaging and storage costs. Dispersibility and bulk density vary with different particle sizes in different milk powder samples. Existing methods to measure dispersibility, bulk density and particle size distribution are post-production and time-consuming in order to determine whether the product meets all necessary specifications. Therefore, two spectroscopic techniques NIR spectroscopy and

HSI are proposed for the testing of instant whole milk powder in this research project. These spectroscopic techniques have promising potential to become a fast and non-invasive method to replace manual testing in the future.

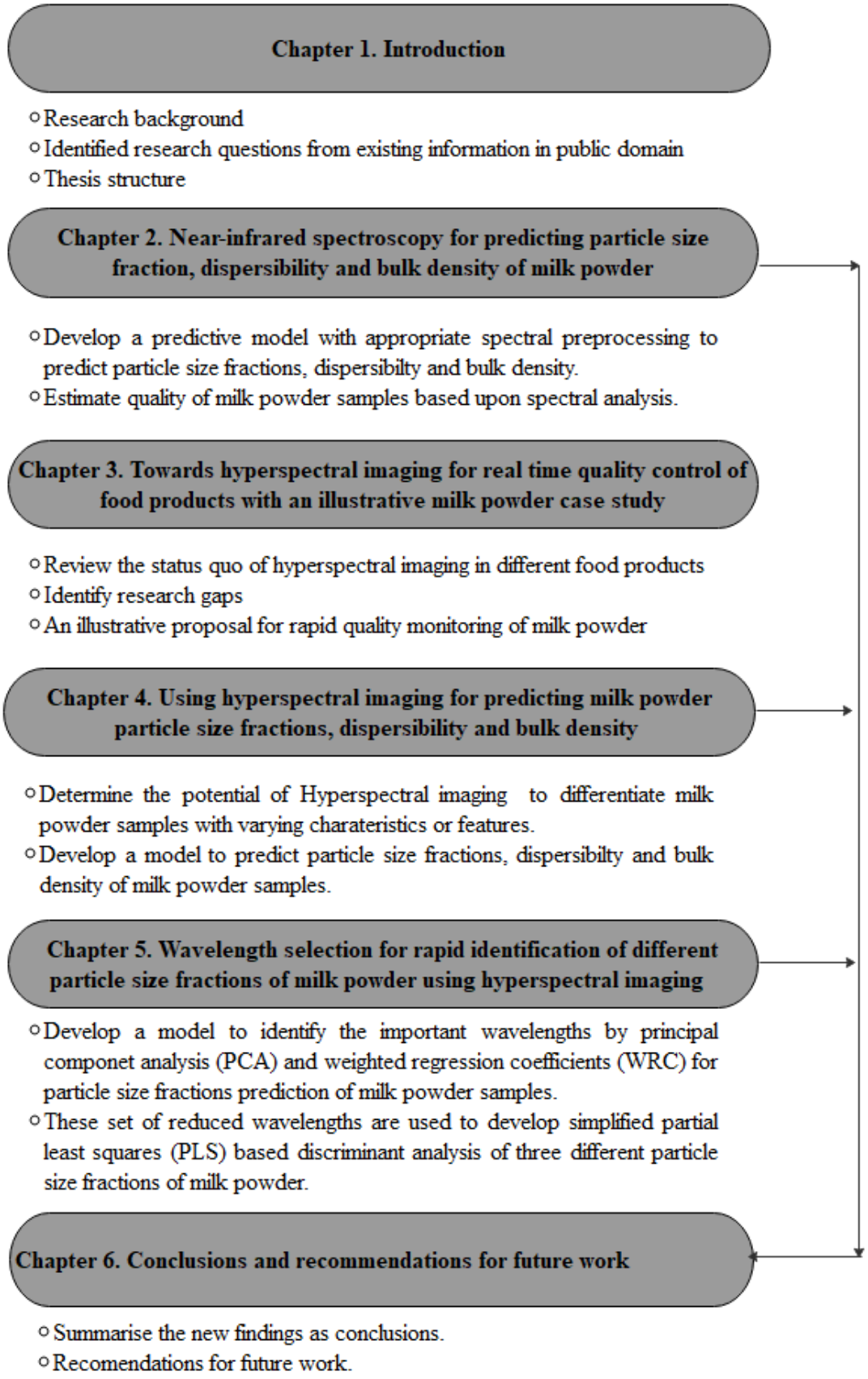

Figure 1.5. Thesis map

Chapter 2. Near-infrared spectroscopy and data analysis for predicting milk powder quality attributes

2.1. Preface

According to the status quo of milk powder quality monitoring practices and future trends discussed in Chapter 1, it was suggested that the rapid monitoring of quality parameters of milk powder would be beneficial. Furthermore, near-infrared (NIR) spectroscopy was introduced as one of the possible solutions for the rapid monitoring of milk powder's physical properties (particle size distribution and bulk density) and functional characteristic (dispersibility).

The first two hypotheses (I & II) as stated in Chapter 1 were considered in order to prepare the samples for the experiments conducted in Chapter 2. Particle size distribution was believed to be influential on bulk density and dispersibility of the milk powder. Furthermore, it was hypothesised that spectral variation could be observed for the samples with different particle size distributions. Therefore, three segregated fractions of milk powder with particles of different size ranges were prepared. These three particle size fractions of milk powder were recombined in seven different proportions to produce a range of samples that were qualitatively different from each other. These seven types of reconstructed milk powder samples were tested for particle size distribution, bulk density and dispersibility in the laboratory. Near-infrared spectra of these reconstructed samples were recorded and preprocessed for data analysis. Partial least square (PLS) based predictive models were developed to predict distribution of fine particle size fraction bulk density and dispersibility of the recombined samples. Model details are given in Appendix A-3.

This work has been published in International Journal of Dairy Technology.

2.2. Abstract

Near-infrared (NIR) spectroscopy is a rapid analytical method that can evaluate the physical and chemical properties of a product sample, and requires little sample preparation. In this study, NIR spectroscopy, multivariate data analysis, and data pre-treatment techniques were used to predict fine particle size fraction, dispersibility, and bulk density of various milk powder samples, which are believed to have a significant impact on milk powder quality. Predictive models using partial least squares (PLS) regression were developed using NIR spectra and milk powder physical and functional properties. Near-infrared spectra were obtained after using different data pre-treatment approaches such as Savitzky-Golay (SG) filtering, standard normal variate (SNV) transformation, multiplicative scatter correction (MSC), and their combinations. The results showed that NIR spectroscopy coupled with data analysis and an appropriate data pre-treatment can be used to rapidly predict milk powder quality in terms of its quality attributes. The fine particle fraction and dispersibility were used as the quality determining attributes of the milk powder samples. However, there was no information found to describe bulk density qualitatively. Confusion matrices based on predicting the fine particle fraction and dispersibility were developed and it was concluded that the PLS models predicted milk powder quality with an accuracy of 80 – 90 percent.

Keywords: Near-infrared spectroscopy; milk powder; particle size fractions; multivariate data analysis; dispersibility; bulk density.

2.3. Introduction

Milk powders are commonly used in the food industry for a wide range of applications due to their nutritional value, and attractive physical and functional properties. During the milk powder production process, liquid milk is standardised, pasteurised, evaporated, and spray dried to produce milk powder. Liquid milk is transformed into powder to increase its shelf-life and ease of its transportation (Kelly et al. 2003). The quality of milk powder is crucial for various food applications such as milk based beverages, yoghurts, milk chocolates, cheeses, and confectioneries, and is usually measured offline after the fact in terms of its dissolution properties using post-manufacture quality tests (*a posteriori* approach) recommended by the International Dairy Federation (IDF). However, these quality tests are off-line, time-consuming, have natural variability, and struggle to describe milk powder quality as quantifiable numeric descriptors (FDA 2004). A failure in milk powder quality tests can mean failing to meet end-user specifications and is unlikely to be industrially feasible. Furthermore, this approach of milk powder quality testing can result in product recall and significant economic loss (Munir et al. 2015).

Milk powder quality is complex because it is dependent on a complex combination of physical and functional properties of milk powder (Sharma et al. 2012). For example, the dissolution behaviour of the milk powder is driven by its physical properties, such as particle size distribution and bulk density, and functional properties such as dispersibility (Oldfield and Singh 2005). An easy to disperse milk powder is desirable in its several applications. Bulk density of milk powder not only affects its functional properties, but it is also significant for its storage and transportation properties. Furthermore, bulk density has a role in the profitability of the milk powder because it determines a precise volume of the product to be packed and shipped (Kim et al. 2002). It is worth mentioning

that these physical and functional properties of milk powder vary with changes in the characteristics of the raw material (i.e. milk) and milk powder processing conditions such as temperature, which impact the end use of the milk powder (Crowley et al. 2015, Kelly et al. 2002).

As a solution to provide rapid quality data, a multivariate data analysis approach coupled with spectroscopic techniques such as near-infrared (NIR) spectroscopy can be used. Amigo et al. (2013) reviewed chemometric tools used to successfully correlate spectral information of various food products to their physical and functional characteristics; however, no information was found on milk powder's spectral data analysis for physical and functional property estimation. Near-infrared spectroscopy has been mostly reported as a feasible method for quantification of milk powder constituents such as proteins and fats (Di et al. 2008, Wu et al. 2008); identification of adulterants in milk powder, such as melamine, urea, starch, etc. (Balabin and Smirnov 2011); and classification of different brands of milk powder (Chen et al. 2018). Most of these NIR studies of the milk powder are based upon lab-scale analysis of the samples. However, Holroyd et al. (2013) tested NIR analyser for the moisture, fat and proteins prediction in the milk powder at the production line and results of their study confirmed that this spectroscopic data-driven approach is technically feasible, can measure milk powder quality (in terms of compositional analysis only) relatively faster than the conventional post-manufacture quality tests, shows less variability than conventional composition test results, can describe milk powder composition as quantifiable numeric descriptors, and is easier to implement in a plant setting for at-line testing. Therefore, potential of NIR spectroscopy for predicting milk powder physical properties and functional performance appears to be promising and needs to be explored.

Near-infrared spectroscopy has been used for real-time quality testing in the pharmaceutical industry for the compositional analysis of active pharmaceutical ingredients (API) and for the estimation of various physical/functional properties such as granulation size of particles, film coating thickness on tablets and powder quality (Kandpal et al. 2017, Märk et al. 2010), following the guidelines provided by the United States Food and Drug Administration (FDA) (FDA 2004). However, one struggles to find published evidence of NIR applications to the physical and functional parameters of dairy products − particularly milk powder. Munir et al. (2015) have presented a comparison of the dairy industry and the pharmaceutical industry's key characteristics for consideration of the real-time quality monitoring of the products. Despite the raw material variations between pharma and dairy industries, the quality control requirements for both industries share the common grounds of safety, traceability and strict quality standards. Near-infrared spectroscopy has the advantage of being a mature and well-developed technology in the pharma industry for real-time testing (Pasquini 2018).

In this study, it was hypothesised that spectroscopy, with the aid of multivariate analysis tools (e.g. partial least square regression, PLS), can predict the physical and functional properties of milk powder such as particle size fractions (e.g. coarse, medium, and fine), bulk density, and dispersibility. Furthermore, the estimation of some of these properties could lead to reliable estimates of the quality of the milk powder samples as well.

The objective of this study is to use NIR spectroscopy for predicting physical and functional property related quality attributes of milk powder such as particle size fractions, dispersibility, and bulk density. Near-infrared spectroscopy was used to get NIR spectra for milk powders. Various spectral data pre-treatment techniques such as Savitzky-Golay (SG), standard normal variate (SNV), multiplicative scatter correction

(MSC), and their combinations (e.g. SG & SNV, and SG & MSC) were used for data pre-treatment. Predictive models for milk powder quality attributes were developed using partial least square (PLS) regression on NIR spectra. The effects of different data pre-treatments on the PLS regression models were evaluated in terms of the regression coefficients of calibration (R_c^2) regression coefficients of prediction (R_p^2). Root mean square errors for calibration ($RMSE_c$) and root mean square errors of prediction ($RMSE_p$) were calculated as well. Model fits with higher R_c^2 and R_p^2 and lower $RMSE_c$ and $RMSE_p$ are desirable. Furthermore, the PLS prediction results were evaluated using confusion matrices to assess the predictive performance of the PLS models.

2.4. Materials and methods

2.4.1 **Milk powder samples**

Instant whole milk powder was obtained from a local supermarket in New Zealand. Milk powder samples with different ranges of particle size distribution, bulk density, and dispersibility were prepared using this commercially available milk powder. The milk powder obtained had passed quality tests in terms of its desired physical/functional properties before it was available to the customers. Therefore, the distribution range of any functional/physical property tests would be narrow if we directly used the milk powder. A reliable model that can unanimously justify a range of samples must be based upon a wider sample distribution range. Therefore, samples for experiments were artificially created in the laboratory to get different particle size distributions and their relevant physical/functional properties.

Milk powder was sieved using a sieve shaker (Retsch AS200–vibratory sieve shaker) to segregate it into three main size fractions: coarse (C; particle size greater than 355 µm), medium (M; particle size range between 180 – 355 µm), and fine (F; particle size less

than 180 µm). In order to create a range of particle size distributions, seven milk powder samples were prepared after mixing three fractions (C, M, and F). Simplex centroid design was used to find out the required number of samples to be analysed and the composition of three size fractions, as shown in Figure 2.1. The table shown in this figure describes the mass percentages of the three different size fractions combined in the preparation of seven samples. Moisture content of these samples were less than 5% which is the maximum acceptable limit of moisture present in instant whole milk powder (Kelly et al. 2003).

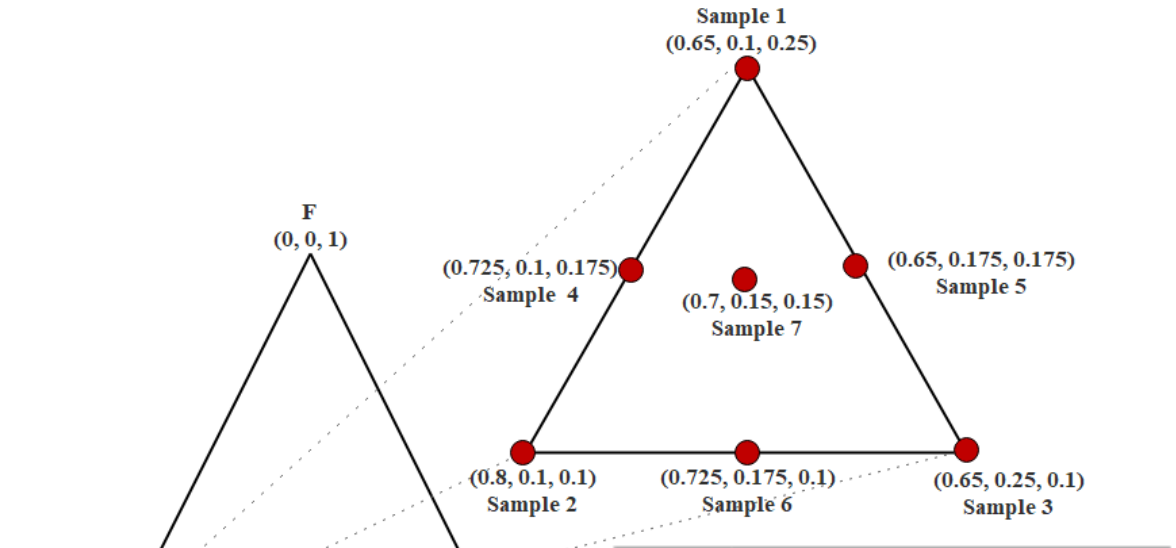

Sample #	Milk powder size fractions (mass percentages)		
	Coarse (C)	Medium (M)	Fine (F)
Sample 1	10	65	25
Sample 2	10	80	10
Sample 3	25	65	10
Sample 4	10	72.5	17.5
Sample 5	17.5	65	17.5
Sample 6	17.5	72.5	10
Sample 7	15	70	15

Figure 2.1. Simplex centroid design for recombined samples of milk powder

2.4.2 **Milk powder particle size distribution**

In order to verify the distribution of the particle size fractions in the recombined milk powder samples, a Malvern Mastersizer 2000 was used. The Mastersizer is capable of measuring dry particle size distribution using laser diffraction. During Mastersizer

operation, approximately 30 g of milk powder was dispersed through a dry dispersion system at 0.1 bar feed pressure, with a laser obscuration of 1 – 5 %. A sample measurement time of 20s, and a refractive index of 1.46 with zero absorption were used in this study. The metallic bearing at the inlet to the Mastersizer was removed to minimise particle breakdown due to attrition. These conditions and parameters during the Mastersizer operation were selected based on preliminary experimentation and previous studies of Boiarkina et al. (2016). It is worth mentioning that the cumulative particle size distribution was also produced for all the samples to find out the cumulative percentage of fine particles i.e. particles with a diameter of 180 µm or less, or the fine particle distribution (X_f).

2.4.3 **Dispersibility measurement**

For dispersibility measurement, a modified New Zealand Dairy Board dispersibility test (NZDB-method) was adopted. The NZDB-method looks at the residue content retained (U) by a mesh directly by comparison with a product-specific standard chart. However, modifications can be made to detect dispersibility directly for skimmed and whole milk powders (Písecký 2012). It is known that a sample with good dispersion properties will leave less residue on the mesh (Crowley et al. 2015, Ji et al. 2016).

Briefly, 26 g of instant whole milk powder, denoted by M_p, was dissolved in 200 ml of water at 318 K for 10 s, and at a mixing speed of 60 rpm using a magnetic stirrer. Immediately after mixing, the undissolved powder was collected on 300 µm mesh by vacuum filtration. It is worth mentioning that the mesh was pre-weighed before use, and was oven dried for 2 h. The percentage of undissolved milk powder was calculated using Equation 2.1 given below.

$$d = \frac{1}{U} = \frac{1}{\left(\frac{M_2 - M_1}{M_p}\right) \times 100} \quad \textbf{2.1}$$

where, d = dispersibility, M_1 = Mesh weight before filtering the mixture (g), M_2 = Mesh weight after filtering the mixture (g), and U = Percentage of undissolved milk powder (%).

2.4.4 **Bulk density measurement**

The bulk density of the milk powder samples was measured using the International Dairy Federation (IDF) Standard 134A method (IDF 2005). A Quantachrome Autotap density analyser with a 250 cm^3 volumetric cylinder was used. The bulk density of all the samples was recorded for 100 tappings with ± 0.01 g/cm^3 repeatability.

2.4.5 **Near-infrared spectroscopy**

For near-infrared spectroscopy data acquisition, a Nicolet 8700 FTIR spectrometer was used which was continuously purged with ultrapure N_2. The FTIR spectrometer was equipped with a CaF_2 beam splitter and an InGaAs detector. The beam splitter splits the incident light into two paths before projecting it on the sample. The light intensities of both are recorded by the detector in the NIR machine and the energy variation (absorption) of the incident light is calculated and reported by the instrument. In this study, the NIR spectra of milk powder samples were recorded for a 1000 – 2500 nm wavelength range. The spectral resolution was 16 cm^{-1} and 110 scans were co-added for each spectrum which includes 3112 wavelengths. Reference reflectance values were obtained with a ceramic block (an accessory provided with the equipment) and dark current measurements.

2.5. Data analysis

Analysis of the spectral data obtained from the NIR spectrometer involves two major steps: data preprocessing or pre-treatment, and multivariate data analysis. Data pre-treatment is necessary to filter noise and extract valuable information required for subsequent data analysis. Data pretreatment methods include data smoothing using techniques such as Savitzky-Golay (SG) filtering (Savitzky and Golay 1964), standard normal variate (SNV) transformation (Barnes et al. 1989), and multiplicative scatter correction (MSC) (Isaksson and Næs 1988). Data pretreatment methods were used individually, and in combination as SG & SNV, and SG & MSC. Afterwards, the partial least square (PLS) (Wold et al. 2001) regression technique was used to develop predictive models. These PLS models were used to predict fine particle distribution (X_f) of the milk powder sample dispersibility, and bulk density using the NIR spectra of the samples. The regression coefficients of the calibration and prediction models were calculated to compare the performance of PLS models. Furthermore, the effect of the aforementioned pre-treatment methods on the regression coefficients of the PLS models was evaluated.

The performance of these PLS models was evaluated by the confusion matrix. The fine particle fraction (X_f) and dispersibility were selected as independent quality attributes for the milk powder samples (details are given in section 2.6.4). The following criteria were independently considered to represent a sample of good quality milk powder (Písecký 2012, Sharma et al. 2012):

i. Milk powder samples having less than 20% fine fraction (particle size less than 180µm)
ii. Milk powder samples having dispersibility more than 1

However, there was no information available in the literature to describe bulk density in qualitative terms. Therefore, prediction of X_f and prediction of dispersibility by PLS were used in the further qualitative analysis of the milk powder samples.

The first criterion was applied to the results of the PLS models developed to predict X_f. Samples that had predicted X_f less than 20% were considered having good quality. All other samples that had X_f 20% or higher were classified as reject samples. These predictions were compared to the actual fine fraction (X_f) of the sample by a confusion matrix.

Similarly, the second criterion was applied to the dispersibility predictive model. All the samples with predictive dispersibility of 1 or higher were considered to be good quality samples. The rest of the samples were considered to be reject quality samples. The confusion matrix for dispersibility prediction was also prepared.

Matlab R2018b (The MathWorks Inc., Natick, Massachusetts, USA) and PLS Toolbox (Eigenvector Research, Inc., Manson, Washington, USA) were used to analyse the NIR spectra in this study.

2.6. Results and Discussion

2.6.1 **Spectral data results**

The NIR spectra of seven different milk powder samples are shown in Figure 2.2. Each sample was prepared from ten different batches of the same brand of milk powder in duplicate and its spectrum was recorded. However, one batch of the spectra is presented in Figure 2.2, illustrating the spectral trend and differences within these seven samples.

It is noteworthy that the raw spectra were distinctive with clear peaks and apparent offsets between them. This observation may be because of the particle size variations in the

recombined milk powder samples which can be related to the spectral information extracted across the whole wavelength range.

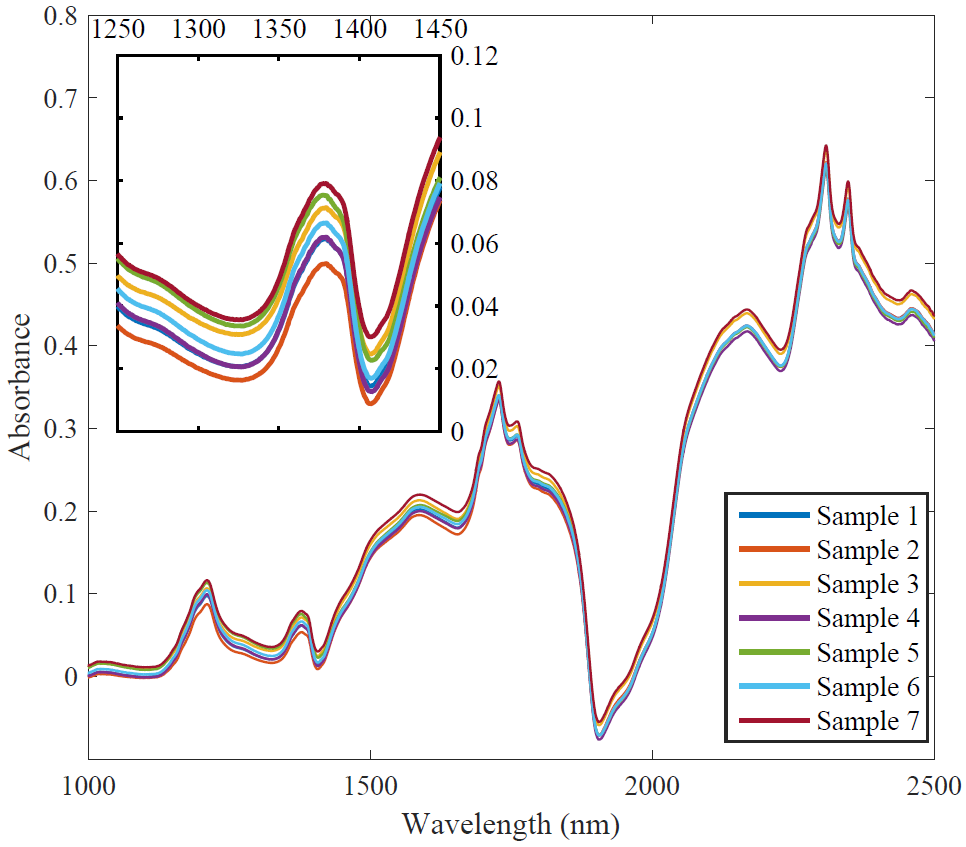

Figure 2.2. Raw near-infrared spectra of milk powder samples with different particle size distribution and quality attributes

As shown in Figure 2.2, each NIR spectrum has some clear peaks that are believed to confirm the position of O-H, C-H, N-H bonds in the powder samples, as reported in various studies such as Moore et al. (2012), Wu et al. (2008). Therefore, these NIR spectra can be used in the compositional analysis of the milk powders. There were offset variations among the spectra which were highlighted in the zoomed subplot of Figure 2.2. These variations in the offsets were believed to be due to differences in physical characteristics of the samples such as different particle size fractions, particle density, and particle shapes, as reported in Andrew et al. (1999).

Before developing the PLS models, all spectra were preprocessed to filter the noise. For this SG, SNV, MSC, and their combinations (SG & SNV, and SG & MSC) were used. Figure 2.3 shows the results of data pretreatment on the spectrum of a milk powder sample (Sample 1) using various techniques such as SG, SNV, and MSC. It is worth mentioning that the SG filter only smoothed the spectrum while retaining the original spectral trends as shown in Figure 2.3. On the other hand, the SNV correction method modified the spectrum by removing the effect of particle sizes within the spectrum of a single sample. Likewise, MSC also eliminated the scattering effect of spectra due to the physical differences of particles within a sample's spectrum. MSC also removed absorption peaks from various atomic bonds (i.e. O-H bonds) from the the spectra and provided a baseline correction for the spectral analysis. The objective of preprocessing of NIR spectra was to obtain a suitable spectrum without unwanted artefacts that could lead to an improved subsequent multivariate data analysis.

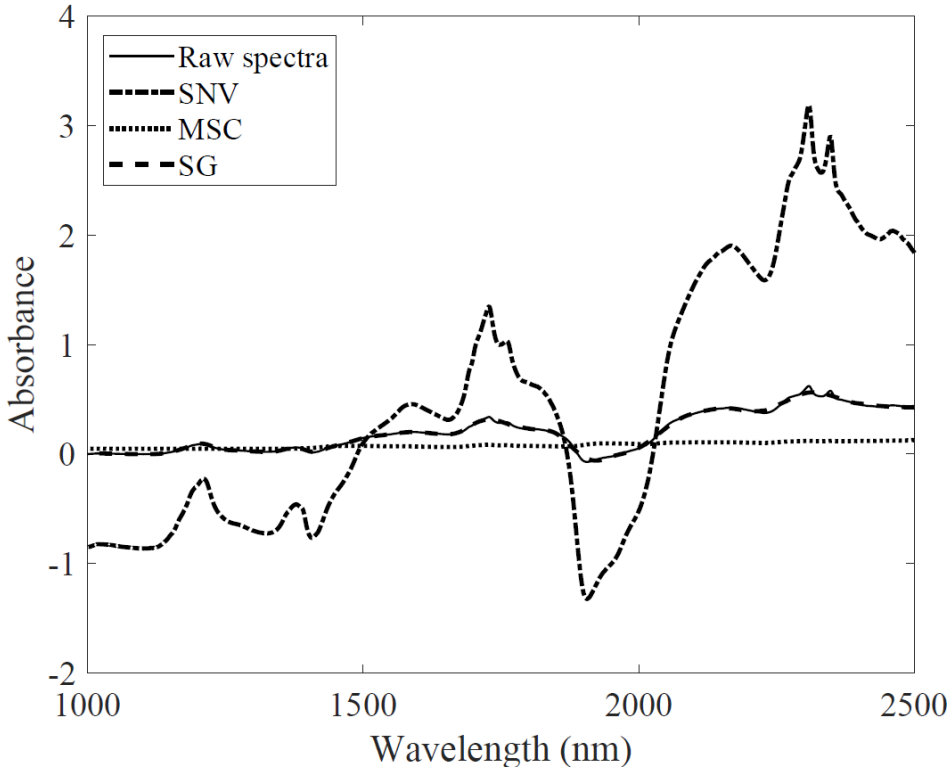

Figure 2.3. Pre-processing of the near-infrared spectrum of a milk powder sample

2.6.2 **Particle size distribution, dispersibility, and bulk density results**

Particle size distribution, dispersibility and bulk density of all the milk powder samples were determined by the methods already discussed in section 2.4.2, section 2.4.3 and section 2.4.4, respectively. These results are summarised in Table 2.1. Dispersibility and bulk density are reported as average values.

Table 2.1. Properties of milk powder samples

Sample #	Milk powder size fractions (mass %)			Dispersibility	Bulk density (g/cm^3)
	Coarse (C)	Medium(M)	Fine (F)		
Sample 1	10	65	25	0.76	0.45
Sample 2	10	80	10	1.84	0.53
Sample 3	25	65	10	1.35	0.60
Sample 4	10	72.5	17.5	1.05	0.42
Sample 5	17.5	65	17.5	0.87	0.46
Sample 6	17.5	72.5	10	1.27	0.55
Sample 7	15	70	15	1.13	0.51

Milk powder samples were reconstituted by using known mass percentages of coarse, medium and fine particle fractions. These distributions were verified by laser diffraction analysis of each sample. The results of laser diffraction were reported as volume percent of particles for different particle size ranges. These results are shown as a histogram in Figure 2.4. Moreover, these discrete fractions were used to develop a cumulative distribution of milk powder samples. The cumulative particle size distribution curve is also presented in Figure 2.4 as a continuous line. From the cumulative size distribution curve, fine particle fraction (X_f) was determined for all the samples. The fine particle fraction (X_f) was the percent volume of the sample having a particle size of 180 µm or less in the sample as shown in Figure 2.4 and it was further used in the data analysis to build the PLS model. It is important to consider that the size distribution analysis by laser diffraction technique was reported and saved as volume percent and the milk powder sample reconstitution was carried by mass percent. However, conversion from one type

of size distribution into another is possible. There was evidence where the mass and volume-based particle size distribution of skimmed milk was close enough to be interchangeable, with the condition that large particles were not dominant in the system (Lammers et al. 1987). For example, sample 6 was prepared by recombining 10% (mass) of fine particle fraction. The results from laser diffraction size analysis of the sample confirmed approx.~11% (vol.) of sample particles were of size 180 µm or less as shown in Figure 2.4.

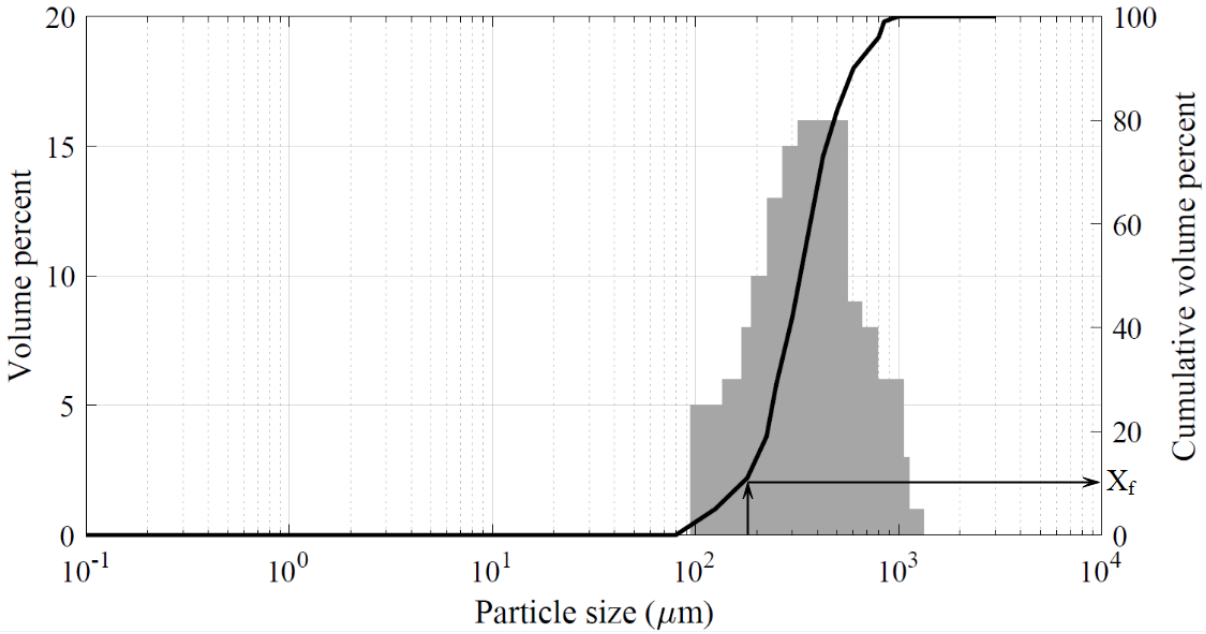

Figure 2.4. Particle size distributions of a milk powder sample with fine particle fraction estimation from cumulative distribution curve

Dispersibility and bulk density results are shown in Table 2.1. It is worth noting that dispersibility results varied from 0.76 (for 25 mass % of fine fraction, sample 1) – 1.84 (for 10 mass% of fine fraction, sample 2). As a result, sample 1, with more fine particles, showed ‘poor’ dissolution performance, and sample 2, with less fine particles, showed ‘good’ dissolution performance. In other words, the distribution of fine particles in the samples influenced dispersibility results and dissolution performance. These dispersibility results and their related dissolution performance are in accordance with the

existing evidence from the published literature such as Ji et al. (2016), Silva and O'Mahony (2016). Similarly, the bulk density results of the samples vary from 0.42 – 0.60 g/cm^3, shown in Table 2.1. Milk powder samples used in this research did not produce a wide range of bulk density when examined in the lab. This observation may be because particle size variation might not be the only factor altering the bulk density. Different process parameters and raw material characteristics have determined the final bulk density of the product (Kelly et al. 2002). These dispersibility and bulk density results from the samples were then used in the data analysis to develop predictive models for milk powder.

2.6.3 **Data analysis results**

Partial least squares (PLS) regression was used to predict the fine particle fraction (X_f), bulk density, and dispersibility of the milk powder samples of the total 70 samples of ten different batches.

Table 2.2 shows the prediction performance of the PLS models in terms of R_c^2, $RMSE_c$, R_p^2, $RMSE_p$ and RPD to predict fine particle fraction (X_f), dispersibility and bulk density of the milk powder samples. Furthermore, the effect of data pre-treatment techniques such as SG, SNV, MSC, and their combinations (e.g. SG & SNV, and SG & MSC) on the prediction performance of the PLS model is presented.

Near-infrared spectra were used to predict the fine particle fraction (Xf) in milk powder samples by PLS regression models as shown in Figure 2.5. It is interesting to note that in Figure 2.5, the PLS model prediction performance for the prediction of fine particle fraction (Xf) using NIR spectra was not significantly affected by the pre-treatment techniques or their combinations. However, the SG technique did improve the prediction model regression coefficient (R_p^2) from 0.668 to 0.703. This observation may be because

SG filtering can smooth the spectra by removing noise without altering the actual spectral trend. Therefore, after smoothing the NIR spectrum of seven types of samples, the offset variation among the spectra was not eliminated and used for differentiating the samples for size analysis. Other pre-treatment techniques such as SNV, MSC or their combinations (e.g. SG & SNV, and SG & MSC) could not achieve a better R_p^2 value than when using the raw spectra. In other words, data pre-treatment techniques mostly did not add significant value in the prediction performance of the PLS model for the prediction of fine particle fraction (X_f) using NIR spectra.

Table 2.2. Regression coefficients for partial least squares models with different spectral pre-treatments

Pretreatment	R_c^2	$RMSE_c$	R_p^2	$RMSE_p$	RPD
			X_f		
No	0.682	5.37	0.668	5.214	1.82
SG	**0.721**	**4.46**	**0.703**	**4.32**	**2.03**
SNV	0.653	4.963	0.645	5.269	1.89
MSC	0.679	5.851	0.651	6.027	1.61
SG and SNV	0.662	5.369	0.628	5.945	1.66
SG & MSC	0.686	4.958	0.648	5.684	1.74
			Dispersibility		
No	0.903	0.1768	0.873	0.1852	2.83
SG	0.962	0.1685	0.942	0.1889	2.71
SNV	0.885	0.1954	0.856	0.2014	2.69
MSC	0.868	0.1453	0.853	0.1985	2.59
SG and SNV	0.893	0.1652	0.879	0.1520	3.84
SG & MSC	**0.981**	**0.1514**	**0.973**	**0.1592**	**3.86**
			Bulk Density (g/cm^3)		
No	0.916	0.104	0.884	0.095	3.51
SG	0.983	0.084	**0.978**	**0.104**	**3.87**
SNV	0.876	0.1056	0.854	0.0961	3.55
MSC	0.935	0.0973	0.907	0.982	3.80
SG and SNV	0.928	0.106	0.872	0.112	3.96
SG & MSC	**0.985**	**0.0814**	0.963	0.0965	3.84

This observation may be because SNV and MSC were used for filtering spectral data from variance and scattering effects due to particle size and density variation, as observed by published studies such as Chang et al. (2001). Therefore, these pre-treatment methods

minimised the spectral variation caused by different sized particles of the milk powder samples and lead to a poor performance prediction model.

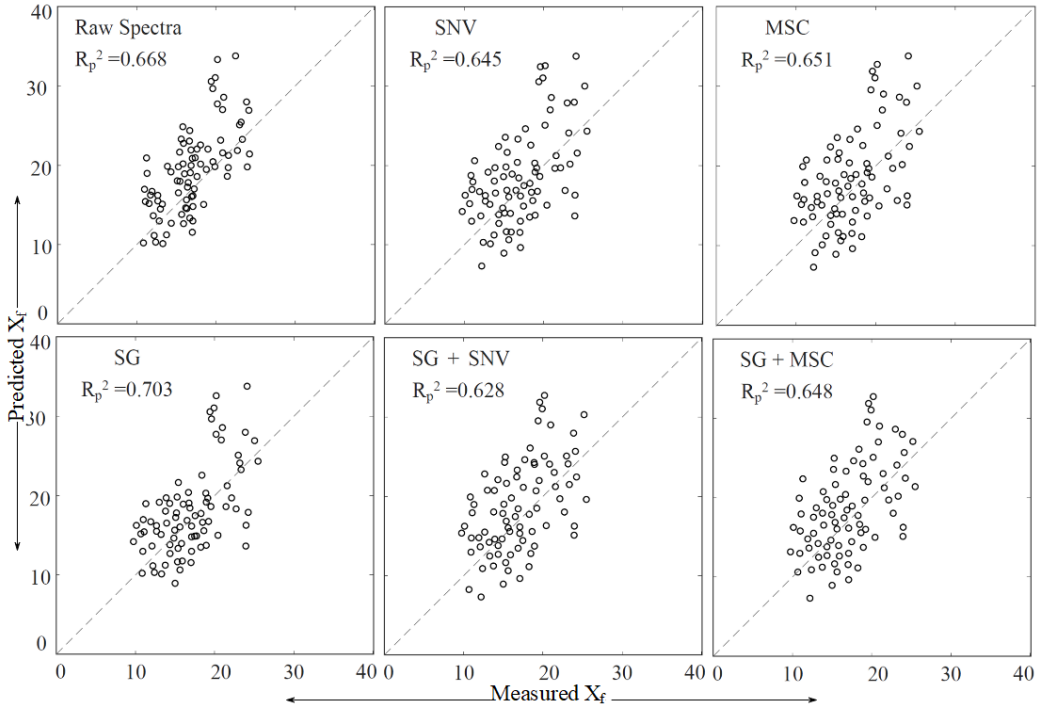

Figure 2.5. Predicted vs measured fine particle fraction (X_f) from the partial least squares model based on near-infrared spectra

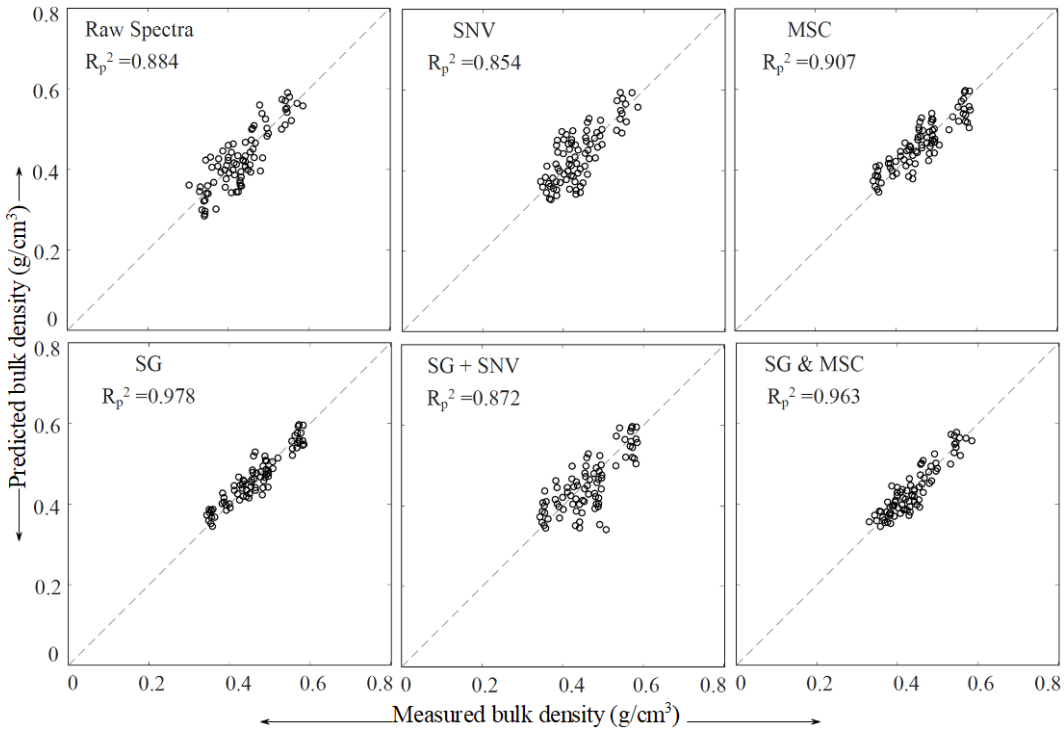

Figure 2.6. Predicted vs measured bulk density from the partial least squares model based on near-infrared spectra

Similarly, Figure 2.6 shows the prediction performance of the PLS model for the prediction of milk powder bulk density using NIR spectra and various data pre-treatment techniques and their combinations. In this case, the SG smoothing technique helped to improve PLS regression prediction performance in terms of R_p^2 value which was 0.978 as compared to 0.884 for the performance of the PLS model based on the raw spectra. The MSC technique slightly improved the prediction performance as the R_p^2 value increased from 0.884 to 0.907. However, SNV worsened the PLS prediction performance as the R_p^2 value decreased from 0.884 to 0.854. The combination of SG and MSC was also effective at improving the prediction performance of the PLS models because the value of R_p^2 increased from 0.884 to 0.963 (Figure 2.6).

Similarly, for the dispersibility prediction models, SG improved the prediction performance of the PLS model in terms of R_p^2 value which was increased from 0.873 to 0.942 (Figure 2.7). Furthermore, SNV and MSC techniques suppressed the prediction performance of the PLS model for the dispersibility prediction of the milk powder samples using NIR spectra. However, the combination of SG and MSC improved the prediction performance of the PLS model in terms of R_p^2 value which increased from 0.873 to 0.974. These observations may be because spectral scattering is a function of particle size in the powder sample i.e. the larger the particles in size, the more scattering of spectra would be observed. However, the dispersibility of the milk powder samples was related to the percentage of fine particles in the samples (Písecký 2012). Thus, a prediction model for a variable (e.g. dispersibility) that was depending upon the fine particles present in the sample would not deteriorate when the scattering was removed from the spectra after smoothing it. Furthermore, the PLS model for the prediction of Xf based on data that underwent SG pre-treatment had a maximum RPD value of 2.03. The higher value of RPD ensures a better predictive performance of the model. In general, an

RPD value greater than three is acceptable (Williams and Norris 1987). However, the PLS model for the prediction of dispersibility based on data after SG and MSC pre-treatment provided an RPD of 3.86. Therefore, the PLS model performed better for the prediction of dispersibility.

Using the results shown in Figure 2.5 to Figure 2.7, the PLS models with the highest R_p^2 values for the prediction of each quality attribute (X_f and dispersibility) were selected for developing confusion matrices (discussed in Section 2.6.4). These were the PLS model based on SG pre-treatment for the prediction of X_f and PLS model based on SG & MSC pre-treatment for the prediction of dispersibility.

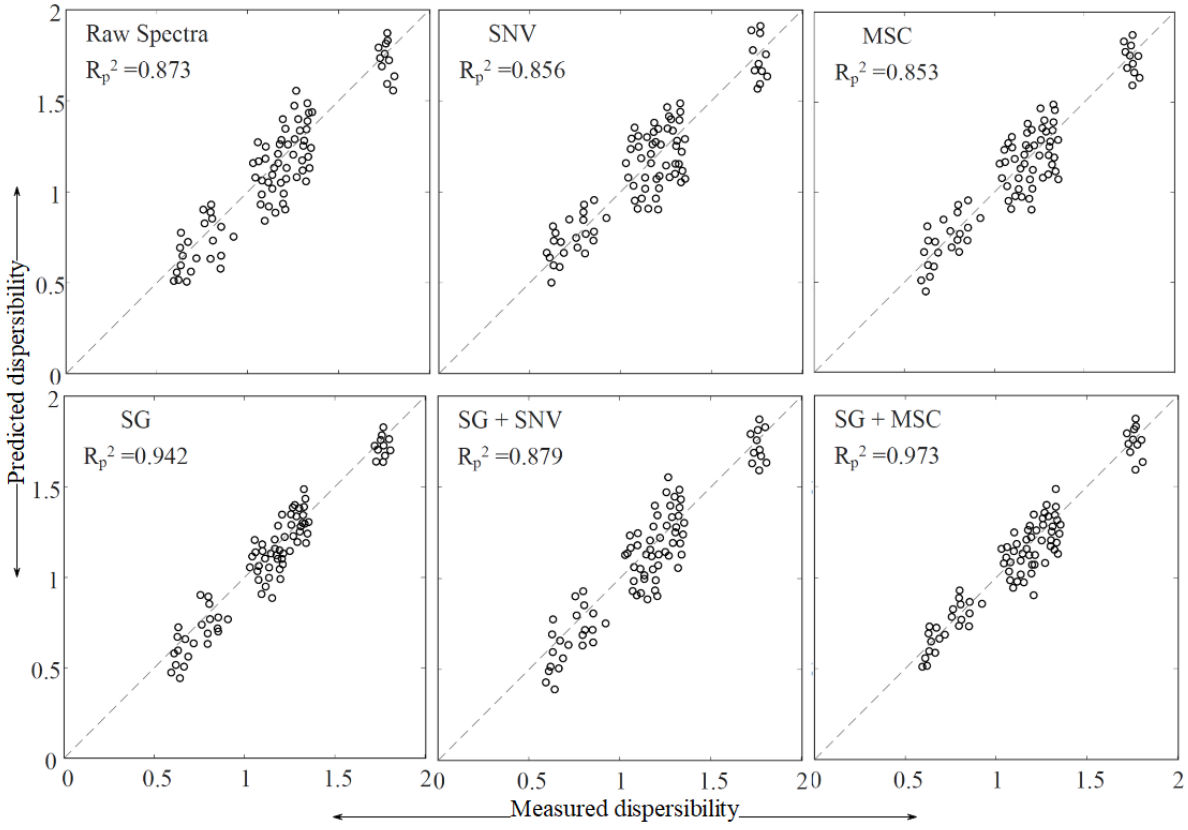

Figure 2.7. Predicted vs measured dispersibility from the partial least squares model based on near-infrared spectra

2.6.4 **Prediction evaluation using confusion matrices**

As discussed before in section 2.3, milk powder quality is dependent on various quality attributes such as the fraction of fine particles and dispersibility. Milk powder samples with a fine particle fraction higher than 20 percent by mass or volume are considered to exhibit 'poor' dissolution properties and lower than 20 percent are considered to have 'good' dissolution properties. Similarly, milk powder samples with dispersibility values smaller than 1 are considered to be 'poor' quality and larger than 1 to be of 'good' quality. Both of these quality attributes were used to develop confusion matrices for evaluating the quality prediction of the milk powder samples.

In order to develop confusion matrices based on the fine particle fraction (X_f), and dispersibility results, class definitions are presented in Table 2.3.

Table 2.3. Classification of milk powder samples for confusion matrix

Fine particle fraction (X_f)	
Positive class I	Milk powder samples of this class contain less than 20 percent fine particles
True positive	X_f is less than 20 percent, and is predicted to be less than 20 percent.
False positive	X_f is more than 20 percent, and is predicted to be less than 20 percent
Negative class I	Milk powder samples of this class contain more than 20 percent fine particles
True negative	X_f is more than 20 percent, and is predicted to be more than 20 percent
False negative	X_f is less than 20 percent, and is predicted to be more than 20 percent.
Dispersibility	
Positive class II	Milk powder samples of this class having dispersibility values more than 1
True positive	Dispersibility of the sample is more than 1, and is predicted to be more than 1
False positive	Dispersibility of the sample is less than 1, and is predicted to be more than 1
Negative class II	Milk powder samples of this class having dispersibility values less than 1
True negative	Dispersibility of the sample is less than 1, and is predicted to be less than 1
False negative	Dispersibility of the sample is more than 1, and is predicted to be less than 1

Table 2.4 presents results of confusion matrices based on the fine particle fraction (X_f), and dispersibility results. The confusion matrices have the advantage of presenting statistically supervised classifications with better visualisation. It is worth noting in Table

2.4 the PLS model developed with pre-treated spectra using SG correctly predicted 49 samples which had less than 20 percent of X_f (i.e. Positive class I, and True positive class I). Furthermore, seven milk powder samples were correctly predicted with more than 20 percent X_f (i.e. Negative class I, and True negative class I). There were nine samples that actually had less than 20 percent X_f, however, were wrongly predicted that they had more than 20 percent X_f (i.e. False negative class I). Similarly, there were eight samples that actually had more than 20 percent X_f, however, were wrongly predicted that they had less than 20 percent X_f (i.e. False positive class I).

Table 2.4. Confusion matrix for the prediction of quality in milk powder samples

X_f prediction results

N / %	Samples predicted as 'Good'	Samples predicted as 'Poor'	Total samples
Actual samples 'Good'	49 / 70.0%	9 / 12.6%	58 / 82.8%
Actual samples 'Poor'	8 / 11.4%	7 / 10.0%	15 / 21.4%
Total samples	57 / 81.4%	13 / 18.6 %	70 / 100.0%

Dispersibility prediction results

N / %	Samples predicted as 'Good'	Samples predicted as 'Poor'	Total samples
Actual samples 'Good'	41 / 58.6%	6 / 8.6%	47 / 67.1%
Actual samples 'Poor'	0 / 0.0%	23 / 32.9%	23 / 32.9%
Total samples	41 / 58.6 %	29 / 41.4%	70 / 100%

Similarly, the PLS model developed with pre-treated spectra using SG and MSC correctly predicted dispersibility value of 1 or higher (i.e. Positive class II, and True positive class II) for 41 samples (Table 2.4). Likewise, a dispersibility value of less than 1 was correctly predicted (i.e. Negative class II, and True negative class II) for 23 samples. There were six samples that had an actual dispersibility value higher than 1, however, the PLS model predicted their dispersibility value less than 1 (i.e. False negative class II).

The confusion matrices based upon these PLS model results have given a statistical explanation to all the predictions made by the models. It is noteworthy that the prediction model regression coefficient (R_p^2) of the PLS models of the fine particle fraction (X_f) and dispersibility was 0.703 and 0.973, respectively. However, the accuracy of the PLS model for X_f prediction was 80 percent based on its correct prediction of X_f in milk powder samples and their classification into Positive class I and Negative class I. There were approximately 11.4 percent of the samples which were in False positive class I. The dispersibility prediction PLS model was 91.4 percent accurate at correctly predicting dispersibility values of the milk powder samples and discriminating them into to Positive class II and Negative class II. Furthermore, none of the samples were characterised into False positive class II. Although, six samples were categorised as False negative class II. The prediction accuracy for the dispersibility model of the milk powder samples was better than X_f predictive model.

2.7. Conclusions

This study shows that spectral information of milk powder samples obtained from NIR spectrometry can be used to predict the fine particle distribution, dispersibility and bulk density of a milk powder sample. Furthermore, milk powder quality, if defined in terms of its underlying parameters like fine particle fraction, can also be estimated with an accuracy of more than 80%. Dispersibility estimation from the spectral data of the milk powder samples was also more than 90 % accurate. The methods presented in this paper can be proposed as an alternative approach to determine the quality of milk powder, which can potentially be implemented at-line on a milk powder production unit.

2.8. Summary

This chapter confirmed that spectral variation exists if there were different size ranges of particles present in different milk powder samples. It also suggests that spectroscopy can be a possible solution to determine milk powder quality in terms of dispersibility. Bulk density was also predicted with a high correlation of prediction, i.e., 0.97; however, the specific numeric value of bulk density could not be found in the literature to differentiate bulk density qualitatively. Milk powder sample quality was also related to the ratio of fine particles present within the sample. Among the total 70 samples, 49 out of 58 good samples and 7 out of 15 poor samples were predicted correctly. However, there were eight samples that were actually poor but predicted as good. This observation made the model less reliable for the quality determination by estimating fine particle percentage in a milk powder sample by NIR spectroscopy.

Chapter 3. A Review towards hyperspectral imaging for real time quality control of food products with an illustrative case study of milk powder production

3.1. Preface

Hyperspectral imaging (HSI) was reported as an emerging technology in Chapter 1 that was a hybrid of spectroscopy and imaging to monitor the quality of food products. Prior to proposing HSI for milk powder quality estimation, it was prudent to review its application towards other food products to understand the similarity and differences. It is noteworthy that an exhaustive review of the application of HSI to food products is not presented in this chapter, although the first part is a summary of recent articles on the subject. There were common shortcomings identified for a successful industrial application for various products. These limitations are discussed separately in this chapter. The last part focuses on the possible use of the technique for real-time quality monitoring during milk powder production and contains generic considerations and comments on the possibilities of HSI on this subject.

This part of the work has been published in the Journal of Food and Bioprocess Technology.

3.2. Abstract

Hyperspectral imaging (HSI) is a relatively fast analytical method that is being used for quality testing of natural foods (e.g. fruits and vegetables). This method has been proposed to replace existing manual off-line sensory quality tests of processed foods (e.g. milk powder). This article reviews the current status of HSI for monitoring natural and processed

food product quality and identifies key knowledge gaps in recent literature that may be responsible for the limited success of HSI especially for processed food (e.g. milk powder) quality testing at both the lab and industrial scales. Furthermore, various strategies to cope with challenges associated with limited HSI success are discussed. From the current literature, HSI has been used primarily as an off-line machine vision technique for quality testing to replace existing manual sensory tests. However, HSI lacks scenarios of testing and controlling product quality in real-time − especially for processed foods. Little has been reported to date on generalising suitable design choices for the 'successful' implementation of HSI. To address this deficiency, the potential of HSI to achieve real-time quality control was examined using the milk powder production process as a case study.

Keywords: Hyperspectral imaging (HSI); milk powders; multivariate data analysis.

3.3. Introduction

Fast analytical methods are essential for monitoring milk powder quality. Ideally, for the successful development of online milk powder quality testing, quality monitoring and control, it would be conducted in real-time to detect problems quickly during milk powder processing and to avoid reject milk powder being produced unnecessarily. However, traditional methods of milk powder quality monitoring such as post-manufacture quality tests are typically offline, time-consuming, expensive, and after the fact. Furthermore, large amounts of sub-standard milk powder can be generated before a processing problem is identified, which leads to milk powder being wasted.

Optical sensing techniques such as hyperspectral imaging (HSI) and spectroscopy are emerging as novel analytical methods for rapid or online food product quality monitoring, which can also be used for milk powder. Hyperspectral imaging has been used in a wide range of applications in the food industry for monitoring the quality of natural foods (e.g. fruits and vegetables, meat, cereals and nuts) (discussed in Section 3.4.1) and processed foods (e.g. milk powder, cheese, processed meat, coffee, food powders, and dried fruits, etc.) (discussed in Section 3.4.2). The term ‘natural’ food here implies foods that are unprocessed post-harvest (e.g. whole fruit), and processed foods are those transformed in some way during processing (such as milk powder).

Hyperspectral imaging technology is a hybrid technology that combines imaging and spectroscopy to generate a spatial map of spectral variations. A three-dimensional ‘hypercube’ of image data (x, y, λ) is generated using this technology by taking a series of two-dimensional spatial (x, y) images as a function of wavelength (λ) and superimposing them. Each image plane of the hypercube is composed of pixels and maps the light absorbance by the sample at a single wavelength, λ_i. Hyperspectral imaging data

can be viewed in various forms: as a three-dimensional hypercube $I(x, y, \lambda)$, as a two-dimensional spatial image $I(x, y)$, and as a collection of spectra $I(\lambda)$ at pixel positions (x, y)(Hussain et al. 2018). Hyperspectral imaging data is of large volume depending on the instrument and camera pixels. A typical short wave near-infrared hyperspectral imaging (SWNIR-HSI) equipment with a wavelength range of 400 – 1000 nm can create image data of around 200 × 2000 pixels which will give approximately 40,000 pixels or spectra measured at approximately 1,000 equally spaced wavelengths from 400 – 1000 nm. The resultant data is big and needs good computing capabilities to process. More detail about the hyperspectral camera and its other hardware components, various modes of operation of HSI and its fundamentals can be found in Gowen et al. (2007), and Wu and Sun (2013).

Hyperspectral imaging can be an effective technology for milk powder quality testing as compared to traditional post-manufacture quality tests, imaging, or spectroscopy alone because it is faster than off-line quality tests and combines the advantages of conventional two-dimensional imaging and spectroscopy (third-dimension). HSI takes two-dimensional images of milk powder at various wavelengths to generate a three-dimensional hypercube, which should provide additional information about milk powder quality compared to imaging or spectroscopy alone. Furthermore, HSI technology can be applied non-invasively as shown by recent studies on natural foods such as fruits and vegetables (Jha et al. 2019, Tung et al. 2018), unprocessed meat (Ma et al. 2019, Zheng et al. 2019), cereals (Erkinbaev et al. 2019, Vermeulen et al. 2018), and nuts (Bai et al. 2018, Nakariyakul and Casasent 2011) However, recent literature lacks HSI case studies of testing and controlling product quality in real-time, especially for processed foods.

Hyperspectral imaging technology is still expensive and requires substantial computing power for online processing of three-dimensional hyperspectral data.

Notwithstanding the various advantages of HSI and its successful applications for monitoring the quality of natural foods, the application of HSI for processed foods (e.g., milk powder) quality testing lags behind natural foods at the lab and industrial scale. It is interesting to note that recent literature has reported HSI as stand-alone off-line machine vision technique for quality testing of natural and processed foods. However, one cannot find any published evidence in the literature showing the application of HSI for testing and controlling product quality in real-time, and successful industrial applications − especially for processed foods. One also struggles to find generalised design choices (e.g. choices for data pre-processing and multivariate data analysis tools) required for HSI applications in the literature. These knowledge gaps were identified and are discussed in more detail in Section 3.5.

Therefore, this article reviews the current status of HSI applications to natural and processed food quality monitoring and identifies key findings and knowledge gaps responsible for the lower number of HSI applications for processed food (e.g. milk powder) quality than natural foods at the lab and industrial scale. Generalised design choices are discussed, especially for monitoring processed food (e.g. milk powder) quality using HSI, which can also be used for natural foods. Improvements in HSI hardware such as advanced cameras, fast and efficient HSI sensors, different lighting arrangements and its impact on various HSI applications could be interesting to discuss; however, this review does not address these elements. Due to the diverse range of food products reviewed in Section 3.4 of this study, it would be appropriate to refer the reader to already published work that has comprehensively covered HSI applications for a

specific product or a similar range of products. For example, Fu and Chen (2019) discussed the software and hardware advancement of HSI, particularly for chicken meat. Lastly, a case study is discussed in which HSI is used as a stand-alone off-line machine vision technique for quality testing linked with the controllable milk powder process variables to show its potential for real-time quality control and its industrial application.

3.4. The current status of using HSI for monitoring food product quality

3.4.1 **Quality monitoring of natural foods**

Hyperspectral imaging (HSI) has been used for monitoring the quality of natural foods at both the lab and industrial scales. The literature in quality monitoring of natural foods using HSI can be classified under four main product categories: unprocessed meats and fish, fruits and vegetables, cereals, and nuts. Table 3.1 shows various applications of HSI, their spectral ranges, important wavelengths or spectral regions and the multivariate data analysis tools used for monitoring the quality of natural foods. It also summarises the performance of these multivariate data analysis tools. In most of the reported studies, HSI has mainly been used for a product property prediction (i.e. regression analysis) or product discrimination (i.e. classification study) using HSI data. For evaluating prediction and classification performances, regression coefficients, root mean square errors and classification accuracy have been employed, also reported in Table 3.1. These statistical descriptors help to determine the suitable data analysis approach in a case study. The studies referred to in Table 3.1 and Table 3.2 have not frequently reported bias and slope from the regression results, so they are not presented here. A diverse range of food products are referred to in this review and the data ranges of various parameters

were not relatable between different products. Therefore, presenting it might create confusion to the reader, and we have thus chosen not to do so.

As shown in Table 3.1, within the meat and fish industry, HSI has been used for determining the origin of salmon fish (Xu et al. 2017), and for predicting meat quality (ElMasry et al. 2012) in terms of various quality attributes, such as tenderness (Pérez-Santaescolástica et al. 2019, Qiao et al. 2015), colour (Kamruzzaman et al. 2016), freshness (Xiong et al. 2015), and for detecting microbial attributes (Feng et al. 2013). Hyperspectral imaging has been used to determine various quality attributes of fruits and vegetables (Giovenzana et al. 2015), such as apple surface defects (Baranowski et al. 2013), ripening of bananas (Rajkumar et al. 2012), lemon taste (Sun et al. 2017), and chemical components (moisture content, acidity, sugar content, and soluble solid content) (Huang et al. 2014a, Li et al. 2018, Rady et al. 2014, Sun et al. 2017). Similarly, HSI has been used for evaluating the quality of natural cereals, such as rice quality (Wang et al. 2015), maize variety (Wang et al. 2016), and protein content prediction in wheat (Mahesh et al. 2015). A few studies on testing nut quality have also been reported. Bai et al. (2018) used HSI to estimate kernel peroxide value, nitrogen, and mineral nutrient concentration, and Nakariyakul and Casasent (2011) used HSI for classification of internally damaged almond nuts. For natural foods, HSI has been used to measure food quality in terms of single or multiple quality attributes. Some attributes were for appearance or surface detection, such as detecting bruises on fruit surfaces, or internal chemistry such as measuring glucose in potatoes, or protein and fat content in meats. Hyperspectral imaging detects surface features by selecting ‘appropriate’ two-dimensional, spatial (x, y) image(s) along with its wavelength range where differences between ‘normal’ and ‘abnormal’ surface features are obvious. For investigating the internal chemistry of

natural foods, HSI uses its spectroscopic capabilities or collection of spectra $I(\lambda)$ at each pixel position (x, y). Hyperspectral imaging records the spectral characteristics of natural foods that are controlled by molecular overtones and bending or stretching of C–H, O–H, and N–H functional groups (Liu et al. 2017).

Table 3.1. Application of HSI for monitoring the quality of natural foods

Objective	Spectral range / Important wavelengths(nm)	Multivariate-data analysis*	Regression analysis			Classification accuracy	Reference(s)
				Regression coefficients	RMSE[+]		
i. Unprocessed meats							
Detected adulteration with duck meat in minced lamb meat	400 – 1000 / 500, 520, 545, 560, 580, 595, 605, 635, 650, 680, 885, 900, 930 and 985	PLSR		0.98[†]	2.51%[†]	--	(Zheng et al. 2019)
Colour and tenderness evaluation in meat	500 – 1850 / --	Spectral analysis		0.96[†]	--	--	(Van Beers et al. 2018)
Determining the origin of salmon fish	964 – 1564 / 470, 490, 510, 600 and 630	PLS-DA		--	--	83.6 – 94.5%	(Xu et al. 2017)
		SVM		--	--	67.3 – 98.2%	
		RF (TreeBagger)		--	--	61.8 – 91.9%	
Lamb meat red colour parameters (L, a, b) prediction	400 – 1000 / 450, 460, 600, 620, 820, and 980	LS-SVM	L	0.96[†]	1.68[†]	--	(Kamruzzaman et al. 2016)
			a	0.89[†]	1.44[†]		
			b	0.85[†]	1.28[†]		
		PLSR	L	0.97[†]	1.72[†]	--	
			a	0.84[†]	1.73[†]		
			b	0.82[†]	1.35[†]		
Muscle classification in lamb meat	380 – 1020	ANN		--	--	85.3%	(Sanz et al. 2016)
		LDA		--	--	83.1%	
		LR		--	--	91.7%	
		SVM		--	--	96.7%	

Objective	Spectral range / Important wavelengths(nm)	Multivariate-data analysis*	Regression analysis			Classification accuracy	Reference(s)
			Regression coefficients		RMSE+		
Rancidity odour and browning on the meat surface	874 – 1734 / 1150, 1355, 1386, 1130, 1072, 1009, 1463, 1328, 1409, 1029, 1598, 1106 and 1214	PLSR		0.81†	0.33†	--	(Wu et al. 2016)
Predicting the tenderness of beef	400 – 1000 / --	SVM		0.45‡	--	--	(Qiao et al. 2015)
Predicting freshness of chicken	400 – 1000 / 400, 405, 461, 519, 533, 550, 578, 669, 939, and 1000	SPA-PLSR		0.81†	0.16†	--	(Xiong et al. 2015)
Detection of bacterial species on chicken fillets	930 – 1450 / 930, 1121 and 1345	PLSR		0.89†	0.33†	--	(Feng et al. 2013)
Predicting beef quality	900 – 1700 / 924, 937, 951, 961, 984, 1044, 1091, 1111, 1117, 1158, 1245, 1251, 1285, 1316, 1342, 1363, 1376, 1406, 1413, 1443, 1476, 1500, 1524 and 1541	PLSR	Colour	0.88‡	1.21‡	--	(ElMasry et al. 2012)
			pH	0.73‡	0.06‡		
			Tenderness	0.83‡	45.7‡		
Predicting the quality attributes of lamb	900 – 1700 / 40, 980, 1037, 1104, 1151, 1258, 1365, 1418, 1518, 1618 and 1652	PLSR	pH	0.65‡	--	--	(Kamruzzaman et al. 2012)
			Colour	0.91‡	1.56‡		
			Drip loss	0.77‡	--		

Objective	Spectral range / Important wavelengths(nm)	Multivariate-data analysis*	Regression analysis			Classification accuracy	Reference(s)
			Regression coefficients		RMSE+		
ii. Fruits and vegetables							
Evaluating the internal quality of nectarines	630 – 900 / 670-730, 760, 970-990	PLS-DA			--	96.5%	(Munera et al. 2019)
		PLSR		0.88†	0.33†	--	
Colour, firmness and soluble solids content in plums	600 – 1610 / --	PLSR	Colour	>0.73‡	<4.2‡	--	(Li et al. 2018)
			Firmness	>0.51‡	<8.2‡		
			Soluble solids	>0.72†	<1.5†		
Determining sweetness and hardness in melon	882 – 1719 / 967, 989, 1010, 1036, 1046, 1092, 1128, 1142, 1191, 1201, 1263, 1335, 1342, 1434, 1492, 1565, 1585, 1619	ANN	Sweetness	0.78†	1.2† 492†	--	(Sun et al. 2017)
			Hardness	0.37†			
		PLSR	Sweetness	0.80†	1.7†	--	
			Hardness	0.37†	503†		
		SVM	Sweetness	0.43†	2.1†	--	
			Hardness	0.20†	553†		
Detection of black spots in potatoes	400 – 1000, 1000 – 2500 / --	PLS-DA			--	94.6%	(López-Maestresalas et al. 2016)
		SIMCA			--	72.4%	
Detection of colour and moisture content in soybeans	400 – 1000 / --	PLSR	Colour	0.86†	1.04†	--	(Huang et al. 2014a)
			Moisture content	0.97†	4.7%†		

Objective	Spectral range / Important wavelengths(nm)	Multivariate-data analysis*	Regression analysis			Classification accuracy	Reference(s)
			Regression coefficients		RMSE+		
Determining glucose, sucrose, soluble solid content, specific gravity and leaf count in potatoes	400 – 1000 / --	PLSR	Glucose	0.95†	3.12†	--	(Rady et al. 2014)
			Sucrose	0.81†	1.64†		
			Soluble solid	0.55†	1.18†		
			Specific gravity	0.61†	1.27†		
			Leaf count	0.95†	3.29†		
Early detection of mechanical stress on mango	600 – 1100 / 700 –780, 890 – 900, and 1070 –1080	Decision-trees		--	--	89 – 96%	(Rivera et al. 2014)
		k-NN		--	--	94 – 98%	
		LDA		--	--	89 – 98%	
Detecting bruises on the apple surface	400 – 1000, 1000 – 2500 / 760, 775, 817, 837, 969, 1017, 1074, 1093, 1188, 1200, 1219, 1263, 1270, 2426, 2432, 2438, 2444, 2450	LLR		--	--	97.7%	(Baranowski et al. 2013)
		BNN		--	--	89.9%	
		SVM		--	--	75.0%	
Detection of bruises on kiwifruit	600 – 1000 / --	PCA		--	--	83.6%	(Lü and Tang 2012)
Detection of bruises on strawberries	960 – 1700 / --	BR		--	--	97.67%	(Nanyam et al. 2012)
Detecting ripening in banana	400 – 1000 / 440, 525, 633, 672, 709, 760, 838, 888, 913, 925, 978, 984, and 1005	MLR	Moisture content	0.87†	--	--	(Rajkumar et al. 2012)
			Firmness	0.91†	--		
			Soluble solids	0.85†	--		

Objective	Spectral range / Important wavelengths(nm)	Multivariate-data analysis*	Regression analysis			Classification accuracy	Reference(s)
			Regression coefficients		RMSE+		
Classifying blueberry fruit and leaves	200 – 2500 / 233, 551, 553 554, 688, 691, 698, 699 and 1373	MLR			--	98 – 100%	(Yang et al. 2012)
		PCA			--	93 – 100%	
iii. Cereals							
Kernel wheat hardness estimation	900 – 1700 / --	ANN		0.94‡	5.38‡	--	(Erkinbaev et al. 2019)
		PCA		--	--		
		PLS		0.81‡	10.85‡		
Identification of maize seed variety	400 – 1000 / 437, 486, 510, 516, 700, and 897	BPNN		--	--	85.1%	(Wang et al. 2016)
		PCA		--	--	87.0%	
		SVM		--	--	91.7%	
Hardness and protein content prediction in wheat	960 – 1700 / --	PCR	Hardness	0.75‡	13.9‡	--	(Mahesh et al. 2015)
			Protein content	0.62‡	1.42‡		
		PLSR	Hardness	0.80‡	12.5‡	--	
			Protein content	0.68‡	1.33‡		
Fungal growth detection in brown rice	400 – 1000 / --	Unsupervised SOM		--	--	--	(Siripatrawan and Makino 2015)
		PLSR		0.97†	0.39†	--	
Discriminate the variety and quality of rice	310 – 1100 / 418, 452, 592, 613, 742, 783 and 965	BPNN		--	--	94.5%	(Wang et al. 2015)
		PCA		--	--	88.1%	

Objective	Spectral range / Important wavelengths(nm)	Multivariate-data analysis*	Regression analysis			Classification accuracy	Reference(s)
			Regression coefficients		RMSE+		
Pre-germination detection in wheat, barley and sorghum	1000 – 2500 / --	PCA		--	--	54%	(McGoverin et al. 2011)
		PLS-DA		--	--	81 – 85%	
iv. Nuts							
Determined kernel peroxide value (PV), nitrogen, and mineral nutrient concentration of nuts	400 – 1000 / --	PLSR	PV	0.81†	2.3†	--	(Bai et al. 2018)
			Nitrogen content	0.80†	1.58†		
			Minerals Fe, Mg, Mn, and S	0.5 – 0.76	0.94 – 2.06		
Classified internally damaged almond nuts	700 – 1400 / 925 and 945	BR		--	--	91.2%	(Nakariyakul and Casasent 2011)

*where, ANN: Artificial neural network, BPNN: Backpropagation neural network, BR: Band ratio, LLR: Linear logistic regression, LS-SVM: Least square support vector machine, LR: Linear regression, k-NN: Kernel-based neural network, MLR: Multinomial logistic regression, PCA: Principal component analysis, PCR: Principal component regression, PLS-DA: Partial least squares discriminant analysis, PLSR: Partial least square regression, RF: Random forest, SIMCA: Soft independent modelling of class analogy, SOM: Self organizing map, SPA-PLSR: Successive projection algorithm-partial least square regression and SVM: Support vector machine

+ Root mean square error

-- no information

‡ results obtained by cross-validation of a model on a complete data set

† results obtained by validating a model on a subset of data

• (Lightness, redness, yellowness)

———— solid line separates research studies

– – – – – – – separates data analysis techniques used within a study

— – — – — separates parameters analysed by a data analysis technique

Table 3.2. Research studies of HSI for monitoring the quality of processed foods

Objective	Spectral range / Important wavelengths (nm)	Multivariate-data analysis*	Regression analysis			Classification accuracy	Reference(s)
			Regression coefficient		RMSE+		
i. Processed meat							
Evaluating protein content of processed pork meats	400 – 1000 / 465, 474, 485, 496, 510, 522, 534, 546, 548, 562, 578, 586, 600, 608, 624, and 630	ANN		0.8318†	8.38†	--	(Ma et al. 2019)
		PLSR		0.7902†	9.48†	--	
Predicting iron content in sausages	405 – 970 / 405, 435, 450, 470, 570, 590, 645, 660, 780, and 870	Lib-SVM	Heme iron	0.880‡	0.158‡	--	(Ma et al. 2016)
			Non-Heme iron	0.879‡	0.316‡		
		PLSR	Heme iron	0.912‡	0.136‡	--	
			Non-Heme iron	0.901‡	0.281‡		
Predicting cooked beef tenderness	400 – 1000 / --	PCA		--	--	96.4%	(Naganathan et al. 2008)
ii. Dairy products							
Visualised and modelled the maturity of long-ripening hard cheeses	937 – 2542 / --	PCA & PLS		--	--	76%	(Priyashantha et al. 2020)
Determining starch content in cheese	200 – 1000 / 765, 874, 910, 948 and 997	PLSR		0.9915‡	0.3979‡	--	(Barreto et al. 2018)
Discriminating quality and origin of various milk powders	400 – 1000 / --	PCA		--	--	--	(Munir et al. 2018)
		PLSR	Dispersibility α	0.99†	--	79-87%	
			Dispersibility β	0.91†	--		
			Origin	0.96†	--		

Objective	Spectral range / Important wavelengths (nm)	Multivariate-data analysis*	Regression analysis			Classification accuracy	Reference(s)
			Regression coefficient		RMSE+		
Quantification of adulterants in milk powder (whey powder, starch, urea and melamine)	1285 – 2500 / --	MCR		--	< 5%	--	(Forchetti and Poppi 2017)
Melamine adulteration in milk powder	900 – 1700 / 1466 and 1490	BR		0.98†	--	--	(Huang et al. 2016b)
Penetration depth of spectra in milk powder	937 – 1654 / --	PLS-DA		--	--	>95%	(Huang et al. 2016a)
Detecting the amount of melamine in milk powders	900 – 1700 / --	EDA SAM SCM		--	--	--	(Fu et al. 2014)
Lactose, $ZnSO_4$, and melamine detection in milk powders	1000 – 2500 / --	PCA		--	--	--	(Huang et al. 2014b)
		PLSR	Lactose	86.03†	--	--	
			Melamine	60.2†			
Discriminating three different blue cheese samples	360 – 1000 / --	PLS-DA		--	--	66%, 100% & 72%	(Kulmyrzaev et al. 2008)
iii. Other food products							
Understand mixing kinetics of cornflour and icing sugar	880 – 1720 / --	PLSR		0.997†	1.26%†	--	(Achata et al. 2018)
Analysis of sucrose, caffeine and trigonelline in coffee beans	1000 – 2500 / --	PLSR	Sucrose	0.65†	0.7†	--	(Caporaso et al. 2018)
			Caffeine	0.85†	0.2†		
			Trigonelline	0.82†	0.1†		
Quality evaluation of dried banana slices, drying process monitoring and control	400 – 1000/ --	PLSR	Water content	0.97†	0.05†	--	(Nguyen-Do-Trong et al. 2018)
			Texture	0.66†	11.8†		

Objective	Spectral range / Important wavelengths (nm)	Multivariate-data analysis*	Regression analysis			Classification accuracy	Reference(s)
			Regression coefficient		RMSE+		
Adulterations in organic wheat flour	900 – 1700 / 1141, 1349, 1362, 1396, 1426, 1443, 1645 and 1658	PLSR	Common wheat flour	0.986†	0.026†	--	(Su and Sun 2017)
			Cassava flour	0.973†	0.036†		
			Corn flour	0.971†	0.038†		
Characterise consistency in coffee brand and roasting class	400 – 1000 / --	LDA	Dark roasted brands	--	--	98%	(Nansen et al. 2016)
			Lightly roasted brands	--	--	45 %	
		PLSR	Extractable protein content	0.76†	--	--	
Determination of surface browning and moisture content of cookies	400 – 1000 / 970, 1440 and 1930	FDA		--	--	100%	(Andresen et al. 2013)
		PLSR	Water content	--	0.22%†	--	

*where, BR: Band ratio, EDA: Euclidian distance measure, FDA: Factorial discriminant analysis, LDA: Linear Discriminant analysis, Lib-SVM, Libraries support vector machine, MCR: Multivariate curve resolution, PCA: Principal component analysis, PCR: Principal component regression, PLS-DA: Partial least square discriminant analysis, PLSR: Partial least square regression, SAM: Spectral angle measure, SCM: Spectral correlation measure, and SVM: Support vector machine

+ Root mean square error

-- no information

‡ results obtained by cross-validation of a model on a complete data set

† results obtained by validating a model on a subset of data

—————— separates research studies

– – – – – – – separates data analysis techniques used within a study

— – — – — separates parameters analysed by a data analysis technique

3.4.2 **Quality monitoring of processed foods**

Hyperspectral imaging has also been used for monitoring the quality of processed foods, though mainly at the laboratory scale, and lags behind quality monitoring of natural foods. In this study, the literature about HSI applications for quality monitoring of processed foods was divided into three product categories: processed meats, dairy products and others foods, listed in Table 3.2. For example, HSI was used to determine the protein content of processed meat (Ma et al. 2019) and iron contents in sausages (Ma et al. 2016). Nguyen-Do-Trong et al. (2018) used HSI for evaluating the quality of dried banana slices, Su and Sun (2017) detected adulteration in various edible flours using HSI, Munir et al. (2018) used HSI for discriminating various milk powders of different quality and of different origin, Fu et al. (2014) used HSI for detecting melamine in milk powder samples, Kulmyrzaev et al. (2008) used HSI to determine starch content in various types of cheese, and Nansen et al. (2016) used HSI to discriminate between different brands of coffee. These studies are shown in Table 3.2. The respective spectral ranges andmultivariate data analysis tools used for analysing the aforementioned processed food quality parameters are also listed in Table 3.2.

It is worth noting that the multivariate data analysis tools used for analysing the natural foods were relatively less complex than those tools used for analysing the processed foods. This observation may be because HSI is mainly used as a quality monitoring and decision-making tool for natural foods, which does not require advanced machine learning and data mining algorithms. On the other hand, advanced machine learning and data mining algorithms were required for the quality monitoring of processed foods because of the complex relation between their processing and quality attributes. For processed foods, different complex regression methods have been reported. For example,

El Jabri et al. (2019) used Bayesian regression model for predicting cheese quality, and employed nonlinear regression models for predicting meat quality (Pan et al. 2016). However, these regression models are difficult to implement in an online fashion.

3.5. Research gaps and potential opportunities

After reviewing the recent literature about applications of HSI for testing the product quality of natural and processed foods, four major research gaps (subsections 3.5.1 - 3.5.4) were identified, which require attention for the online application of HSI to test quality and achieve quality testing and control in real-time − especially for processed foods (e.g. milk powder).

3.5.1 **Applications of HSI in processed foods lags behind natural foods**

From the summary shown in Section 3.4, it is evident that the applications of HSI in processed foods lags behind natural foods. This trend may be because the machine vision route for quality testing of natural foods is more reproducible, reliable, customer-focused, non-invasive and requires limited, or no processing (García-Cañas et al. 2012). In fact, HSI can act as machine vision for quality testing and grading of natural foods and can replace existing manual, sensory, or quality tests.

The applications of HSI for quality testing of processed foods can be enhanced by using HSI as a quality monitoring tool instead of using conventional manual quality testing due to the additional advantages of machine vision in that they are less time consuming, non-invasive, and have less variability of results. More studies are required on the evaluation of HSI as a process analyser coupled with predictive multivariate regression models to test the product quality of processed foods.

3.5.2 **HSI is mostly used as a stand-alone machine vision tool, and real-time quality control is mostly neglected**

As shown in Section 3.4, most of the HSI applications found in the public domain literature about natural foods in general and processed food in particular reported HSI as a stand-alone machine vision method for off-line quality testing, and lack on-line applications for quality testing required to achieve control in real-time. However, various commercial companies have claimed the success of on-line applications of HSI for quality testing − especially for natural foods (Bannon 2009). On the other hand, it was hard to find a claim in literature or by commercial companies regarding the success of on-line quality testing using HSI for processed foods. This observation may be because unlike processed food, there is not much room for linking machine vision with the process because limited or no processing is involved for most of the natural foods.

For achieving quality testing and control in real-time, HSI needs to be applied online − not as an off-line machine vision tool for quality testing. Especially for processed foods, there is much room for on-line quality control in real-time because more processing is involved in transforming raw food materials into value-added processed foods for various quality objectives, such as extended shelf life, better taste, or ease of transportation.

For achieving real-time quality control, HSI needs to be linked with the product quality and controllable process variables through multivariate data models. A limited number of wavelengths at which product quality differences are more obvious need to be identified and used during data processing. It is worth mentioning that for product quality monitoring using HSI, either the full spectral range or a particular segment of the spectrum like infrared (IR), ultraviolet (UV), or visible ranges can be used because, in some cases, selected wavelengths from the spectrum show more discrimination between

product samples than using a full-range spectrum. The selected spectral range (e.g. infrared) data can also be processed faster because of the smaller data volume. Various techniques such as the grey-level co-occurrence matrix (GLCM) can be employed for selecting desired regions of the spectrum. The GLCM technique is an image-processing technique first described in Haralick et al. (1973), and is designed to extract certain information from grey-scale images, which can then be used to classify them.

Furthermore, faster data analytical tools and algorithms need to be developed and used for the faster processing of HSI data required for its online application. There are only a limited number of studies that have highlighted the requirements for more accurate and efficient HSI algorithms; these requirements are to shorten the time for image acquisition and data pre-processing to enable real-time HSI quality monitoring.

3.5.3 **Applications of HSI have rarely reported on generalised design choices**

Another research gap identified in Section 3.4 was limited information about the selection of generalised design choices (e.g. choices for data pre-processing and multivariate data analysis tools) which are required for quality testing of natural or processed food using HSI. The design choices include options for data pre-processing and multivariate data analysis tools because product quality testing can have different qualitative or quantitative results for different pre-processing and multivariate data analysis tools. It is worth mentioning that multiple steps are involved in data pre-processing and multivariate data analysis, and various tools are available for each step and task. These are design choices, and generalised design choices can help the experimenter, who has limited guidance on choosing suitable data pre-processing and multivariate data analysis tools required for spectral data.

For example, data cleaning within data pre-processing has several steps such as region of interest (ROI) selection, and identifying and removing dead pixels, spikes, and outliers (Zhang and Henson 2007). Various techniques for each of these pre-processing steps are available in the literature. For example, a ROI is selected manually, or using histograms (Vidal and Amigo 2012). In many cases, a random selection of pixels, or pixel selection near the centre of the image, can be appropriate for further analysis. Similarly, several techniques have been used for locating and removing dead pixels such as thresholding from median spectra, and the minimum volume ellipsoid (MVE) (Burger and Geladi 2005). Manual supervision, nearest neighboring pixel comparison (Zhang and Henson 2007), median filtering (Behrend et al. 2002), wavelets (Cannistraci et al. 2009), and Fourier analysis (Feuerstein et al. 2009) are all commonly used techniques to identify and remove spikes and outliers.

Similarly, spectral pre-processing is the next step of data pre-processing which includes data normalisation, de-noising, smoothing, filtering, and taking derivatives of the spectra. Several algorithms, such as standard normal variate (SNV), and grey-level co-occurrence matrix (GLCM) selection can be used for spectral pre-processing (Rinnan et al. 2009). Various smoothing schemes such as locally estimated scatterplot smoothing (LOESS) (Cleveland et al. 1988), splines (Reinsch 1967), Savitzky-Golay filters (Savitzky and Golay 1964), and Whittaker filters (Whittaker 1922) can be used for spectral smoothing. The choice of smoothing scheme can be critical for subsequent data analysis, as each scheme has a different performance related to its strengths and weaknesses.

In some cases, spectral derivatives (1^{st} order, 2^{nd} order) are also used when building multivariate data analysis models, such as Principal Component Analysis (PCA) and Partial Least Squares (PLS) regression, because derivatives can enhance spectral features

by removing additive and multiplicative effects in the spectrum. However, derivatives of a noisy spectrum as is the case of HSI can also deteriorate spectral features by enhancing data noise. In other words, a derivative action is opposite to data smoothing.

In addition, multivariate data analysis involves multiple steps and has different tools, as shown in Table 3.1 & Table 3.2. For example, PCA and PLS regression are most commonly applied to find differences and make predictions (Gowen et al. 2007). Furthermore, decision trees (Kong et al. 2013), discriminant analysis (Kamruzzaman et al. 2011), neural networks (ElMasry et al. 2009), and support vector machines (Pierna et al. 2004) are some of the other multivariate data analysis tools that have been reported in the literature.

Therefore, there is a need for an optimised formulation of generalised design choices for quality monitoring using HSI. An optimised formulation of design choices includes: tuned spectra subsampling for plotting a significant number of spectra, spectral region selection for multivariate data analysis, the appropriate level of data smoothing to observe discrimination between products of different quality, a suitable order of spectral derivatives (first two derivatives computed using finite differences) to enhance spectral features, and the choice of appropriate, subsequent multivariate analysis techniques to see the differences between products and predictions. For this objective, more studies are required to develop an overview and illustrate design choices for various products. Furthermore, algorithms need to be developed for automatic selection of suitable design choices for a given product, and the effects of various design choices on quality testing by HSI need to be quantified.

3.5.4 **Limited industrial applications of HSI especially for processed foods**

It is also worth noting from Section 3.4 that despite the significant claims that have surfaced for the implementation of HSI in the field of natural foods, the industrial application of HSI is rarely found in literature. However, a few case studies on HSI applications in natural foods have been reported. For example, Compac owned by TOMRA has used HSI commercially for apple and kiwifruit sorting and grading in New Zealand, and Headwall Photonics USA has used HSI for almond and fruit grading. However, most of the published literature reports that HSI has mainly been used at the laboratory scale for quality monitoring of processed foods, and industrial applications of HSI were rarely found. There are significant reasons for this: the complex nature of data and its analysis associated with HSI, traditional testing facilities and methods for calibrating data, limited desktop and industrial computing capabilities, and challenges associated with HSI integration with in-line, or online control practice in the processed food industry.

It is worth mentioning that the industrial application of HSI is challenging because its analysis can be affected by various external factors in industrial settings such as ambient light, sample collection, and preparation. For a ‘successful’ industrial application of HSI, it is critical to understand the effect of various external factors on the HSI analysis, calibrate the HSI instrument in an industrial setting, cover the HSI instrument with a black box to minimise ambient light effects on analysis, and to fix sample size, orientation, and frequency for each product (Kandelbauer et al. 2012). Tatzer et al. (2005) have presented a balanced approach for the robust and suitable application of HSI in industrial settings, where time required for the data processing and classification was calculated.

Though the high cost of HSI instrumentation may act as a barrier to its industrial utilisation, the value of HSI may soon be recognised (Amigo et al. 2013). However, in order to explore the full potential of this technique, comprehensive research and development is required.

For the successful industrial application of HSI, especially for processed foods, various steps are required. For example, the performance and economic potential of HSI as compared to conventional quality tests need to be studied and reported. Furthermore, initiatives from standards organisations such as the U.S. Food and Drug Administration (FDA) are required for achieving the real-time quality of processed foods using HSI. More detailed feasibility studies at the lab and pilot plant scales and validation of the practicability, performance, and precision of multivariate data analysis techniques in industrial scenarios can also contribute to the development of successful industrial applications of HSI. Future developments in HSI systems, such as efficient cameras, faster computing hardware, and more accurate and efficient algorithms, can all help to reduce the time for image acquisition and data pre-processing to encourage industrial applications of HSI for quality monitoring.

3.6. Implementing HSI for online quality control of processed foods: Milk powder processing as a case study

Like other processed foods, the application of HSI for product quality testing of milk powder also lags behind natural foods at the lab or industrial scale. This observation may be because milk powder quality is complex and is measured in terms of various interlinked variables such as texture, appearance, colour, taste, and dissolution properties. Furthermore, milk powder is produced after complex processing and involves various sensitive variables which can change milk powder quality.

The online quality control of milk powder using HSI has two main aspects:

i) implementing HSI as a machine vision technique for milk powder quality testing, and ii) linking product quality tested by HSI with milk powder process variables which are controllable by process control.

3.6.1 **Milk powder process description**

Liquid milk is converted into milk powder after processing through various unit operations to increase its shelf life, provide ease of transport, and enhance storage capacity.

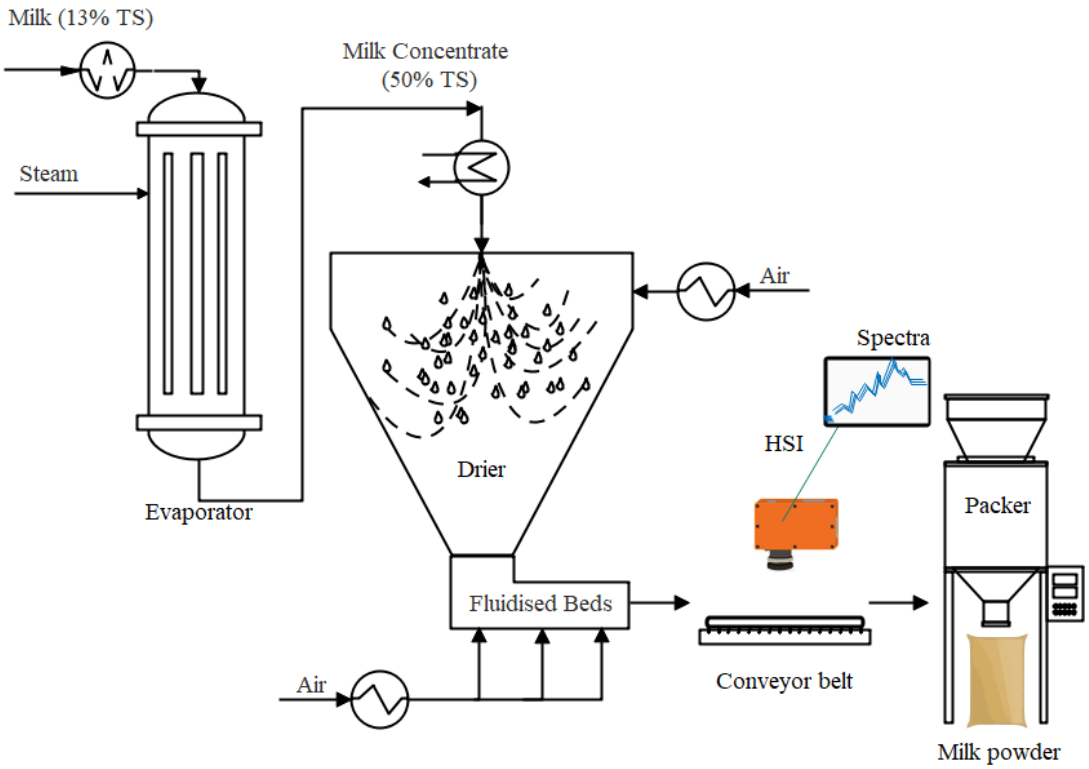

Figure 3.1. Milk powder production process schematic adapted from Bylund (2003), and proposed hyperspectral imaging location

After initial receipt and storage, pasteurisation, centrifuging, standardisation and preheating, milk is passed through evaporators to concentrate milk from approximately 13 weight percent (wt. %) to approximately 50 wt. % total solids under vacuum at

temperatures between 40–70 °C, Figure 3.1. The concentrated milk from the evaporator is spray dried in the dryer where hot air contacts with milk droplets, to further dry them, and make milk powder. Moist milk powder is passed through fluidised beds to attain dried milk powder which is then sent to the packer (Bylund 2003).

3.6.2 **HSI as a machine vision tool**

An HSI instrument can be installed after fluidised beds around the conveyor belt to scan milk powder product and obtain HSI data. The objective of this installation is to discriminate between different milk powders of various qualities and variety. It is worth noting here that HSI can discriminate milk powders of different qualities and origins. The results from (Munir et al. 2018) show HSI can potentially be used to replace existing off-line, manual, sensory testing of milk powder quality, origin and appearance. Fu et al. (2014) used HSI to detect melamine in milk powders and Forchetti and Poppi (2017) used HSI to quantify melamine, urea, whey powder and starch adulteration in milk powder. Huang et al. (2014b) also predicted the $ZnSO_4$ and lactose contents as well as melamine adulteration in milk powder samples. Furthermore, the same group extended their research findings to quantitatively analyse melamine detection on selective wavelengths by band ratio (Huang et al. 2016b) and estimated penetration depth of NIR light of HSI equipment for milk powder samples (Huang et al. 2016a). The speed of milk powder discrimination can be increased by identifying critical wavelengths at which differences between ‘good’ and ‘poor’ quality powders are obvious because analysing hyperspectral data at selected wavelengths has a reduced computation load and the results can be processed faster. Furthermore, milk powder discrimination at a faster pace is also required for transforming HSI data to calibration models, and selection of suitable design choices, as discussed in Section 3.5.3.

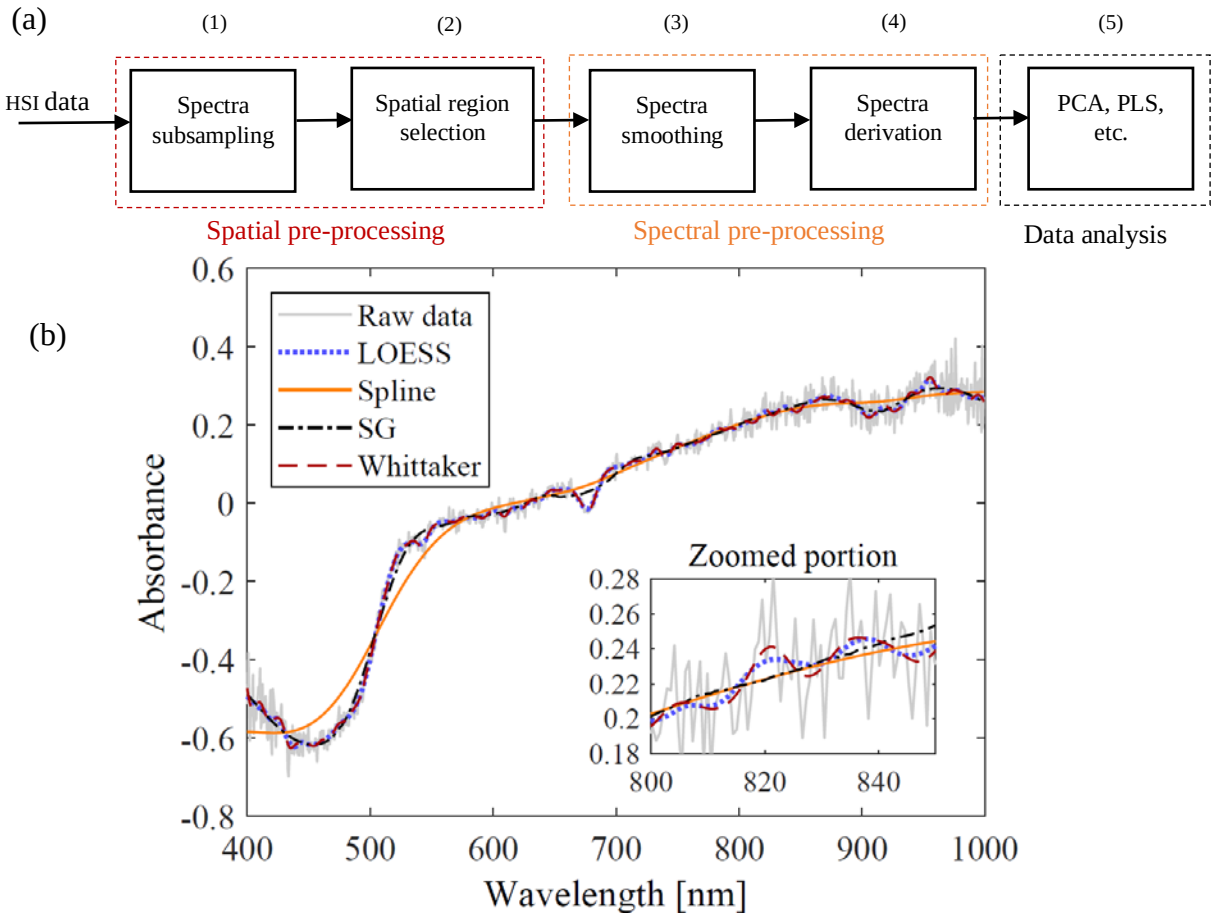

Figure 3.2. (a) Data pre-processing steps (e.g.(Munir et al. 2018)) (b) Comparing LOESS, spline, SG, and Whittaker smoothing schemes (This work)

The transformation of HSI data to calibration models is divided into five major steps as presented in Figure 3.2 (a) (also discussed in Section 3.5.3). Figure 3.2 (a) presents an overview of the HSI data pre-processing major steps and subsequent data analysis techniques. These five steps are design choices, and a generalised, optimal approach is required for suitable design choices that the experimenter must use (also discussed in Section 3.5.3). For example, the number of spectra to plot, which spectral region (UV, IR, or visible) to keep, the degree of smoothing and the smoothing technique to use, what order of derivation to be used, which multivariate data analysis technique to be used (PCA, PLS, or others), and what number of principal components to retain (in the case of PCA) are all factors the experimentor must consider.

Spectral smoothing is one of the main design choices required for milk powder quality testing using HSI. Figure 3.2 (b) shows a comparison of spectrum smoothing by various smoothing techniques such as LOESS, spline, SG, and Whittaker filtering. The outcome of each smoothing technique is a unique smooth spectrum, which can significantly affect subsequent multivariate data analysis results. For milk powder quality testing, Munir et al. (2018) reported on suitable design choices after testing and quantifying the effects of various design choices on quality testing by HSI. The 'clean' pre-processed data should have an understandable format and be suitable for input into multivariate data analysis models for further processing. Improper selection or application of data pre-processing technique can cause loss of important information or introduce new artefacts and noise. The choice of multivariate data analysis tools and specific details of each tool are important. For example, PCA can be used to show discrimination between various milk powders and specific principal components (PC_1, PC_2 or higher) can be selected which show more obvious discrimination (Munir et al. 2018). Similarly, a variety of multivariate data analysis tools and the specific details of each tool have been used and documented in the literature (Esbensen et al. 2002). Simple algorithms based upon linear regression to the complex versions that can deal with data mining and involve training of models (e.g. ANN, BPNN, and SIMCA) have been reported in the literature. For example, the prediction of a chemical adulterant or nutrient in milk has been linearly correlated with its spectra (Jawaid et al. 2013), and texture analysis of puffed snacks has been non-linearly correlated with its freshness using ANN (Sanahuja et al. 2018).

Standalone, off-line HSI for quality monitoring of milk powder cannot achieve online quality control because the machine vision, in this case, is not connected with the milk powder process variables. As milk powder quality is not linked with the process variables

in a standalone, offline monitoring system, it is thus difficult to control milk powder quality in real-time.

3.6.3 **Linking HSI with process variables for online quality control**

Milk powder quality tested by HSI needs to be linked with milk powder process variables which are controllable by process control to achieve online quality control. For example, milk powder quality is dictated by its physical and functional properties. The particle size distribution of milk powder is one of the main factors that affects the physical and functional properties of milk powder. Milk powder with less fine particles has better functional properties in terms of its dissolution characteristics. It is worth noting that milk powder particle size is linked to process conditions and understanding of these links is critical for achieving online quality control. For example, milk powder particle size is controlled by the viscosity of the milk-concentrate stream which is controlled by its temperature. At higher temperatures, the viscosity of the milk-concentrate stream is lower and produces smaller milk droplets in the dryer, which results in finer particles (Sharma et al. 2012). On the other hand, a lower temperature of the milk-concentrate stream increases its viscosity which results in larger droplets of milk and thus particles with higher coarseness. Multivariate interactions between milk powder particle size and milk-concentrate stream viscosity, temperature, and other critical process or design parameters need to be evaluated. Understanding these multivariate interactions can subsequently be used for controlling milk powder particle size in real-time, and the resulting milk powder properties could be linked with HSI data, Figure 3.1. Following this strategy, using HSI as machine vision can be proposed to link with the milk powder process variables and can be used to achieve online quality control by controlling process variables linked with milk powder quality.

3.7. Conclusions

Product quality is a direct result of operating conditions on a product throughout its processing. In the views expressed in current literature and existing thoughts around process control and operations, it is clear that there is potential for the application of HSI technology with existing processes and their control architectures − especially for processed foods. The streamlining of HSI algorithms will provide product quality information at a rate that is appropriate for process control implementation, and continued study of these integrations, whether at the pilot or industrial scale, will allow for growth in the body of knowledge about design choices surrounding relevant calibration and processing of HSI data, and therefore the optimal integration of said data into feedback control loops. With an example focussing on possible applications in the dairy industry, the study of off-line use of HSI as a machine vision tool in other areas of application shows, by the same token, that with more research into this still-emerging field, real-time quality control in many industries is a likely future possibility.

3.8. Summary

This chapter introduced HSI to the reader as an alternative technique for the quality monitoring of a diverse range of food products. Limitations currently preventing successful implementation of these HSI applications at the industrial scale were highlighted. Furthermore, the possibility of an HSI based quality monitoring route for milk powder at the production facility was presented.

Chapter 4. Using Hyperspectral imaging for predicting milk powder particle size fractions, dispersibility and bulk density

4.1. Preface

The potential of hyperspectral imaging (HSI) to predict the physical and functional properties of milk powder is explored in this chapter. Instant whole milk powder reconstructed samples were prepared by recombining the coarse, medium and fine particle fractions as adopted in Chapter 2. Moreover, HSI data cubes were produced for samples of individual particle size fractions and reconstructed samples. The importance of HSI data pre-treatment was already highlighted in Section 3.6. Therefore, an appropriate pre-treatment routine was identified by preliminary analysis reported in the Appendix A-1. These results suggested that the smoothing of HSI spectral data might improve the discrimination between milk powder spectra and support hypothesis III, presented in Chapter 1. Therefore, a suitable degree of smoothing was performed prior to spectral data analysis.

Afterward, it was observed that HSI spectral data of coarse, medium and fine particle fractions could be differentiated from each other. The average spectrum of each of coarse, medium and fine particle fractions was then calculated.

The ability of HSI to record spectral information along the spatial coordinates of the milk powder samples was helpful in order to estimate the distribution of individual particle size fractions in a reconstructed milk powder sample. The similarity of spectra from multiple spatial locations to the average spectra of individual particle size fractions has been used to predict their ratio in a reconstructed sample. Furthermore, dispersibility and bulk density of the reconstructed samples have been correlated with the relevant HSI data cubes as well.

Stepwise calculation of the important model/s parameters is available in the Appendix (A-2, A-3 and A-4).

This part of the work has been submitted to the Journal of Food Measurements.

4.2. Abstract

Milk powder quality is measured in terms of its dissolution properties, and in recent literature, powder particle size was hypothesised as one of the main variables that controls powder quality. This article reports upon a study carried out to evaluate the potential of hyperspectral imaging (HSI) analyser with spectral range of 400 nm -1000 nm for predicting milk powder quality and milk powder particle size analysis. As an initial step of this analytical method, HSI and Principal Component Analysis (PCA) were used to discriminate milk powder samples based on their different particle sizes. The PCA results showed that HSI can distinguish milk powder samples of different particle sizes. In a subsequent step, Partial Least Squares (PLS) regression was employed to predict the milk powder particle size fractions, physical property (bulk density) and functional property (dispersibility). The PLS results showed that one can also predict milk powder particle sizes using hyperspectral images. Comparing various pixel spectra of the samples with the spectra of individual size fractions of milk powders has enabled the prediction of the ratio of these fractions in the sample. The findings of this study may potentially be used to implement HSI for at-line milk powder testing in the near future after linking it with the milk powder production process.

Keywords: Hyperspectral imaging (HSI), milk powders, particle size, multivariate data analysis

4.3. Introduction

Liquid milk is transformed into milk powder to reduce its transportation costs (i.e. by reducing the milk solids' volume to be transported), and increase shelf-life. Milk powders have a wide range of applications in the food industry such as their use in dairy beverages, confectionaries, cheeses, yoghurts, and animal foods (Bhandari et al. 2013). A good quality milk powder with desired physical and functional properties behaves well for the customer and has attractive reconstitution properties. Achieving good quality performance of a milk powder for a variety of applications is challenging because milk powder quality is measured by a complex combination of physical and functional properties (Oldfield and Singh 2005).

Various physical and functional properties such as powder particle size distribution, appearance or structure, particle density, bulk density, flowability, stickiness, heat stability, scorched particles, caking, hygroscopicity, and rehydration or reconstitution properties all play a crucial role in determining milk powder quality (Sharma et al. 2012). Reconstitution properties are measured in terms of powder wettability, sinkability, dispersibility, and solubility. These are important for instant whole milk powder in particular (Crowley et al. 2015). These physical and functional properties are highly associated with each other. For example, particle size distribution affects the physical and functional properties of milk powder (Boiarkina et al. 2017). Achieving the desired physical and functional properties of milk powder for each batch is essential for customer satisfaction and economic benefits.

It is worth noting that the physical and functional properties of milk powder are dependent on various input variables before, during, and after milk powder production (Rimpiläinen et al. 2015). After collecting liquid milk from multiple farms, milk is standardised, pasteurised, evaporated and dried to produce milk powder during the milk powder production process (Kelly et al. 2003). Milk powder quality, in terms of it's physical and functional properties,

is mostly tested manually by sampling the final product after production using standard quality tests recommended by the International Dairy Federation (IDF).

However, these offline quality tests, also called *a posteriori* approach, are usually time-consuming, invasive, have natural variability, are only discrete, and struggle to describe quality attributes in terms of quantified numeric descriptions. Another major drawback of *a posteriori* testing approach is that an out-of-specification production batch is identified sometime after production (Munir et al. 2018). This approach can result in product recall, and significant economic losses because the out-of-specification product is usually downgraded or disposed of.

Replacing existing offline quality tests by machine vision for quality tests may minimise some of the challenges associated with offline quality tests (Dufour 2011). For achieving this goal, various machine vision options such as HSI need to be tested for milk powder quality testing. Hyperspectral imaging produces information-rich data, has advantages of spatial imaging and spectroscopy, and is non-invasive. Furthermore, it has the potential to be implemented for at-line/online milk powder quality prediction in the near future after linking HSI with the milk powder production process through predictive multivariate regression models such as principal component analysis (PCA), and partial least squares regression (PLS). This strategy may potentially be used to control milk powder product quality in real-time without off-line sensory quality tests. More detail regarding HSI is given in Amigo et al. (2013).

The main purpose of hyperspectral data analysis is to reduce the dimensionality and retain useful data for discrimination or qualitative analysis. Hyperspectral data requires data pre-processing before building multivariate data analysis models. These pre-processing steps have various impacts on spectra but the main reason for their use is to eliminate the scattering

effect and unwanted spectral variability (Gowen et al. 2007). Various data pre-processing techniques such as standard normal variate (SNV) smoothing (Barnes et al. 1989), multiplicative scattering correction (MSC) (Isaksson and Næs 1988), Whittaker weighted kernel smoother (Whittaker 1922), and the Savitzky-Golay (SG) smoother (Savitzky and Golay 1964) have been reported in literature. For baseline correction and scaling of the spectra, SNV and MSC have been reported (Huang et al. 2015). Similarly, the Savitzky-Golay filter is the classic and popular smoother that has been reported for spectral smoothing (Savitzky and Golay 1964).

Previously, various multivariate data analysis techniques such as PCA, PLS, band ratio and multivariate curve resolution (MCR) have been used in the dairy industry for discrimination of products, and predictions of quality. For example, Munir et al. (2018) used PCA and PLS to discriminate between various types of milk powders and for predicting milk powder quality, Huang et al. (2016b) employed band ratio for quantitative analysis of melamine in milk powders, and Lachenmeier and Kessler (2008) used MCR for the determination of artificial food colours. These stated evidence as well as other evidence found in published literature has established an understanding that HSI can act as a machine vision tool for quality testing and grading of various food products and can replace existing manual, sensory testing or quality tests (Dale et al. 2013, Reis et al. 2018, Wang et al. 2015). A combination of recording spectral data along with the spatial information of a sample simultaneously makes HSI a suitable choice for various applications. Its other advantages are no sample preparation/pre-treatment required, it is non-invasive, and it has the ability to extract information rich data from the sample. However, advanced data analysis tools, the latest computing machines and/or leading-edge cameras & spectrograph hardware improvements need to be explored to realise its full potential for online/at-line quality testing and incorporating it into a control scheme.

It is worth mentioning that HSI with multivariate data analysis techniques was previously proposed to discriminate various milk powders based on their quality which is dependent on various physical and functional properties such as powder particle size (Gowen et al. 2011). However, this has not been fully tested yet. The hypothesis of this study was that powder particle size mainly influences milk powder quality. Instant whole milk powder size has been reported as a potential proxy to measure complex offline quality parameters (Boiarkina et al. 2017). Furthermore, Blanco and Peguero (2008) performed the near-infrared spectral analysis of various pharmaceutical powders with size variation and concluded that PLS regression was effective and accurate for the prediction of particle size distributions identical to that obtained by sieving. Therefore, in this paper, we are examining the potential of HSI to discriminate milk powders based on their particle size and their quality.

The objective of this study was to assess the potential of HSI to discriminate various size fractions of milk powder and predict the powder particle size fractions using their hyperspectral images. To achieve this objective, milk powder was segregated according to the size of particles present in it, PCA was used to discriminate between the various size fractions, and PLS was used to predict the particle size fractions using their hyperspectral images. The effects of data pre-processing such as spectra smoothing, was also studied to evaluate the robustness of the regression models. Moreover, these samples of individual particle size fractions were used in the prediction of particle size distribution in the reconstructed samples (details given in section 4.4.1). Both actual particle size distribution and predicted particle size distribution of milk powder reconstructed samples were compared to quantify the performance of the prediction model itself.

4.4. Materials and methods

4.4.1 **Milk powder samples**

Instant whole milk powder was obtained from a local supermarket, and was segregated into three commercially relevant size fractions: coarse (denoted by 'C', and with particle size range >355 µm), medium (denoted by 'M', and with particle size range 180 –355 µm), and fine (denoted by 'F', and with particle size range <180 µm). These particle size fractions of the milk powder were made using a sieve shaker (as described in section 2.2). Instant milk powder with particles in size range 180 – 355 µm is assumed to exhibit desirable functional characteristics (Písecký 2012). Therefore, milk particles either smaller than 180 µm or larger than 355 µm were minimised in the composition in the commercial grade milk powder. After segregating milk powder into three main size fractions, these fractions were recombined in different mass ratios to prepare seven reconstructed samples as shown in Table 4.1.

Table 4.1. Composition of reconstructed samples and their respective quality (dispersibility) and bulk density data

Size fractions	Reconstructed milk powder samples						
	Sample 1	Sample 2	Sample 3	Sample 4	Sample 5	Sample 6	Sample 7
Coarse (mass %)	10	10	25	10	17.5	17.5	15
Medium (mass %)	65	80	65	72.5	65	72.5	70
Fine (mass %)	25	10	10	17.5	17.5	10	15
Total (unit)	100	100	100	100	100	100	100
	Functional results						
Dispersibility	0.74 ± 0.22	1.76 ± 0.12	1.41 ± 0.18	0.97 ± 0.08	0.82 ± 0.08	1.24 ± 0.16	1.08 ± 0.07
Bulk density (g/cm^3)	0.44 ± 0.01	0.53 ± 0.01	0.59 ± 0.01	0.42± 0.01	0.46 ± 0.01	0.54 ± 0.01	0.50± 0.01

The simplex centroid design method was used to obtain the composition of these reconstructed samples (Eriksson et al. 1998). The boundaries of each individual fractions' compositions were carefully selected so that it could cover the minimum to a maximum

range of an individual size fraction seen in the commercially available milk powder. Detail regarding dispersibility and bulk density of the milk powder samples are given in section 4.4.4.

A total of nine replicated were acquired from different batches of milk powder for each of the fine, medium and coarse fractions for HSI analysis. Thus, there were a total 27 images for three individual size fractions. Reconstructed milk powder samples were also produced from fine, medium and coarse fractions of these nine different bacthes. The hyperspectral images of reconstructed milk powder samples were used in the predictive model to estimate particle size fraction distribution, bulk density and dispersibility of these samples.

4.4.2 **Particle size segregation and particle size analysis**

In this study, sieving was used for the particle size segregation into the three size fractions (coarse, medium and fine). For this objective, a Retsch AS200–vibratory sieve shaker was used for 30 min with two sieves of 180 and 355 µm aperture sieves to separate 100 g of milk powder in each run. As a result, approximately 3 kg of milk powder from each batch was segregated into three size fractions: particle size range greater than 355 µm (coarse (C), approximately 250 g), particle size range 180–355 µm (medium (M), approximately 2050 g), and particle size range less than 180 µm (fine (F), approximately 700 g).

Reconstructed samples of milk powders were produced by recombining the above stated fractions. However, to verify or quantify particle size distribution within these samples, the Malvern Mastersizer 2000 was employed. The Mastersizer is capable of measuring dry particle size distribution using laser diffraction. During Mastersizer operation, approximately 30 g of milk powder was dispersed through a dry dispersion system. Metallic ball bearing at the inlet were removed to avoid particle breakdown. Settings of 0.1 bar feed

pressure, laser obscuration of 1–5 %, sample measurement time of 20 s, and refractive index of 1.46 with no absorption were used in this study (Boiarkina et al. 2016).

4.4.3 **Hyperspectral imaging experimental set-up**

In this study, a Headwall Photonics Hyperspec™ hyperspectral camera with visible and near-infrared spectral range (400–1000 nm), also called VNIR, was used for experiments.

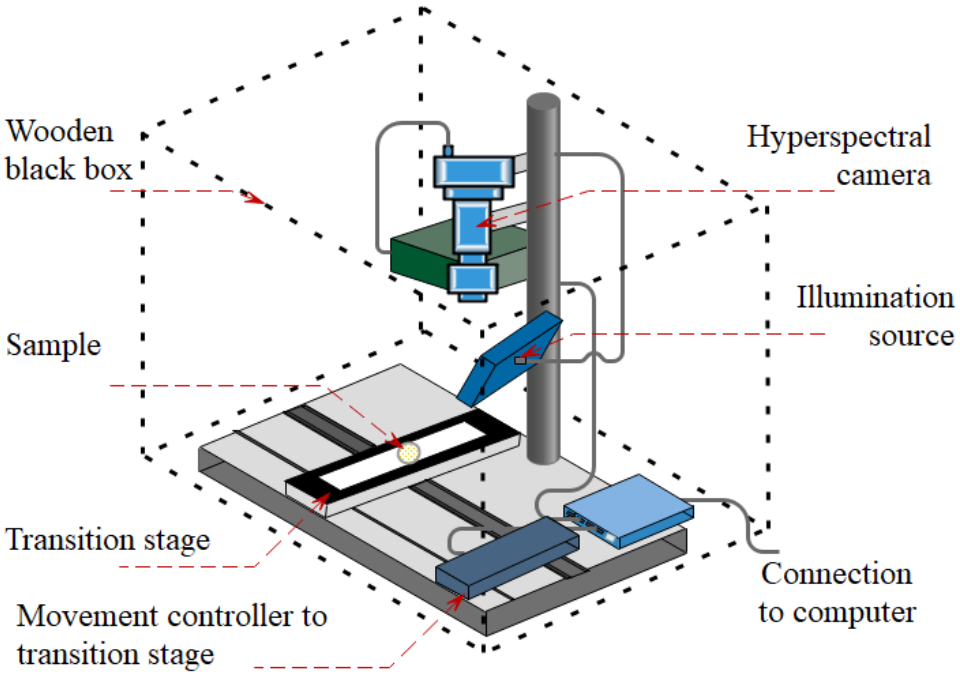

Figure 4.1. A schematic of the hyperspectral imaging set-up

Figure 4.1 shows the experimental set-up and experimental procedure used in this study for scanning the milk powder samples using a HSI camera. The HSI experimental set-up has four main parts: the transition stage, the lamp or light source, the hyperspectral camera (Schneider-Kreuznach Xenoplan 1.4/23), and the spectrograph. Each sample of milk powder was transferred into a small, quartz petri dish (30 × 15 mm), and placed on the moveable transition stage for scanning. The lamp or LED light source mounted directly above the transition stage illuminates the milk powder sample uniformly. The camera mounted above the transition stage and in parallel with the lamp captures images at various wavelengths

(933 equally spaced wavelengths) within the 400 – 1000 nm range. The spectrograph mounted with the camera records spectra at the level of each pixel and produces a 3D (2 spatial and 1 spectral dimension) hypercube to be used for subsequent data analysis. It is worth mentioning that before milk powder scans, the HSI experimental set-up was covered with a black box to avoid ambient light effects which can have significant effects on HSI analysis.

The HSI instrument was calibrated before hyperspectral scans to minimise the effects of various reflectance and spatial issues associated with the instrument. For example, reflectance calibration was carried out following a standard procedure recommended by the literature to deal with a dark camera response caused by a dark current and a white background spectral response of the instrument, also called bright response (Amigo et al. 2015). The dark camera response (*D*) was obtained by recording an HSI scan without any sample while covering the camera lens and without a light source. The bright response (*W*) was obtained by scanning a uniform high reflectance tile which reflects 99 % light without any sample. The lighting source was on during the bright response measurement. After the dark camera and bright response measurement, the corrected reflected value of an image (*I*) was calculated using the following formula given by Gowen et al. (2007).

$$I = \frac{I_{sample} - D}{W - D} \quad \textbf{(4.1)}$$

Where

$I =$ Corrected image reflectance

$I_{sample} =$ Actual image reflectance recorded by the camera

$D =$ Dark response

$W =$ Bright response

Repeatability and reproducibility of the instrument was also tested before experiments by scanning a single sample multiple times and no significant variation in spectral data was observed.

4.4.4 **Milk powder functional properties**

i. Dispersibility

The New Zealand Dairy Board dispersibility test (NZDB-method) was adopted for dispersibility measurements (Písecký 2012), where the percentage of undissolved dry mass of milk powder retained at 300μm mesh was recorded for a specific stirring speed and dispersion time. The dispersibility value was estimated as the inverse of the percentage of the undissolved dry mass of the milk powder. The main purpose of this test was to categorise the reconstructed samples in terms of a commonly used quality parameter in the New Zealand milk powder production industry.

ii. Bulk density

International Dairy Federation (IDF) Standard 134A was followed in this study as it is a widely accepted test for the bulk density measurement of milk powder (IDF 2005). A quantachrome autotap density analyser with 250 cm^3 volumetric cylinder was used to measure bulk density. The bulk density of all the samples was recorded for 625 tappings with ± 0.01 g/cm^3 repeatability.

4.4.5 **Multivariate data analysis**

After each HSI scan, a significantly large amount (20,000 spectra) of hyperspectral data was generated. Processing such a large volume of data for developing multivariate regression and prediction models was challenging. Furthermore, hyperspectral data in its original form had irregular spatial orientation and image dimensions due to manual sample placement on the transition stage; had spectral noise along spectra, possibly due to calibration and ambient

environment settings; and diminishing spectral features, possibly due to insufficient camera resolution.

Spatial image orientation and its dimensions must be consistent for each HSI scan to be comparable with other HSI scans. Furthermore, the raw HSI data needs to be subsampled to 2000 spectra for a manageable data volume (approximately $1/10^{th}$ of original 20,000 spectra), spectral data needs smoothing to minimise external noise effects on the multivariate analysis, and spectral differentiation may be used to enhance spectral features required to observe differences between samples. In order to reduce unwanted artefacts and noise from the spectra, smoothing was performed.

For example, the region of interest (ROI) from the middle portion of each scan was selected. To avoid irregular spatial orientation and image dimensions, the hyperspectral data from the already selected ROI was further subsampled randomly (2000) spectra to generate manageable data volumes for subsequent analysis. Spectral noise was filtered using the SNV smoother. Smoothing was performed by the Matlab function `smoothn` Garcia (2010). This method of smoothing is preferred for accommodating n-dimensional data. Suitable smoothing results were obtained by a similar pre-processing approach in the work of Munir et al. (2018).

In this study, the multivariate technique of PCA was used to discriminate between milk powder samples based on their particle size fractions (coarse, medium, and fine), and PLS was used to predict particle size fractions using hyperspectral data.

Principal component analysis (PCA) is a multivariate data analysis tool that is used to reduce the dimensions of a large data set with a large set of variables to a reduced data set. The reduced data set after PCA still contains most of the relevant and meaningful information of the large data set. Furthermore, PCA is a data visualisation tool where data sets are

discriminated upon based on their variance and splitting data into orthogonal vectors (Wold 1966). A linear combination of these vectors across new, unknown variables, named as principal components (PC's), reduces the dimensionality of spectral data. The hyperspectral data matrix $\boldsymbol{D}$ $(x \times y \times \lambda)$ was integrated into its respective scores $\boldsymbol{T}$ $(x \times y, n)$ and loadings $\boldsymbol{P^T}$ $(n \times y)$ and a residuals matrix $\boldsymbol{E}$ $(x \times y, \lambda)$ (Amigo et al. 2015), Equation (4.2). Where x & y are the spatial dimensions of the hypercube and λ is the wavelength vector for that hypercube. Moreover, *n* represents the number of principal components. Three PC's were examined in this study.

$$\boldsymbol{D} = \boldsymbol{T}\boldsymbol{P}^T + \boldsymbol{E} \quad \textbf{(4.2)}$$

A PLS discrimination model (Model-I as shown in Figure 4.2) was developed to predict each particle size fraction of the milk powder. In this model we had spectra of each size fraction as a predictor matrix **X**, which was a function of a variable **Y**. This **Y** variable was assigned discrete values of 1, 2, 3 which were a respective reference to class C, M, and F.

Mean spectra for every HSI image was saved as a spectral feature. Hence, we had three spectral features for each size class i.e. for the coarse fraction (λ_c), fine fraction (λ_f), and medium fraction (λ_m).

A hyperspectral image is comprised of multi-pixel data. It is practical to consider 'pixel as a sample' approach (Al-Sarayreh et al. 2017). We selected a random set of N pixels from a single hyperspectral image of a reconstructed sample and compared the spectrum to an already saved, reference set of spectral features. A second model (Model-II as shown in Figure 4.2) with average spectra of coarse (λ_c), fine (λ_f) and medium (λ_m) fractions of milk powder was used to predict the membership of the selected 'N' pixels to either of the three

particle size fractions. This was done by calculating the Euclidean distance of these spectra with the average spectrum of each size fraction (Jain et al. 1999).

$$d_\lambda = (x_i, x_j) = \left[\sum_{k=1}^{l} (x_{i,k} - x_{j,k})^2\right]^{1/2} \quad \textbf{(4.3)}$$

where,

x_i = Absorbance intensity at a particular wavelength from spectrum of a random pixel

x_j = Absorbance intensity at a particular wavelength from spectrum of an individual fraction

l = particular wavelengths

This Euclidean distance served as a similarity index. This similarity index d_λ was calculated with reference to each coarse fraction (λ_c), fine fraction (λ_f), and medium fraction (λ_m). The least value would represent the minimum distance from respective fractions. Hence, the respective fraction class was assigned to that pixel. Similarly, all *N* pixels were assigned a class and composition of these classes were calculated.

$$N = n_c + n_f + n_m \quad \textbf{(4.4)}$$

where,

n_c = Total number of pixels assigned to class 'Coarse'

n_f = Total number of pixels assigned to class 'Fine'

n_m = Total number of pixels assigned to class 'Medium'

In this way, we predicted the particle size distribution in terms of coarse particle fraction, medium particle fraction and fine particle fraction in a reconstructed sample and compared it to the distribution of these size fractions already stated in Table 4.1. A similar approach

was adopted by Diezma et al. (2013) for classification of three quality grades of spinach leaves by their HSI data in 400 – 1000 nm range of wavelengths.

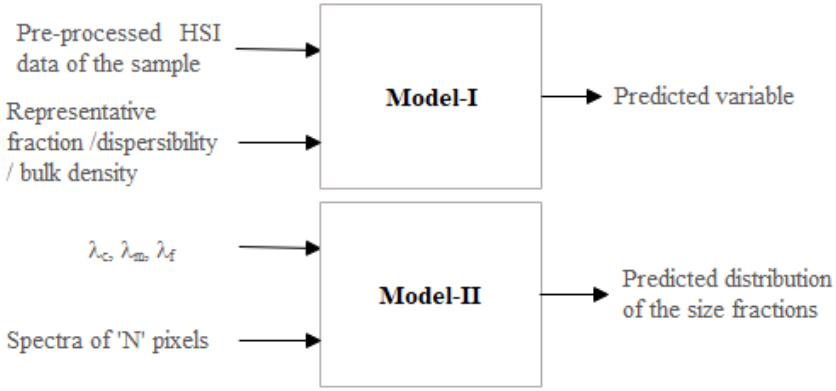

Figure 4.2. Summary of input and output from the models

For the prediction of dispersibility and bulk density of the reconstructed samples, we used the PLS regression method (Abdi 2010) similar to Model-I. The predictor matrix **X** was based upon the spectra of these seven samples. However, the **Y** variable was the respective bulk density / dispersibility value of each sample.

4.5. Results and Discussion

4.5.1 **Selection of suitable design choices for subsequent multivariate analysis**

After scanning milk powder samples, spatial images at selected wavelengths, the raw hyperspectral data, and smoothed hyperspectral data representing each size fraction were plotted (Figure 4.3). Figure 4.3 (a) shows spatial images or absorbance maps of three size fractions of milk powder plotted at three different wavelengths. Similarly, a stack of such plots can be plotted at different wavelengths. Each slice in the stack of such plots represents a spatial image or absorbance map at a particular wavelength. These spatial images are slightly different from each other. However, one cannot describe quantitative differences between these particle size fractions of the milk powder without an appropriate method of

analysis. It appears to be that higher camera resolution might be required to show significant visual differences in the spatial images of the three size fractions.

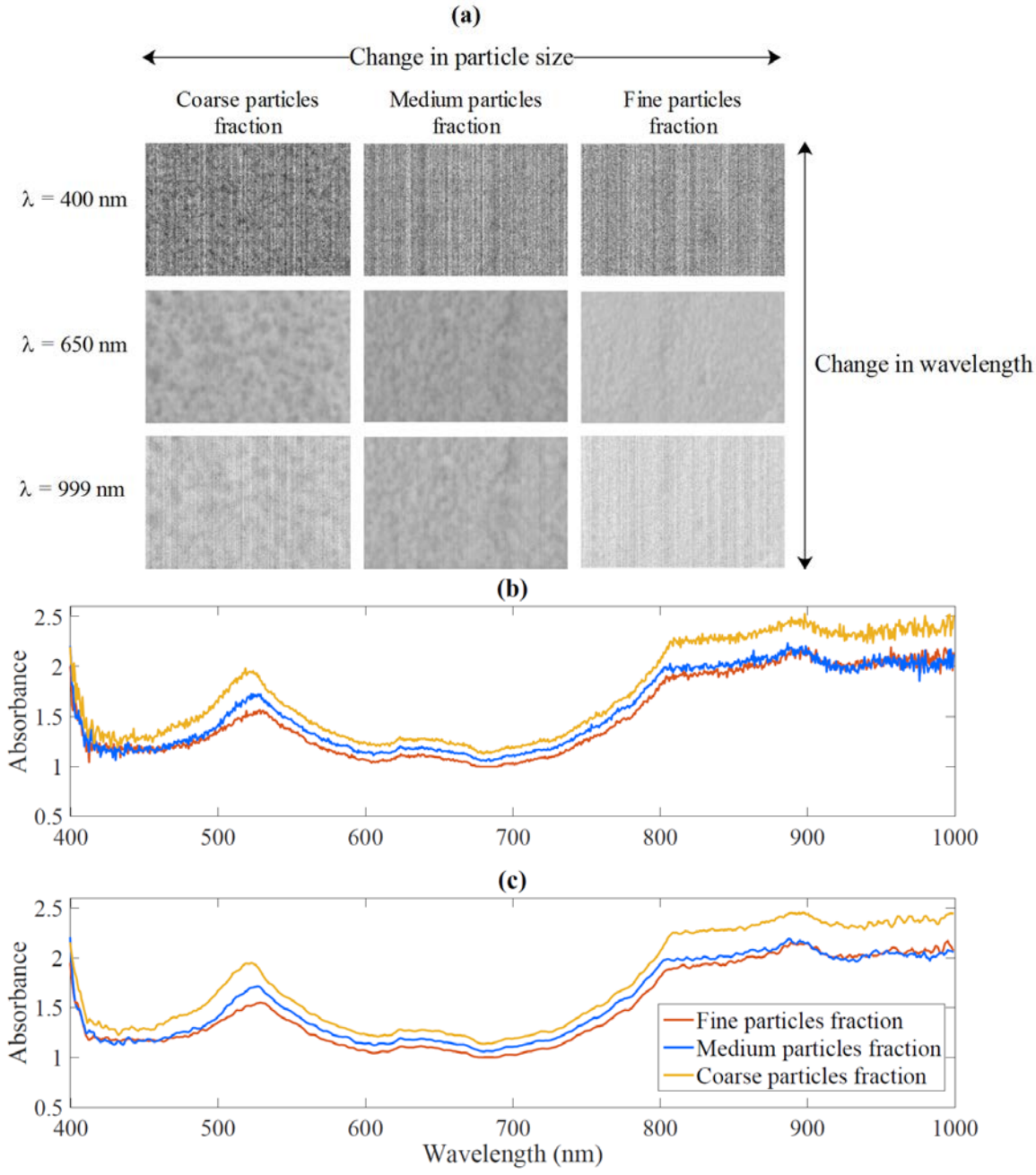

Figure 4.3. (a) Spatial maps of three size fractions of milk powder at three different wavelengths, (b), raw spectra plot, and (c) spectra after spectral smoothing

From further analysis and developing multivariate models, 2000 randomly selected raw spectra of each size fraction of the milk powder were selected using (x, y) spatial information, and then were plotted. Figure 4.3 (b) shows three average spectra obtained from

randomly selected raw spectra of each size fraction of the milk powder. As mentioned previously, the raw HSI data was subsampled to a manageable data volume for processing the data and developing the multivariate model. However, a single spectrum from each particle size fraction is only shown for illustration of the representation of possible spectral variations among the three different particle fractions. The general trends of the spectra of the coarse and the medium size fractions are similar to each other with an offset in absorbance values. However, if we split the spectral differentiation over different wavelength segments, it is worth noting that the average spectrum of the medium and fine size fractions overlapped with each other − especially in the infrared (~ 700 – 1000 nm) and blue (~ 400 – 500 nm) regions. Furthermore, the medium and the fine size fractions did not overlap each other in the visible region. Conversely, the coarse size fraction seems different from the medium and the fine fractions through the whole range studied (400 – 1000 nm). An offset in the spectral behaviour was reported for other different materials where the particle size among the sample varied and was analysed by near-infrared spectrometry (Gupta et al. 2004). This offset in the spectra of three different particle size fractions of milk powder was expected as these three size fractions were derived from the same bulk package of the milk powder which were derived from the same raw materials and were processed through similar conditions in a single batch of operation. The major difference among the samples was the fact that they had particles of different size ranges.

It is evident in Figure 4.3 (b) that the raw spectra exhibit spectral noise, which needs to be filtered or smoothened before developing multivariate data models because spectral noise can significantly affect them. For spectral smoothing in this study, the `smoothn` function developed in MATLAB by Garcia (2010) was employed because it is robust, automatically selects the required smoothing extent, and is efficient at high dimensions. Figure 4.3 (c) shows smoothened spectra of three size fractions of the powder. Other smoothing techniques

such as the Savitzky-Golay smoothers (Savitzky and Golay 1964), Whittaker weighted kernel smoother (Whittaker 1922), and locally estimated scatterplot smoothing (LOESS) (Cleveland et al. 1988) are also available in the literature in the field of spectrometry. However, the use of these techniques is challenging for smoothing hyperspectral data, because they require a choice of various crucial tuning factors that adjust the degree of smoothing. The experimenter usually has a limited understanding of the choices of suitable smoothing tuning factors for a desired degree of smoothing. It is worth noting that the degree of smoothing has important implications in developing multivariate models and the subsequent analysis.

After making the data pre-processing design choices discussed above, the prepared hyperspectral data was used for developing multivariate PCA, and PLS data models. For the PCA model, the first three principal components (PCs) with differing levels of spectral smoothing were tested to decide suitable design choices of PCA such as the number of PCs to retain, and the desired level of spectral smoothing which can discriminate between different size fractions of the powder. Smoothing level here refers to the window size that gives the closest possible residual for a certain noise of the spectra. A detailed description of this can be found in Vivó-Truyols and Schoenmakers (2006). The first three PCs were selected because they accounted for approximately more than 70% of the total variation in the spectra. Addition of more PCs to the PCA model did not add significant value. For evaluating the spectra smoothing effect on the PCA analysis, the smoothing factor (measured in terms of smoothing tuning variables) was varied from 0.0001 to 10. The objective was to evaluate suitable design choice parameters for the discrimination of different size fractions of the milk powder.

Two separate predictive models were used in this study. Model-I was developed from the pre-processed spectra obtained from HSI images of three segregated size fractions. We had nine images for each size fraction, six of which were used in a training model while three were kept in a validation set. Model-II was based upon the average spectrum of the three different size fractions. Furthermore, it was applied on the HSI images of reconstructed samples at the pixel level. We selected a certain number of pixels from a single image of the reconstructed sample and evaluated the prediction of the model. With a lesser number of pixels, the correlation coefficients (R^2) of the model were lower. However, the correlation coefficient or model accuracy increased with increasing number of selected pixels as shown in Figure 4.4. Incorporating at least 50 pixels in the prediction analysis resulted in a correlation coefficient higher than 0.9. This test was repeated at least 10 times to evaluate consistency.

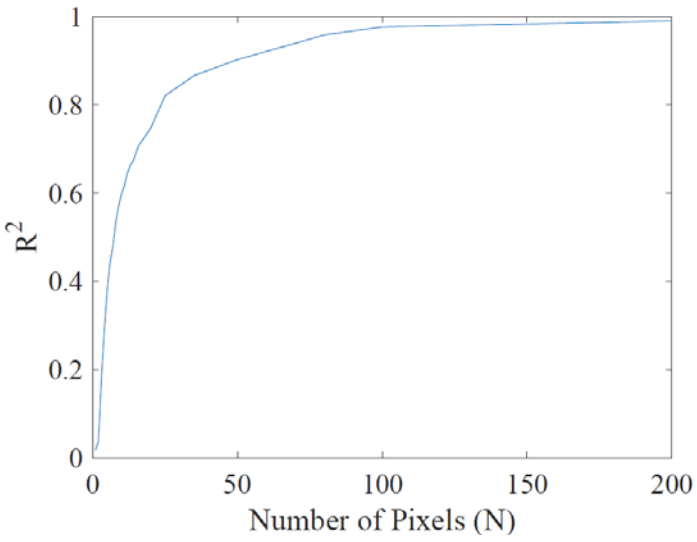

Figure 4.4. Prediction correlation coefficient and number of pixels selected from an HSI image

4.5.2 **Milk powder discrimination results using the PCA techniques**

For discriminating milk powder on the basis of its size fractions, PCA score plots of the spectra obtained from the scans of three size fractions (coarse (C), medium (M), and fine (F)) of the milk powder were plotted together. The first three PCs with varying levels of

spectral smoothing were plotted in an array of plots as shown in Figure 4.5, where, the rows of the array present subplots between the first three PCs, and the columns of the plot present subplots of the first three PCs at differing levels of spectral smoothing. It is worth mentioning that smoothing level was varied by varying the smoothing factor, which was obtained by combining different smoothing tuning factors, and is mentioned in the first row of the subplots. A similar array pattern was followed for the other PCA plots. Figure 4.5 shows the PCA scores plot of first three PCs with varying levels of spectral smoothing of the spectra obtained from the scans of three size fractions of the powder. The scores and 95% confidence interval ellipses of the three size fractions were presented with different colours, following the same colour code used above, for the discrimination of the three size fractions. Each ellipse illustrates the 95% confidence region, which means that there is 95% probability of the scores data to lie with each ellipse. However, only ellipses were plotted without their data points for better data visualisation, Figure 4.5. As stated previously, the first three PCs contributed approximately 70% or more to the total variance, which means that more than 70% of the variance contained in the spectral data is retained by the first three PCs (PC_1 = ~62%, PC_2 = ~8%, and PC_3 = ~ 2%).

As shown in Figure 4.5, the selected pairs of PCs (PC_1 vs PC_2, or PC_2 vs PC_3, or PC_1 vs PC_3), and smoothing factor have a significant effect on milk powder discrimination on the basis of size fraction. Three size fractions of the powder were separated from each other along PC_1 for a smoothing factor of 10 (Figure 4.5). The first principal component refers to the variable that describes the maximum variance in the spectral data (Mattila et al. 2007), which is milk powder particle size in this case. Therefore, PC_1 could be linked with milk powder particle size, and PC_2 could be related to the quality of the powders. Earlier, Munir et al. (2018) also referred to the first principal component correlating with appearance of

the powder particles. Consequently, HSI can discriminate between the milk powder samples based on their size fractions using PCA.

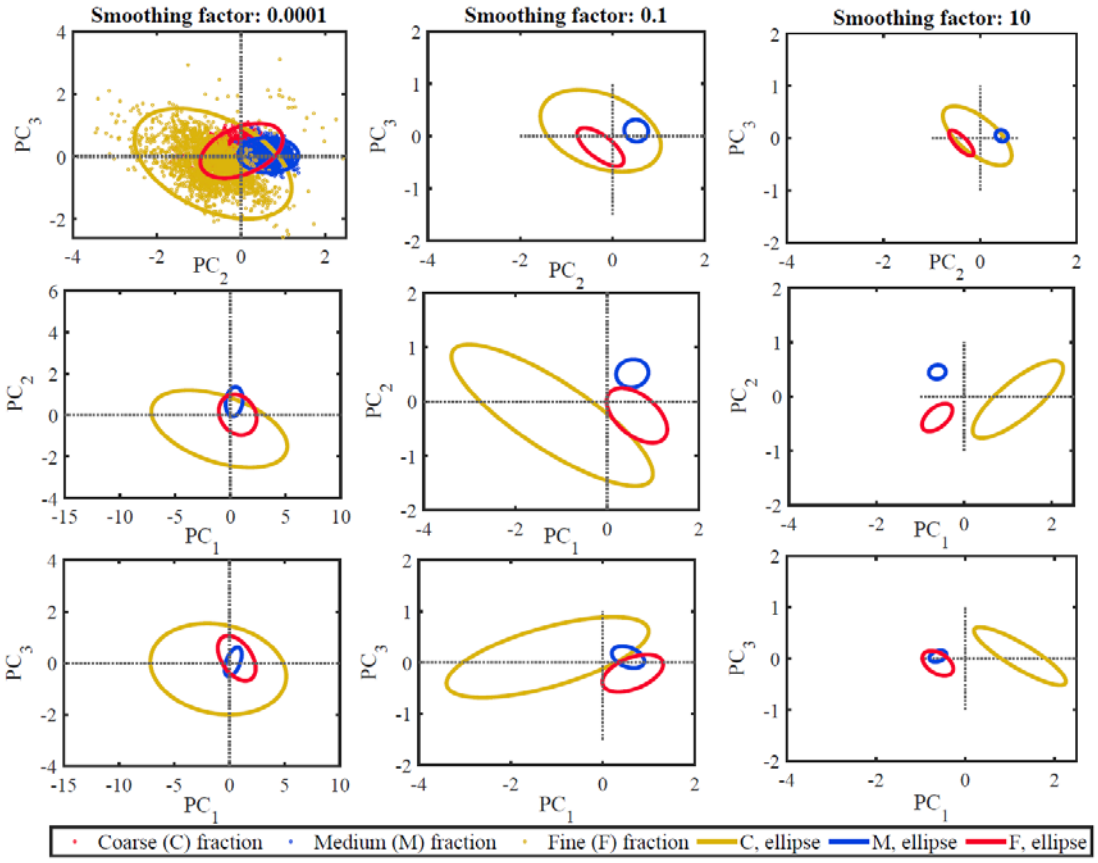

Figure 4.5. Principal component plots for the three individual particle size fractions

4.5.3 **Prediction of milk powder size using the PLS technique**

For predicting milk powder particle sizes, Model-I was developed using the spectra obtained from the scans of the three size fractions of coarse (C), medium (M), and fine (F). Figure 4.6 shows PLS model fitting (i.e. calibration) and validation plots for the particle size fractions. In this case, 2/3 of the samples were used for the PLS model calibration and 1/3 of the samples were used for the PLS model validation. A standard deviation of 0.015, in the form of a Gaussian distributed noise source, was added to the abscissa to show the spread of the data. The colour coding used for three size fractions of the milk powder was the same as used above in sections 4.5.1 and 4.5.2.

It is evident from Figure 4.6 that the PLS model can successfully predict milk powder particle size fractions using the spectral data, because the correlation coefficient values for the calibration and validation of the PLS model were ≥ 0.94. This observation may be because the spectral features of the three size fractions of the milk powder have significant differences among them.

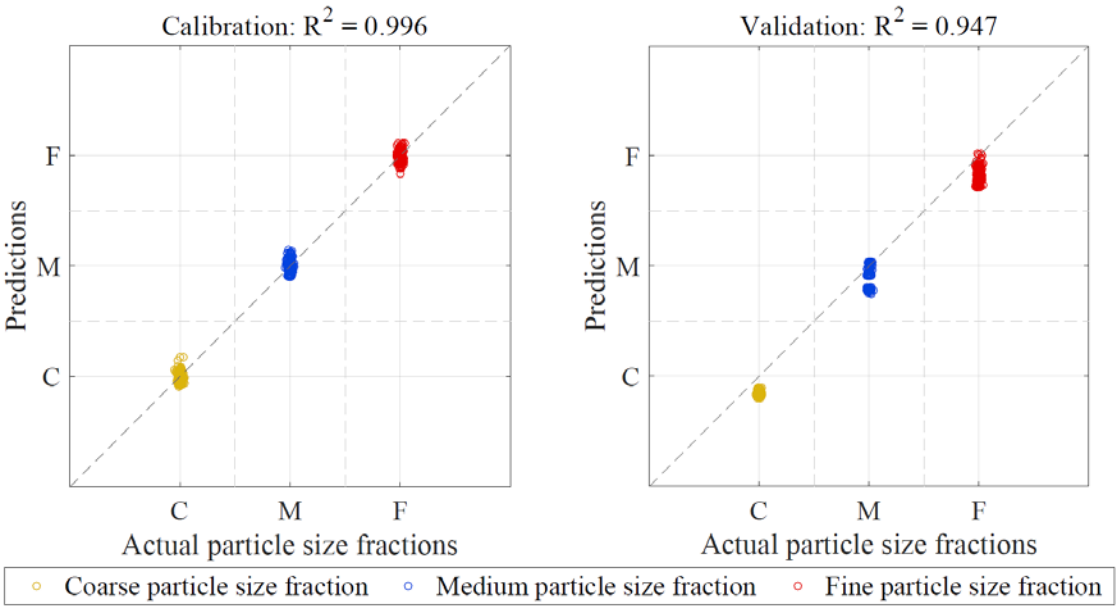

Figure 4.6. Partial least squares regression of three separate size fractions of milk powders

For predicting powder particle size fractions in the seven samples, the average spectrum for each particle size fraction and the spectra obtained from the scans of the samples (described in Table 4.1) were used.

Figure 4.7 shows results for predicting the distribution of three particle size fractions in the seven samples. The size fraction results were presented as mass percentages of the three size fractions in the seven reconstructed samples. The predicted results were presented with error bars which account for the possible standard deviation.

It is worth noting that in Figure 4.7 the Model-II successfully predicted the powder particle size fractions in the seven samples in comparison with their actual values. The correlation

coefficient of this predictive model was 0.98. As discussed before in this section, this observation might be due to the presence of three size fractions (having significantly different spectral features) in the samples. These results strengthen the idea of using spectral features of a milk powder sample for the proxy-measurement of its physical and functional properties.

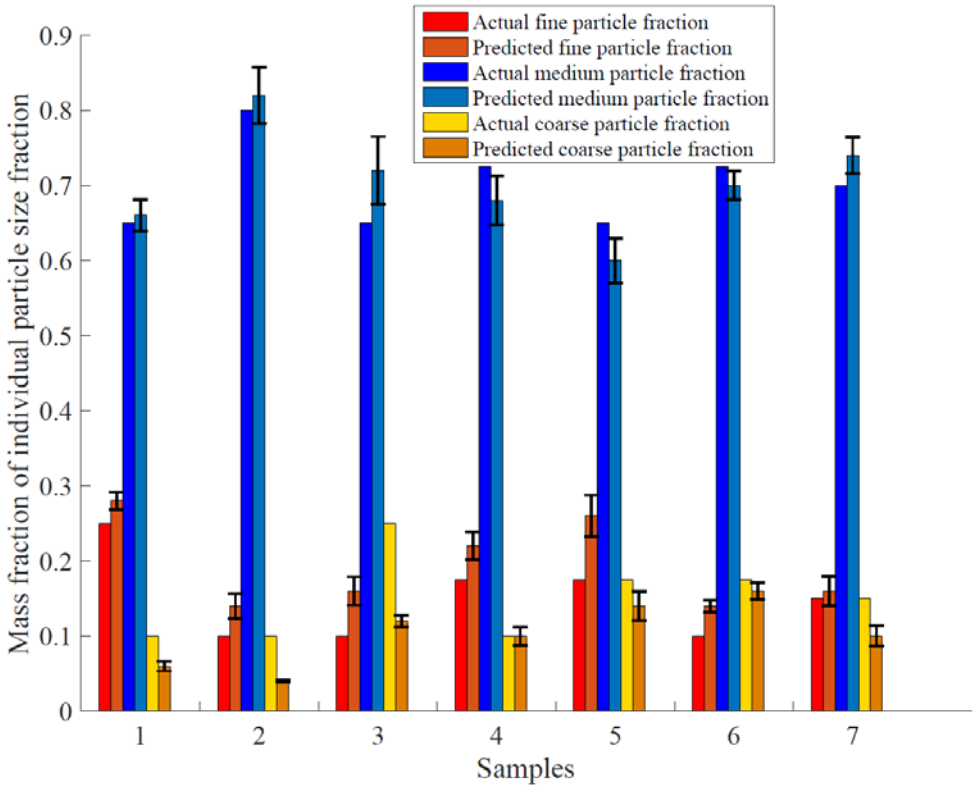

Figure 4.7. Comparison of actual and predicted fractions of particles in seven reconstructed milk powder samples

A PLS model can be used for the prediction of the dispersibility and bulk density of the reconstructed seven samples as well. The correlation coefficients for calibrating the data (R^2) and validation of data (R^2) both were greater than 0.980 and 0.865 respectively for the prediction of the dispersibility as shown in Figure 4.8. Similarly, Figure 4.9 shows these correlation coefficients were 0.979 for calibration and 0.896 for validating data sets respectively for the prediction of the bulk density of milk powder samples that varied with the particle size distribution. This supports the hypothesis that the spectral features or

behaviour of these milk powder samples might have the potential to correlate with the functional and physical properties that are directly related to the size of milk powder particles present within a sample.

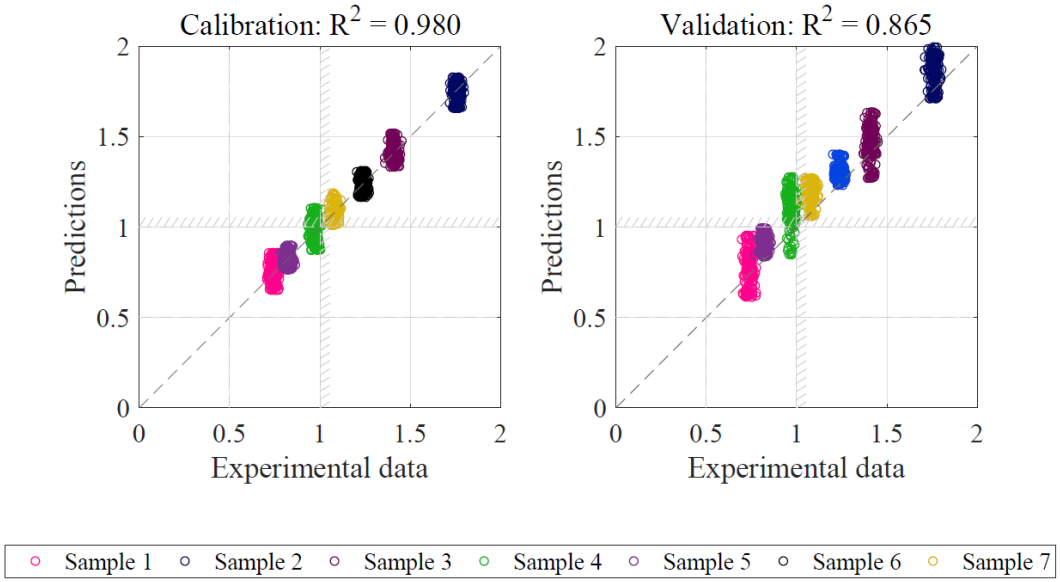

Figure 4.8. Partial least squares model prediction of dispersibility

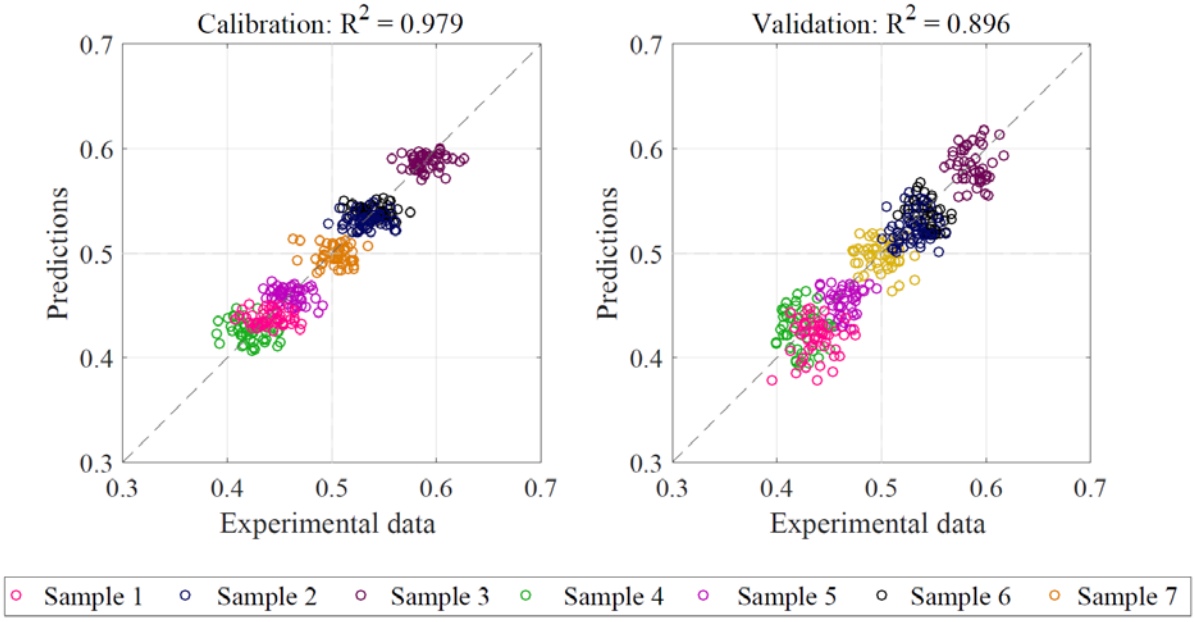

Figure 4.9. Partial least squares model prediction of bulk density

4.6. Conclusions

In this study, HSI with multivariate data analysis tools PCA and PLS were used for predicting milk powder particle size fraction or, indirectly, milk powder quality. The hypothesis of this study seems to be correct in that HSI can discriminate between milk powders based on their particle size fractions or their quality. It is worth noting that while spatial images or absorbance maps of three size fractions were not able to differentiate between them, PCA modelling was able to discriminate between the powder size fractions. Furthermore, PLS model successfully predicted the powder size fractions individually, and their distribution in the seven reconstructed samples was also estimated. It was also found that the spectral smoothing technique and its degree of smoothing have significant implications in developing multivariate models such as PCA, and PLS.

This study indicates that HSI coupled with multivariate data analysis tools can potentially be further developed, as an analytical method, to replace existing off-line quality tests of milk powder. However, more detailed studies in the future are required to achieve real-time quality prediction of milk powder during its processing.

4.7. Summary

The results of this chapter were promising. It was evident from the PCA analysis that the three particle size fractions were differentiable from their pre-processed HSI data cubes. The impact of pre-processing on the subsequent PCA was significant. This PCA analysis of three particle size fractions will be used further in Chapter 5.

A similar approach to Chapter 2 was followed to develop predictive models for the estimation of reconstructed milk powder samples' physical and functional properties. A significantly improved prediction coefficient was obtained from HSI data analysis for the estimated distribution of particle size fractions than NIR data from Chapter 2. However, for

bulk density and dispersibility prediction coefficients of prediction were slightly less than NIR data analysis.

Chapter 5. Wavelength selection for rapid identification of different particle size fractions of milk powder using hyperspectral imaging

5.1. Preface

Hyperspectral imaging (HSI) data analysis provided encouraging results for differentiating three particle size fractions of milk powders in Chapter 4. Principal component analysis (PCA) is reproduced with another set of samples prepared from different batches of IWMP. Hyperspectral data analysis is extended to identify a reduced set of wavelengths from PCA and weighted regression coefficient (WRC) analysis. Partial least square discriminant analysis has been conducted for HSI data obtained from three particle size fractions, with the complete wavelength data and two reduced sets of wavelengths.

This part of the work has been published in Journal "Sensor" for their special issue "Non-destructive Sensors and Machine Learning for Food Safety & Quality Inspection".

5.2. Abstract

Hyperspectral imaging (HSI) in the spectral range of 400 – 1000 nm was tested to differentiate three different particle size fractions of milk powder. Partial least squares discriminant analysis (PLS-DA) was performed to observe the relationship of spectral data and particle size information for various samples of instant milk powder. The PLS-DA model on full wavelengths successfully classified the three fractions of milk powder with a coefficient of prediction 0.943. Principal component analysis (PCA) identified

each of the milk powder fractions as separate clusters across the first two principal components (PC_1 and PC_2) and five characteristic wavelengths were recognised by the loading plot of the first three principal components. Weighted regression coefficient (WRC) analysis of the partial least squares model identified 11 important wavelengths. Simplified PLS-DA models were developed from two sets of reduced wavelengths selected by PCA and WRC and showed better performance with predictive correlation coefficients (R_p^2) of 0.962 and 0.979 respectively, while PLS-DA with complete spectrum had R_p^2 of 0.943. Similarly, the classification accuracy of PLS-DA was improved to 92.2% for the WRC based predictive model. Calculation time was also reduced to 2.1 and 2.8 s for PCA and WRC based simplified PLS-DA models in comparison to the complete spectrum model that was taking 32.2s on average to predict the classification of milk powder samples. These results demonstrated that HSI with appropriate data analysis methods could become a potential analyser for non-invasive testing of milk powder in the future.

Keywords: milk powder, hyperspectral imaging, principal component analysis, weighted regression coefficients analysis

5.3. Introduction

Milk powder quality is complex as it is measured in terms of different quality attributes such as milk powder appearance, taste, aroma, and its dissolution performance in water. These quality attributes of milk powder depend on various physical (e.g. particle size distribution, bulk density) and functional properties (e.g. wettability, sinkability, dispersibility and solubility) of milk powder. The physical properties determine the storage and transport properties of milk powder, and functional properties describe how well the milk powder performs when recombined. Mostly, milk powder quality is measured after the fact and offline using various quality tests which include quality test(s) for measuring powder bulk density, powder flowability and dispersibility in water, etc. These quality tests have inherent variability and lack numeric descriptors which makes milk powder quality quantification challenging. Furthermore, this offline strategy of testing milk powder quality is not helpful to detect milk powder quality in real-time which is described as Process Analytical Technology (PAT) by the U.S. Food and Drug Administration (FDA, 2004). Consequently, manual offline quality testing of milk powder needs to be replaced by machine vision for quality testing, which is relatively faster, has less variability and has numeric descriptors.

Process analysers such as HSI may potentially be used for testing milk powder quality and replacing existing manual quality tests because HSI is non-invasive, relatively faster than manual quality tests, and it can test powder quality in terms of quantifiable numeric descriptors. Hyperspectral imaging is popular because it combines the advantages of conventional imaging and spectroscopy to achieve the benefits of both techniques. During HSI data acquisition process, HSI instrument captures two-dimensional spatial (x, y) images at different wavelengths which is also called the spectral (λ) range. As a result, three-dimensional hypercube is obtained. Further details of HSI image acquisition

and hypercube analysis are given in Amigo (2019). It is worth mentioning that imaging and spectroscopy are acknowledged techniques in the food industry. For example, in the food industry, imaging is used for visual defect detection (Vote et al. 2003), and spectroscopy is used for compositional analysis of food products and the identification of adulterants (Sun 2009). Hyperspectral imaging has been previously used in the food industry and other applications such as remote sensing, airborne surveys, astronomy, agriculture, biomedical, mineralogy and pharmaceuticals (Geladi and Manley 2010). In the food industry, HSI has been used for qualitative assessment of products, for example, monitoring the freshness and quality of meat (Qiao et al. 2015), identifying the types and varieties of cereals (Sendin et al. 2018), detecting defects in fruits and vegetables (Nanyam et al. 2012), and exploring varieties of cheese and its quality (Barreto et al. 2018).

The hypercube obtained after data acquisition needs appropriate multivariate data analysis tools that can relate the hyperspectral data with milk powder quality attributes. Principal component analysis (PCA), discriminant analysis (DA), and partial least square (PLS) regression are among the common multivariate data analysis tools reported in the literature which can be used to explore the relationship of spectral variation with the chemical/physical/functional properties (Burger and Geladi 2006, Rajalahti and Kvalheim 2011). Furthermore, suitable data pre-processing techniques such as normalisation, de-noising, smoothing, filtering, and/or taking derivatives of the spectra are required for preparing data sets for subsequent data analysis.

Hyperspectral imaging usually generates large data sets of information. Nevertheless, there might be redundancy of information in the consecutive bands of HSI data. These highly correlated wavelengths of similar information could affect the performance of

multivariate data analysis (Liu et al. 2014). Hyperspectral imaging data analysis can be utilised in real-world applications if vital wavelengths can be identified. However, one struggles to find standard selection criteria for obtaining the important wavelengths from the full spectrum. Several key wavelengths are usually recognised through more than one strategy such as PCA (Chang et al. 1999), weighted regression coefficient (WRC) analysis (Osborne et al. 1997), successive projection algorithm (SPA) (Araújo et al. 2001), uninformative variable elimination (UVE) (Cai et al. 2008), and stepwise regression coefficient analysis (Chong and Jun 2005). This reduction in the number of selected wavelengths is called feature selection in multivariate data analysis. Selected wavelengths are used to propose a reliable multispectral imaging system that could represent the complete spectrum well. The accuracy and fast acquisition of the results are important considerations for the development of real-time quality monitoring systems. On this basis, the selection of reduced wavelengths is essential for reducing the amount of data acquisition and processing for a HSI application.

In previous studies HSI has been used for detection of adulterants (such as, melamine, urea , etc.) in milk powders (Forchetti and Poppi 2017, Fu et al. 2014, Huang et al. 2014b). Huang et al. (2016b) reported two important wavelengths 1447 nm and 1466 nm due to low reflectance ability of melamine in the region 1450 – 1550 nm and analysed spectral data by band ratio technique. Munir et al. (2018) tried to discriminate milk powders of varying quality produced at different production locations by HSI. However, there is no reported example for identifying vital wavelengths for estimating the milk powders quality attributes (either physical or functional properties) by HSI.

This paper aims to evaluate the potential of HSI techniques to facilitate the rapid testing of milk powder. This article has three main specific objectives. The first objective was to

develop a PLS-DA model to differentiate and classify milk powders according to the varying size range of particles, because, the published literature has shown that powder particle size and particle size distribution are influential to functional performance (rehydration characteristics) and quality of milk powder (Schuck 2011, Silva and O'Mahony 2016). The second objective was to identify the important wavelengths by PCA and WRC methods because data reduction to a manageable size is required for real-world applications. The last objective was to develop simplified PLS-DA models with a reduced number of wavelengths to classify the particle size fractions of milk powder which can be implemented for real-time quality monitoring in the future.

5.4. Materials and Methods

5.4.1 **Milk powder sample preparation**

Ten different batches of commercial grade milk powders of a locally manufactured brand were purchased from the supermarket. A Retsch AS200 - vibratory sieve shaker was used with two sieves of 180μm and 355μm aperture to segregate the milk powder into three discrete particle size fractions: coarse particles fraction (labelled as ‘C’, having particle diameter larger than 355μm), medium particles fraction (labelled as ‘M’, having particle diameter larger than 180μm and smaller than 355μm) and fine particles fractions (labelled as ‘F’, having particle diameter smaller than 180μm). Three sets of each particle size fraction were prepared from a single batch and a total of 30 samples of each particle fraction was used in further analysis.

A recombined sample of milk powder was prepared with 17.5%(wt./wt.) fines particle fraction, 65%(wt./wt.) medium particle fraction and 17.5%(wt./wt.) coarse particle fraction. This recombined sample was used for visualisation of classification results only.

5.4.2 **Hyperspectral imaging setup**

In this study, we employed a Headwall Photonics Hyperspec^{TM} - VNIR HSI instrument. This HSI instrument had a sensor covering VNIR (visible and near-infrared) wavelengths in the range from 400 – 1000 nm. The HSI instrument consists of four basic components: a spectrograph, camera (Schneider-Kreuznach Xenoplan 1.4/23), lamp, and transition stage. The camera captured spatial images of samples that had pixels, and each pixel represented a spectrum through the images. The lamp provided a lighting source, and the transition stage provided a moveable platform for placing samples for the analysis. The HSI equipment was enclosed in a black box while analysing the samples to minimise the impact of ambient light. Hyperspectral imaging analysis involves various steps involving data acquisition, image calibration, spectra pre-processing, and data analysis. A flowchart is presented in Figure 5.1 that overviews these steps performed in this research.

Reflectance calibration was performed on all the images recorded by the hyperspectral equipment. A white reference image (*W*) was recorded from a standard Teflon tile provided by the manufacturer as an accessory with the equipment. A dark image (*D*) was saved as a response of the camera in the absence of light. The corrected image (*I*) of each sample was obtained from the respective recorded image (I_{sample}) by Equation (5.1) and saved as a hypercube.

$$I = \frac{I_{sample} - D}{W - D} \quad \textbf{(5.1)}$$

Three hyperspectral images of every sample of milk powder were recorded. Matlab R2018 (The MathWorks Inc., Natick, Massachusetts, USA) with the PLS Toolbox (Eigenvector Research, Inc., Manson, Washington, USA) and the Unscrambler HSI

(Camo Analytics AS, Norway) were used for processing and analysis of the hypercube generated by the HSI.

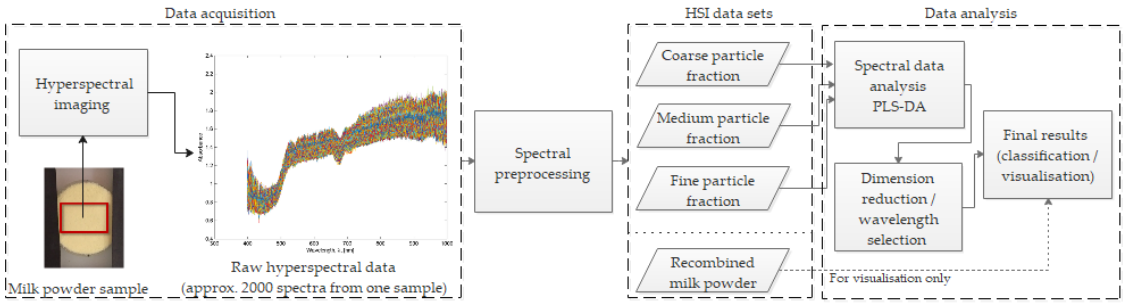

Figure 5.1. Flow chart of the key steps involved in hyperspectral imaging analysis

5.4.3 **Data pre-processing**

A square region of interest (ROI) with the same spatial resolution was manually selected for all the images. The standard normal variance (SNV) (Barnes et al. 1989) was used for spectral data normalisation for each image of the milk powder sample. The HSI data was noisy when plotted as a function of wavelength. Therefore, spectral smoothing was implemented by the Matlab function `smoothn` developed by Garcia (2010). This method was preferred for accommodating multi-dimensional data and providing robust smoothing of spectra generated by HSI. Earlier Munir et al. (2018) reported this pre-processing method for HSI data of milk powders of varying quality obtained from different production locations.

5.4.4 **Multivariate data analysis**

i. Partial least square discriminant analysis (PLS-DA)

Partial least square discriminant analysis (PLS-DA) is a supervised classification technique (Brereton and Lloyd 2014). It was used to classify hyperspectral images of coarse, medium and fine milk powder samples to their respective particle size fraction. In this model, we had spectra of each HSI image as a predictor matrix **X**, which was a function of **Y**, a variable set of assigned dummy values of 1, 2, 3 which were a respective

reference to class C, M, and F. The parsimonious number of latent variables (LVs) from PLS analysis was determined by analysing the root mean square error of cross-validation (RMSECV).

Validation of the model is an important step in any data analysis. It provides the comparison of output provided by the model to the actual variable measured and has a significant impact on the reliability of the model. The samples were divided into calibration and prediction sets. Each particle size fraction had 30 samples prepared from 10 different batches. A total of 21 samples from 7 batches were kept for calibrating the model. Whereas, 9 samples from 3 batches were used in the prediction models. The performance of the calibration model was estimated by the correlation coefficient (R_c^2) and root mean square error of calibration (RMSEC). Cross-validation of the calibration model was used for internal validation of the model by the correlation coefficient of cross-validation (R_{cv}^2) and RMSECV respectively. The prediction performance was also measured in terms of correlation coefficient of prediction (R_p^2) and root mean square error of prediction (RMSEP). For a good performance of the model correlation coefficients terms were expected to be close to 0.9 while the root mean square error terms should be close to zero (Williams and Norris 1987). Residual predictive deviation (RPD) was also calculated for the model. This is the ratio of the standard deviation of the calibration set to the sum of prediction errors. It is believed that a good model performance is associated with a high value of RPD. In general a RPD value greater than three is acceptable (Williams and Norris 1987). The significance of these validating terms is comprehensively explained in Sun (2008). Confusion matrices for the prediction of coarse, medium and fine particle fractions were also created. These confusion matrices show the true positive prediction rate for each particle fraction. Accuracy, sensitivity and specificity of the classification was also determined from these confusion matrices.

Hyperspectral imaging data has the advantage of producing distribution maps for better visualization over traditional spectroscopic techniques. Presence of fine particles has a significant impact on the quality of the milk powder (Boiarkina et al. 2017). Therefore, chemical images and a distribution map were produced by pixel spectra of the milk powder sample and the regression coefficient of a model.

5.4.5 **Wavelength selection**

Accuracy and speed are required for HSI application in industrial settings. It would be expedient to use the big data generated from the HSI directly. However, data analysis based upon the full spectral range of 400 – 1000 nm could be affected by the collinearity of the similar spectral information of the consecutive wavebands. This high dimensionality of the HSI data has its impact on the computation speed and it could make data processing a time-consuming step. However, the data acquisition and its processing could be made more efficient and robust if optimum wavelengths that carry valuable information were identified.

i. Principal component analysis (PCA)

Principal component analysis (PCA) is a well known technique for dimension reduction in big data systems. PCA gives an overview of the data set on a new axis called the principal components (PCs). PCA extracts the systematic variation of data by projecting it into a new space across these PCs (Wold 1966). This technique was applied to the spectral data of the samples of three milk powder fractions from the seven batches assigned to calibration. It transformed the data in such a way that the projections of the transformed data (termed as the principal components) exhibit maximal variance among three fractions of milk powder. This data transformation was represented in the score plots of PCA. Three PCs were retained that represented the 75% variance of the data.

Principal component analysis is also one of the most extensively used feature selection methods. Chang et al. (1999) present a band prioritisation method based on the PCA. The loading plot represents the influence of wavelengths on the PCs. The influential wavelengths were extracted from local minima or maxima of the retained PCs. A similar approach was used by Xing and De Baerdemaeker (2005) for identifying six key wavelengths for apple bruise detection from HSI. Zhang et al. (2015) also recognised influential wavelengths by three PC loadings to classify plastic and cotton using HSI technology.

ii. Weighted regression coefficient (WRC) analysis

This method was based upon the regression coefficient analysis of the wavelengths obtained from the partial least squares model as shown in Equation (5.2).

$$\mathbf{Y} = \boldsymbol{\beta}\mathbf{X}' \quad \textbf{(5.2)}$$

Whereas $\mathbf{X}'$ was the standardised wavelength matrix obtained by dividing wavelength vectors by their standard deviation and $\mathbf{Y}$ was the predictor matrix. Both $\mathbf{X}'$ and $\mathbf{Y}$ were related by a regression vector β. The weighted regression coefficient (WRC) method was performed on the calibration data set with full cross-validation. The absolute value of β indicates the importance of the corresponding wavelength. Wavelengths with large β values (irrespective of the sign) were the most influential. A detailed explanation of this method is given in Mehmood et al. (2012). Various studies have reported using WRC for key wavelength selection in different applications of HSI. For example, Zhang et al. (2017) extracted 12 important wavelengths to determine the caffeine content from HSI data of coffee beans. ElMasry et al. (2012) used weighted regression to recognise 6, 24 and 15 important wavelengths for colour, pH and tenderness prediction of beef slices, respectively.

5.5. Results & Discussion

5.5.1 **Full-Range PLS-DA Model**

One thousand spectra were randomly selected from every single hyperspectral image used in the model. For predicting milk powder particle size classes, the discriminant analysis was performed by the PLS method using spectra obtained from the three size fractions (coarse (C), medium (M), and fine (F)). This model was trained (i.e. calibrated) and validated with the milk powder size fractions of different batches. As mentioned earlier, the samples from seven batches were used for the model calibration and the samples from the other three batches were used for the model validation. Figure 5.2 shows that the parsimonious number of latent variables (LV) was three as more than three LV did not significantly reduce RMSECV.

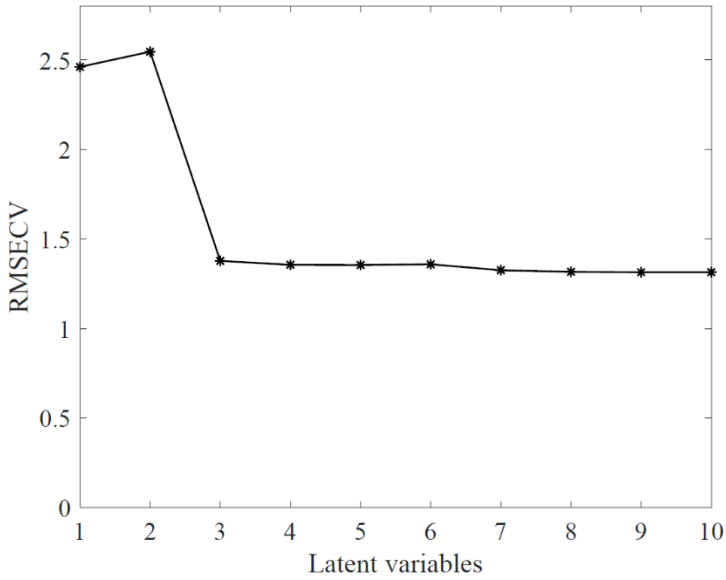

Figure 5.2. Latent variable selection using the root mean square error of cross-validation

Spectral pre-treatments are usually applied prior to developing the PLS-DA model. Pre-treatments including differentiation, and smoothing were tested before the data analysis, and smoothing showed improvements compared to taking derivatives of the spectra. Therefore, smoothing was applied to all spectra of milk powder samples before the PLS-

DA model. A standard deviation of 0.015, in the form of a Gaussian distributed noise source, was added to the abscissa to show the spread of the data. It was observed that the PLS-DA model can successfully predict the milk powder particle size fractions using the spectral data, as the correlation coefficient values for the calibration and prediction of the PLS model were ≥ 0.94.

Classification accuracy, sensitivity and specificity for selected spectra from samples of individual particle size fractions have been presented in section 5.5. However, it is worth mentioning that all of the 27 samples from the validation set of discrete particle size fractions were correctly classified to their respective class C, M or F.

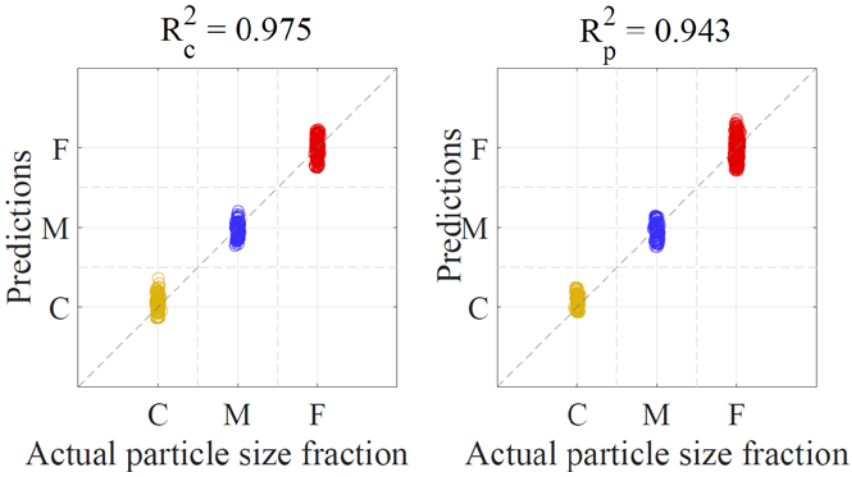

Figure 5.3. Prediction of milk powder samples into coarse, medium and fine fractions

5.5.2 **Selection of wavelengths**

iii. Reduced number of wavelengths based upon principal component analysis (PCA)

After pre-processing by spectral smoothing and noise reduction, PCA was performed on the spectra of three size fractions of milk powder, and hence a large amount of spectral information of each pixel was represented by three PCs.

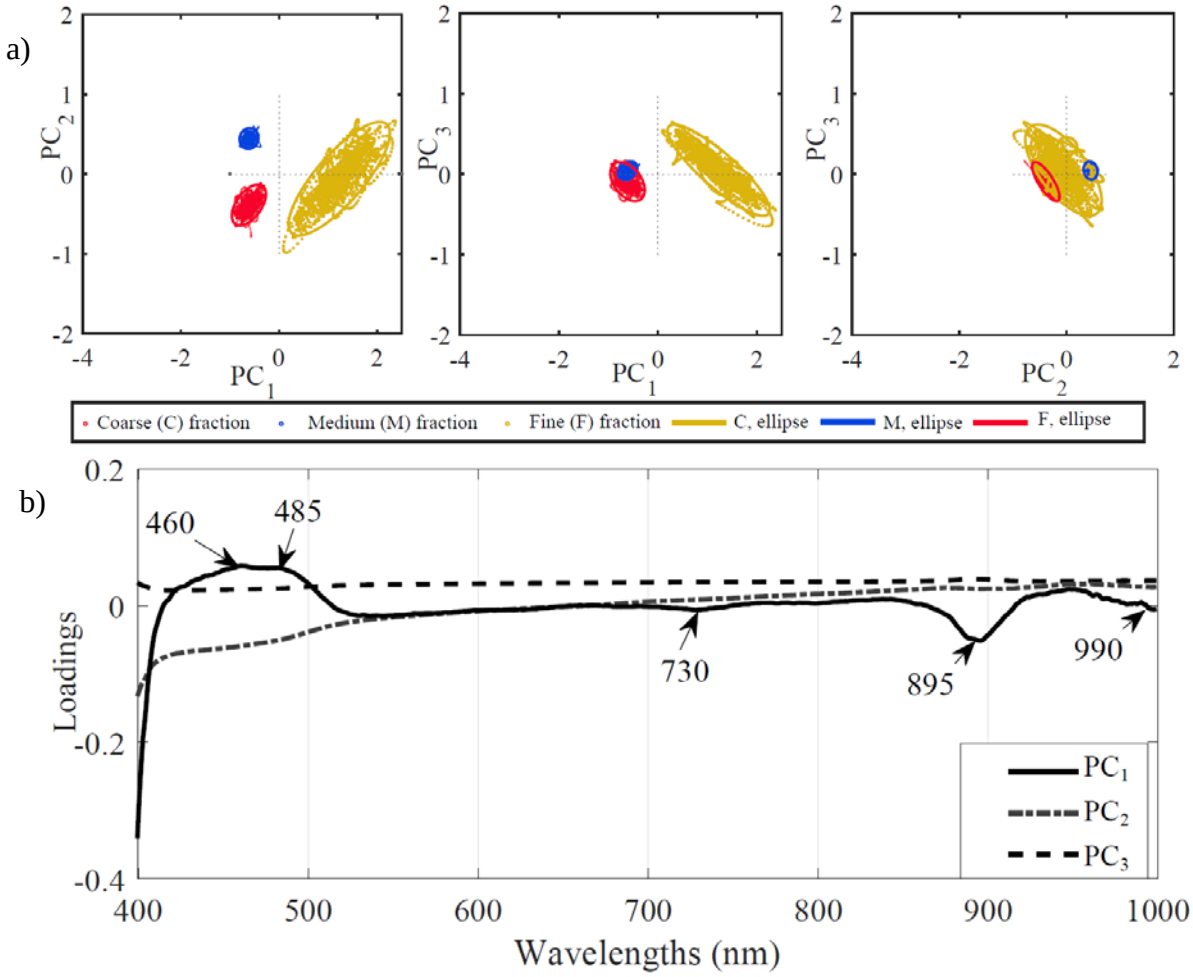

Figure 5.4. Principal component analysis of medium, coarse and fine fraction of milk powder samples.

a. score plots; b. loading plots

The score and loading plots of the PCA are presented in Figure 5.4. Different colours were used to represent pixel spectra of the different particle size fractions of milk powder. An ellipse was drawn across each cluster to present the 95% probability of occurrence of the sample within the confined area. The score plots show the three PCs (PC_1, PC_2 and PC_3) that comprised approximately 75% variance of all the spectral data of the three milk powder fractions. Almost 73% variance was associated with PC_1 and PC_2. The score plots differentiated the three milk powder fractions clearly across PC_1 and PC_2. The spectral information of various pixels of samples was presented as one single point on the PCA score plot.

The loading plot in a PCA shows the explanatory strength of the PCs towards the original data set's wavelength variable. The wavelengths having high loading values (regardless of sign) are good candidates to be effective wavelengths (ElMasry et al. 2011). The loading plot also indicated that PC_1 was most influenced by wavelengths in the 400 – 550 nm and 850 – 1000 nm regions, while PC_2 was also affected by the 400 – 550 nm wavelengths. The third principal component PC_3 seemed least related across the whole wavelength range. With three PCs, at least three original wavelengths were needed for re-modelling the data. Therefore, loading vectors of the three PC's plotted over the complete spectral range and it was observed that at least five local minima and maxima on PC_1 and PC_2 could be obtained, as shown in Figure 5.4. Wavebands of these minima and maxima were important to the clustering analysis in PCA (Rutlidge and Reedy 2009). Therefore, centred wavelengths within these minima and maxima regions from the loading curve were chosen. According to the loadings of PC_1 to PC_3 (Figure 5.4), two wavelengths of 460 and 485 nm were selected mutually from PC_1 and PC_2, and a further three wavelengths of 730, 895 and 990 nm were selected from PC_1, respectively. A model developed with these five wavelengths was named as PCA-PLS-DA.

iv. Reduced number of wavelengths based upon weighted regression coefficient (WRC)

This technique reduced the number of wavelengths by selecting only those wavelengths that highly contribute toward the regression coefficient β. For this purpose, the spectral data was adjusted to the same scale. Afterwards, weighted regression coefficient β was plotted for entire spectral range, as shown in Figure 5.5. Higher values of β reflected the significance of the wavelengths. However, no particular threshold value was selected. Peak values of the regression coefficient β plot could be chosen (Anzanello and Fogliatto 2014).A set of 11 wavelengths was identified. These wavelengths were used to replace

the full spectrum to build a simplified PLS-DA model. This model was named as WRC-PLS-DA. These wavelengths were 413, 425, 440, 458, 493, 515, 578, 596, 624, 669 and 922nm. It is interesting that 10 out of 11 wavelengths belong to the visible region of the spectrum. This confirms the importance of the visible region in the multivariate data analysis of the milk powder samples with varying size particles.

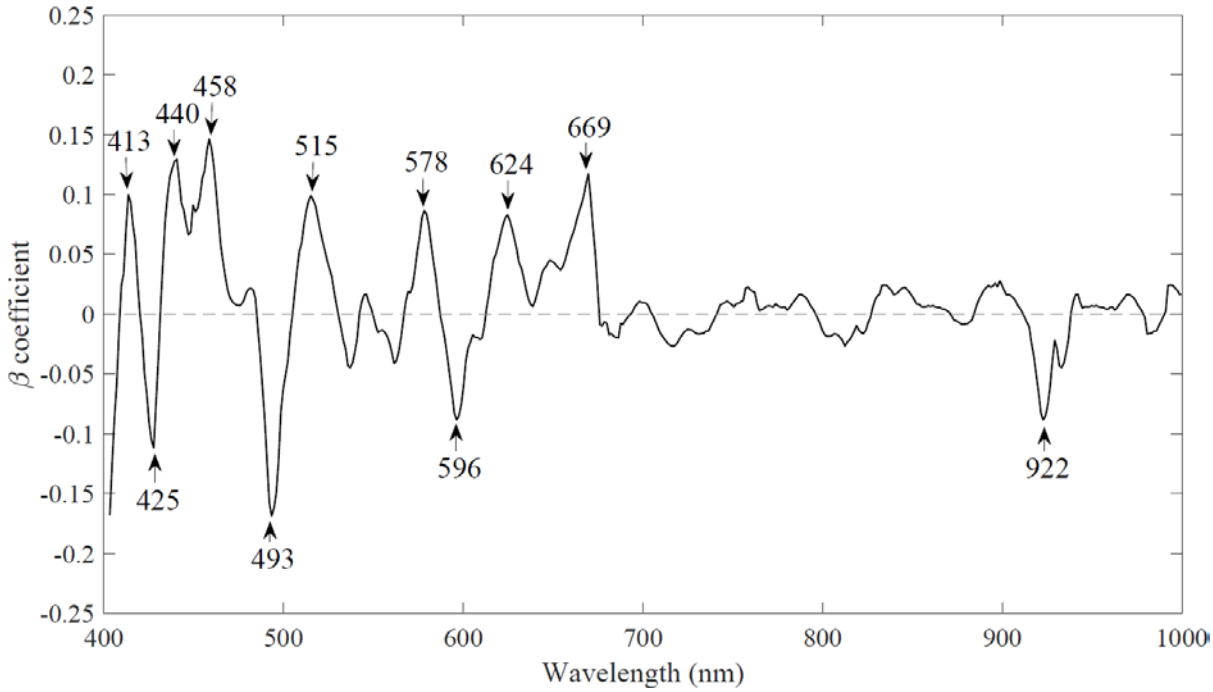

Figure 5.5. Selection of eleven wavelengths from the weighted regression coefficient method

5.5.3 **Validation of selected wavelengths models**

Notwithstanding the encouraging results found using the full wavelengths model, it is beneficial to use only a few variables for accurate, simplified, and robust classifications from hyperspectral data (Ravikanth et al. 2017). In section 5.5.2, five wavelengths were selected by PCA loading analysis and 11 wavelengths were identified by the weighted regression coefficient technique. Simplified PLS-DA models with a reduced number of wavelengths were developed. Table 5.1 shows a comparison of models in terms of calibration performance (i.e. R_c^2, RMSEC, R_{cv}^2 and RMSECV), prediction performance (i.e. R_p^2 and RMSEP), residual predictive deviation (RPD) and computation time.

Computation time was recorded as execution time for model to produce a results data set by an Intel Core i7 CPU with the dual-processor running at 2.60 GHz & 2.10 GHz with a memory capacity of 16 GB. Models were run 20 times and execution time was recorded. The average execution time is presented in Table 5.1. Fast computation was observed for the reduced wavelength models as it took 2.13 s on average for the model using five wavelengths identified by PCA loadings, while 2.82 s was the average execution time with 11 wavelengths of WRC-PLS-DA model for the classification of three individual fractions of milk powder. However, a model built with full spectral information of milk powder fractions was taking more than 30 s on average to produce results.

Table 5.1. Performance of models for prediction of particle size fraction of milk powder

Model	Wavelengths	LVs	Calibration		Prediction		Cross-validation		RPD	Computation time (s)
			R_c^2	RMSEC	R_p^2	RMSEP	R_{cv}^2	RMSECV		
PLS-DA	933	3	0.975	0.1283	0.943	0.1471	0.954	0.1296	5.835	32.2±1.5
WRC-PLS-DA	11	3	0.982	0.0158	0.979	0.0134	0.979	0.0153	5.942	2.8±0.3
PCA-PLS-DA	5	3	0.971	0.0617	0.962	0.0662	0.964	0.648	5.716	2.1±0.2

Where PCA principal component analysis, PLS-DA partial least squares discriminant analysis, RMSEC root-mean-square errors estimated by calibration, RMSECV root-mean-square errors estimated by cross-validation, RMSEP root-mean-square errors estimated by prediction, RPD residual predictive deviation, and WRC weighted regression coefficients

The regression coefficient R_p^2 was slightly improved from 0.943 for the PLS-DA model to 0.962 for PCA-PLS-DA. The best regression coefficient R_p^2 was for the WRC-PLS-DA model with 0.979. However, significant differences were observed when PLS-DA models were evaluated by RMSEP and computational time. Root mean square error was reduced from 0.142 for a complete spectrum model to 0.066 for the model that was based upon reduced wavelength ranges derived from PCA and 0.013 for model built with wavelengths selected by PCA. In terms of R_p^2 and RMSEP, WRC-PLS-DA resulted in better performance. The prediction performance of WRC-PLS-DA was better than the

other models in terms of R_p^2 and RMSEP. Residual predictive deviation for all models was greater than five which indicates satisfactory performance of all models.

Table 5.2. Classification performance of models for prediction of particle size fraction of milk powder

PLS-DA		Predicted class			FN	Sensitivity
		C	M	F		
Actual class	C	37651	3964	385	4349	0.897
	M	1236	31295	9469	10705	0.745
	F	1061	5067	35872	6128	0.854
FP		2297	9031	9854	Overall accuracy	0.832
Specificity		0.967	0.890	0.875		
WRC-PLS-DA		Predicted class			FN	Sensitivity
		C	M	F		
Actual class	C	40511	1086	403	1489	0.964
	M	1909	36854	3237	5146	0.877
	F	63	3112	38825	3175	0.924
FP		1972	4198	3640	Overall accuracy	0.922
Specificity		0.975	0.949	0.955		
PCA-PLS-DA		Predicted class			FN	Sensitivity
		C	M	F		
Actual class	C	38456	2946	598	3544	0.916
	M	1380	35591	5029	6409	0.847
	F	345	3047	38608	3392	0.919
FP		1725	5993	5627	Overall accuracy	0.894
Specificity		0.977	0.928	0.929		

Whereas, C, M and F respective class of coarse, medium and fine particle fraction, FN false negative, FP false positive, Green cells TP true positive and red cells false negative.

Performance of these models were evaluated for their respective classification accuracy as well (as presented in Table 5.2). Classification performance indicators such as sensitivity, specificity and overall accuracy of the model were calculated. Prediction of class from a thousand spectra taken from single samples of milk powder of three classes - coarse, medium or fine - was analysed. There was a total of 21 samples in duplicate (i.e. 2 × 21 ×1000 spectra of each particle size fraction). Green cells in the table show the number of true positives (TP) of each particle size class e.g. a spectrum extracted from a coarse particle fraction of milk powder samples was predicted to be class ‘C’. False

negative (FN) prediction was also estimated for the three particle size classes. A false negative number is the number of spectra that were assigned to an incorrect class. Furthermore, sensitivity and specificity of each class were also calculated. Sensitivity determined the ratio of the true positive prediction number to total number of spectra in a respective particle size class. It is noteworthy that the WRC-PLS-DA model showed the highest sensitivities of 0.964, 0.877 and 0.924 for coarse, medium and fine particle size classes, respectively. Similarly, specificity referred to the actual negative prediction number ratioed to the total number of spectra that were not part of a respective class. It was observed that the coarse particle fraction had a greater than 96% probability for not being misclassified. A lower specificity may show a higher chance of predicting a false positive for the medium and fine particle spectra in these classification models. The highest overall accuracy in these three models was observed for WRC-PLS-DA i.e. 92.2%. Notwithstanding the similar predictive performance of these models, their classification performance indicators were distinctive.

The prediction maps of three discrete particle size samples and one recombined milk powder sample are shown in Figure 5.6. These maps present the classification of spatial pixels of a milk powder sample to their predicted particle size class. These maps show a clear visual discrimination between the coarse, medium and fine particle size fractions. A reference scale is also presented here to refer to the range of the predicted ‘dummy’ variable and its respective class of PLS-DA model. The result from the recombined milk powder sample suggests the feasibility of using hyperspectral imaging to visualise milk powder samples having varied particle size fractions. However, an even more comprehensive study with a large set of milk powder samples with varying particle sizes could be helpful for industrial applications where milk powder particle size affects the physical and functional properties of the final product.

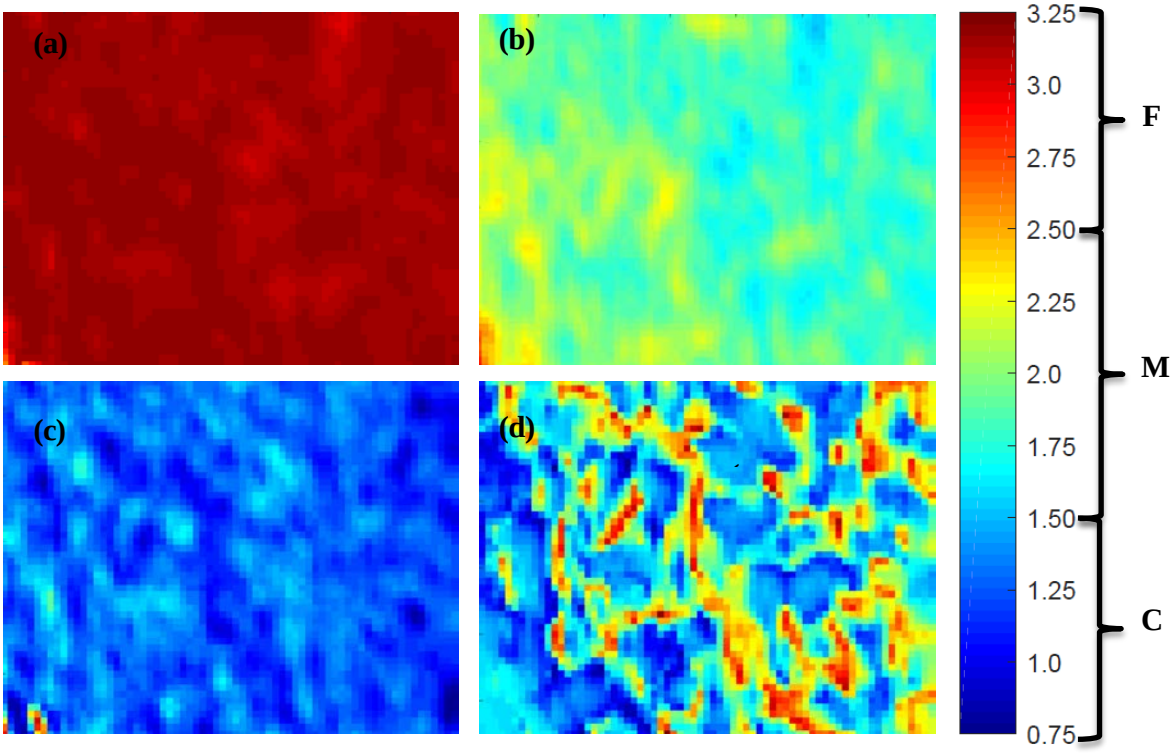

Figure 5.6. Example of prediction map of discrete particle fractions of milk powder (a) fine particle fraction sample; (b) medium particle fraction sample; (c) coarse particle fraction sample; and (d) recombined fractions sample.

5.6. Conclusions

This research was conducted to explore the potential suitability of visible and near-infrared (400 – 1000 nm) HSI for classifying three discrete particle size fractions of milk powder. Based on full spectral wavelengths, the PLS-DA model with R_p^2 of 0.943 was able to classify coarse, medium and fine fractions of milk powder in 32 s on average. Important wavelengths identified by the PCA were five and by weighted regression coefficient were 11. Simplified PLS-DA models based upon these reduced numbers of wavelengths improved the prediction performance of the models. The WRC-PLS-DA model yielded better predictability with R_p^2 0.98, RMSEP 0.013, RPD 5.94 and 92.2 % classification accuracy. However, the fastest average computation time was recorded as 2.13 s for the PCA-PLS-DA model. These results established that this method could be feasible for rapid and non-invasive measurements of milk powder particle size for future

at-line/on-line applications. It could also contribute to the design of future sensors by an initial choice of decisive wavelengths allowing maximum discrimination between different particle size particles.

5.7. Summary

This chapter focused on further enhancing the differentiation among the milk powder samples having a different size range of particles already performed in Chapter 4. By reducing the number of wavelengths, discriminant analysis was improved by higher prediction correlation, reduced error of prediction and fast calculation. These results validated hypothesis IV presented in Chapter 1.

Chapter 6. Conclusions and recommendations for future work

This research was based upon instant whole milk powder (IWMP), which was split into three discrete fractions of coarse particles (C), medium particles (M) and fine particles (F). These fractions were recombined to produced IWMP reconstructed samples that had varying quality parameters for analysis purposes. This chapter summarises the key findings of this study and recommendations for future work. At first this research involved near-infrared (NIR) spectral data analysis to assess quality attributes of instant whole milk powder (IWMP) samples such as powder particle size, dispersibility, and bulk density. For the next part of the study, hyperspectral imaging (HSI) was trialled as a potential analysis to rapidly predict IWMP quality in terms of quality attributes (e.g. powder particle size, dispersibility, and bulk density). Hyperspectral imaging produced an enormous amount of spectral data as compared to NIR spectroscopy; therefore, as the last part of the study, important wavelengths were identified to simplify the data analysis.

6.1. Estimation of milk powder quality by near-infrared (NIR) spectroscopy

Near-infrared spectroscopy was investigated for predicting quality attributes of IWMP such as particle size analysis, dispersibility and bulk density. It is noteworthy that an appropriate pre-processing of the spectra was mandatory to obtain the best predictive model of each quality attribute. Therefore, spectral data pre-treatment techniques such as Savitzky-Golay (SG), standard normal variate (SNV), multiplicative scatter correction (MSC), and their combinations (e.g. SG & SNV, and SG & MSC) were used. Partial least squares (PLS) regression models were developed.

For predicting dispersibility of IWMP, NIR spectra pre-treated with SG & MSC gave the highest R_p^2 value which was 0.978 with the lowest $RMSE_p$ 0.159. This PLS regression model discriminated 91.5% samples accurately if they had dispersibility greater than 1 (good) or less than 1 (poor). This predictive model presented null false positive results which was encouraging. However, 8.5% milk powder samples were predicted false negative.

Bulk density of IWMP reconstructed samples was also accurately predicted with SG treated NIR spectra with R_p^2 of 0.973 and $RMSE_p$ of 0.104. This predictive model could not be analysed further due to lack of qualitative information for bulk density.

In comparison to above prediction results, the prediction models of milk powder particle size analysis, in terms of fine particle fraction percentages in the powder samples, were least accurate with maximum R_p^2 of 0.703 achieved for SG treated NIR spectral analysis with $RMSE_p$ of 4.32. This model was 80% accurate in predicting whether fine particle fraction percent was less than 20% (good) or higher than 20% (poor) in a reconstructed IWMP sample. However, the prediction model of milk powder particle size analysis was prone to false positive predictions. Approximately 11% of poor-quality exhibiting milk powder samples that had a fine particles percentage higher than 20% were predicted as good quality samples with less than 20% fine particles by the model.

6.2. Estimation of milk powder quality by Hyperspectral imaging (HSI)

Hyperspectral imaging (HSI) technique was tested for the estimation of IWMP's rehydration performance in terms of dispersibility and related physical properties (particle size analysis and bulk density). Hyperspectral imaging data coupled with multivariate data analysis tools such as principal component analysis (PCA) successfully

differentiated between the three size fractions. It is worth mentioning that the spectral differences between the three size fractions were more obvious along the first two principal components (PC_1 and PC_2). Furthermore, partial least squares discriminant analysis (PLS-DA) classified the samples as coarse, medium and fine particle fractions from their pre-processed HSI data. Loading plots of the first three principal components (PC_1, PC_2 and PC_3) from the PCA were plotted and centre of local minima and maxima were identified at 460, 485, 730, 895 and 990 nm. These wavelengths were used for a simplified classification model. Weighted regression coefficient (WRC) analysis of the HSI data highlighted 11 wavelengths at 413, 425, 440, 458, 493, 515, 578, 596, 624, 669 and 922nm that had the highest contribution towards the regression coefficient of the standardised spectrum (where all spectra were divided by standard deviation). These reduced wavelengths were used to build simplified PLS-DA models for the classification. These simplified models provided rapid prediction of three milk powder particle size fractions and improved coefficients of prediction as well.

Hyperspectral images of coarse, medium and fine particle fractions were recorded. Spectral features, in terms of the average spectra, were produced for each of these milk powder fractions. Although the study found that spectral variation was evident in the samples of milk powders that belong to three different particle size ranges. However, actual products of instant whole milk powder production consist of all of these particle size fractions and can be any combination of coarse, medium and fine particle fractions. Therefore, seven types of reconstructed milk powder samples were prepared by recombining coarse, medium and fine particle fractions. Hyperspectral imaging was used to extract the spectral and spatial information for reconstructed milk powder samples. Euclidean distance was used for the classification of pixels to coarse, medium or fine in a reconstructed milk powder sample. Moreover, the distributions of coarse, medium and

fine pixel classes were compared with the actual, known distribution of coarse, medium and fine particle fractions in the prepared samples. It was interesting to note that the two distributions were close with a correlation coefficient of 0.98. These reconstructed milk powder samples were manually tested for bulk density and dispersibility. Partial least squares regression models successfully predicted bulk density and dispersibility of these samples with prediction coefficients of 0.896 and 0.865, respectively.

6.3. Near-infrared spectroscopy and/or hyperspectral imaging for milk powder quality

The current research was mainly focused for analysing the potential of two analysers (near-infrared spectrometer and hyperspectral imaging) for estimating the quality of instant milk powder in-terms of dispersibility, bulk density and distribution of three discrete particle size fractions. Prediction and classification results of the two analysers have been already discussed thoroughly in the relevant chapters. The spectral ranges of both instruments were entirely different. Near-infrared spectrometer has operational wavelength range of 1000nm – 2500nm. Hyperspectral imaging equipment has performed between the 400nm – 1000nm spectral wavelength range. Therefore, a comparative analysis of two might not be useful at this stage. However, NIR has predicted bulk density and dispersibility with higher accuracy than predicting the distribution of fine particle fraction in a milk powder sample within the 1000nm – 2500nm. Furthermore, hyperspectral imaging was more accurate in predicting the distribution of particle size fractions than dispersibility and bulk density of a milk powder sample in the spectral range of 400nm -1000nm. A possible reason could be that HSI is capable to get more spectral information of a milk powder sample than one spectrum produced by NIR analyser. This feature might have helped to better analysed and predict the distribution of discrete particle size fraction of milk powder. On the contrary, one

average spectrum per sample generated by NIR spectrometer was sufficient enough to predict bulk density and dispersibility of that sample. However, it is important to emphasised again that a comprehensive comparison of both analysers can be performed only if the two equipment would analyse milk powder samples for a similar wavelength range.

6.4. Limitations

1. The current research can present particle size distribution information only in terms of three particle size fractions. Therefore, it may not replace the detailed particle size distributions produced by specialised size analysis equipment.

2. Wu et al. (2008) have reported similar type of milk powders from different commercial brands had compositional variations. Distinct manufacturing units and operating conditions might be the reason for these protein and fat content variation. Therefore, a single commercial brand of IWMP was used in this research and the calibration and prediction results of the models may be specific to this brand. However, it is worth mentioning that results of this research provides a proof of concept for any dairy powder manufacturing brand to adopt, modify and improve the methods for their product.

3. The current research was based upon instant whole milk powder (IWMP) only and different observations may be obtained if another type of milk powder is analysed.

6.5. Future Recommendations

Some recommendations for future work may include the following.

1. Particle size ranges of the milk powder fraction can be narrowed to increase the number of fractions in the subsequent analysis.

2. Multivariate data analysis of the HSI data can be extended by other statistical methods such as soft independent modelling of class analogy (SIMCA) for supervised classification.

3. Simplified wavelength models presented in Chapter 5 can be further used to produce prediction maps of particle size fractions in the milk powder sample for visualisation purposes. Furthermore, image analysis methods can be applied to these prediction maps to reproduce the distribution of various particle size fractions in the milk powder sample.

4. Considering the process parameters with the product quality and spectroscopic data in the analysis domain may be beneficial towards the potential of at-line / on-line monitoring of IWMP quality.

Each of the topics mentioned above could stand alone as a research idea, expanding horizons into even more potential improvements and beneficial application.

References

Abasi, S., S. Minaei, B. Jamshidi, D. Fathi and M. H. Khoshtaghaza (2019). "Rapid measurement of apple quality parameters using wavelet de-noising transform with Vis/NIR analysis." Scientia Horticulturae **252**: 7-13.

Abdi, H. (2010). "Partial least squares regression and projection on latent structure regression (PLS Regression)." WIREs Computational Statistics **2**(1): 97-106.

Abdi, H. and L. J. Williams (2010). "Principal component analysis." Wiley interdisciplinary reviews: computational statistics **2**(4): 433-459.

Achata, E. M., C. Esquerre, A. A. Gowen and C. P. O'Donnell (2018). "Feasibility of near infrared and Raman hyperspectral imaging combined with multivariate analysis to assess binary mixtures of food powders." Powder Technology **336**: 555-566.

Al-Sarayreh, M., M. M. Reis, W. Q. Yan and R. Klette (2017). Detection of adulteration in red meat species using hyperspectral imaging. Pacific-Rim Symposium on Image and Video Technology, Springer.

Alessandrini, L., S. Romani, G. Pinnavaia and M. Dalla Rosa (2008). "Near infrared spectroscopy: An analytical tool to predict coffee roasting degree." Analytica Chimica Acta **625**(1): 95-102.

Amigo, J. M. (2019). Data Handling in Science and Technology, Elsevier.

Amigo, J. M., H. Babamoradi and S. Elcoroaristizabal (2015). "Hyperspectral image analysis. A tutorial." Analytica Chimica Acta **896**: 34-51.

Amigo, J. M., I. Martí and A. Gowen (2013). Chapter 9 - Hyperspectral Imaging and Chemometrics: A Perfect Combination for the Analysis of Food Structure, Composition and Quality. Data Handling in Science and Technology. M. Federico. United Kingdom, Elsevier. **Volume 28:** 343-370.

Andresen, M. S., B. S. Dissing and H. Løje (2013). "Quality assessment of butter cookies applying multispectral imaging." Food Science & Nutrition **1**(4): 315-323.

Andrew, J. O. N., D. J. Roger and C. M. Anthony (1999). "Measurement of the cumulative particle size distribution of microcrystalline cellulose using near infrared reflectance spectroscopy." Analyst **124** 33-36.

Anzanello, M. and F. Fogliatto (2014). "A review of recent variable selection methods in industrial and chemometrics applications." European J. of Industrial Engineering **8**: 619.

Araújo, M. C. U., T. C. B. Saldanha, R. K. H. Galvão, T. Yoneyama, H. C. Chame and V. Visani (2001). "The successive projections algorithm for variable selection in spectroscopic multicomponent analysis." Chemometrics and Intelligent Laboratory Systems **57**(2): 65-73.

Ariana, D. P. and R. Lu (2008). "Detection of internal defect in pickling cucumbers using hyperspectral transmittance imaging." Transactions of the ASABE **51**(2): 705-713.

Bai, S. H., I. Tahmasbian, J. Zhou, T. Nevenimo, G. Hannet, D. Walton, B. Randall, T. Gama and H. M. Wallace (2018). "A non-destructive determination of peroxide values, total nitrogen and mineral nutrients in an edible tree nut using hyperspectral imaging." Computers and Electronics in Agriculture **151**: 492-500.

Baiano, A. (2017). "Applications of hyperspectral imaging for quality assessment of liquid based and semi-liquid food products: A review." Journal of Food Engineering **214**: 10-15.

Balabin, R. M. and S. V. Smirnov (2011). "Melamine detection by mid- and near-infrared (MIR/NIR) spectroscopy: A quick and sensitive method for dairy products analysis including liquid milk, infant formula, and milk powder." Talanta **85**(1): 562-568.

Bannon, D. (2009). "Cubes and slices." Nature photonics **3**(11): 627-629.

Baranowski, P., W. Mazurek and J. Pastuszka-Woźniak (2013). "Supervised classification of bruised apples with respect to the time after bruising on the basis of hyperspectral imaging data." Postharvest Biology and Technology **86**: 249-258.

Barnes, R. J., M. S. Dhanoa and S. J. Lister (1989). "Standard Normal Variate Transformation and De-trending of Near-Infrared Diffuse Reflectance Spectra." Applied Spectroscopy **43**(5): 772-777.

Barreto, A., J. P. Cruz-Tirado, R. Siche and R. Quevedo (2018). "Determination of starch content in adulterated fresh cheese using hyperspectral imaging." Food Bioscience **21**: 14-19.

Behrend, C. J., C. P. Tarnowski and M. D. Morris (2002). "Identification of Outliers in Hyperspectral Raman Image Data by Nearest Neighbor Comparison." Applied Spectroscopy **56**(11): 1458-1461.

Bhandari, B. R., N. Bansal, M. Zhang and P. Schuck (2013). Handbook of food powders: processes and properties, Elsevier.

Blanco, M. and A. Peguero (2008). "An expeditious method for determining particle size distribution by near infrared spectroscopy: Comparison of PLS2 and ANN models." Talanta **77**(2): 647-651.

Blyth, A. W. (1896). Foods: Their Composition and Analysis: A Manual for the Use of Analytical Chemists and Others" C. Griffin.

Boiarkina, I., N. Depree, W. Yu, D. Wilson and B. Young (2017). "Rapid particle size measurements used as a proxy to control instant whole milk powder dispersibility." Dairy Science & Technology **96**(6): 777-786.

Boiarkina, I., C. Sang, N. Depree, A. Prince-Pike, W. Yu, D. I. Wilson and B. R. Young (2016). "The significance of powder breakdown during conveying within industrial milk powder plants." Advanced powder technology **27**(6): 2363-2369.

Boiarkina, I., C. Sang, N. Depree, A. Prince-Pike, W. Yu, B. Young and D. Wilson (2016). "The significance of powder breakdown during conveying within industrial milk powder plants." Advanced powder technology **27**(6): 2363-2369.

Brereton, R. G. and G. R. Lloyd (2014). "Partial least squares discriminant analysis: taking the magic away." Journal of Chemometrics **28**(4): 213-225.

Brown, S. D. (2017). "The chemometrics revolution re-examined." Journal of Chemometrics **31**(1): e2856.

Burger, J. and P. Geladi (2005). "Hyperspectral NIR image regression part I: Calibration and correction." Journal of Chemometrics **19**(5-7): 355-363.

Burger, J. and P. Geladi (2006). "Hyperspectral NIR image regression part II: dataset preprocessing diagnostics." Journal of Chemometrics **20**(3-4): 106-119.

Bylund, G. (2003). Dairy processing handbook, Tetra Pak Processing Systems AB.

Cai, W., Y. Li and X. Shao (2008). "A variable selection method based on uninformative variable elimination for multivariate calibration of near-infrared spectra." Chemometrics and Intelligent Laboratory Systems **90**(2): 188-194.

Cannistraci, C. V., F. M. Montevecchi and M. Alessio (2009). "Median-modified Wiener filter provides efficient denoising, preserving spot edge and morphology in 2-DE image processing." Proteomics **9**(21): 4908-4919.

Caporaso, N., M. B. Whitworth, S. Grebby and I. D. Fisk (2018). "Non-destructive analysis of sucrose, caffeine and trigonelline on single green coffee beans by hyperspectral imaging." Food Research International **106**: 193-203.

Caric, M. (2004). "Dairy: milk powders." Principles and Applications: 319.

Chang, C.-I., Q. Du, T.-L. Sun and M. L. Althouse (1999). "A joint band prioritization and band-decorrelation approach to band selection for hyperspectral image classification." IEEE Transactions on Geoscience and Remote Sensing **37**(6): 2631-2641.

Chang, C.-W., D. A. Laird, M. J. Mausbach and C. R. Hurburgh (2001). "Near-infrared reflectance spectroscopy–principal components regression analyses of soil properties." Soil Science Society of America Journal **65**(2): 480-490.

Chelladurai, V. and D. S. Jayas (2014). Near-infrared Imaging and Spectroscopy. Imaging with Electromagnetic Spectrum: Applications in Food and Agriculture. A. Manickavasagan and H. Jayasuriya. Berlin, Heidelberg, Springer Berlin Heidelberg**:** 87-127.

Chen, H., C. Tan, Z. Lin and T. Wu (2018). "Classification and quantitation of milk powder by near-infrared spectroscopy and mutual information-based variable selection and partial least squares." Spectrochimica Acta Part A: Molecular and Biomolecular Spectroscopy **189**: 183-189.

Chong, I.-G. and C.-H. Jun (2005). "Performance of some variable selection methods when multicollinearity is present." Chemometrics and Intelligent Laboratory Systems **78**(1-2): 103-112.

Cleveland, W. S., S. J. Devlin and E. Grosse (1988). "Regression by local fitting: Methods, properties, and computational algorithms." Journal of econometrics **37**(1): 87-114.

Crowley, S. V., B. Desautel, I. Gazi, A. L. Kelly, T. Huppertz and J. A. O'Mahony (2015). "Rehydration characteristics of milk protein concentrate powders." Journal of Food Engineering **149**: 105-113.

Dale, L. M., A. Thewis, C. Boudry, I. Rotar, P. Dardenne, V. Baeten and J. A. F. Pierna (2013). "Hyperspectral Imaging Applications in Agriculture and Agro-Food Product Quality and Safety Control: A Review." Applied Spectroscopy Reviews **48**(2): 142-159.

Destremau, K. and P. Siddharth (2018). How does the dairy sector share its growth? An analysis of the flow-on benefits of dairy's revenue generation. Wllington, NZ Institute of Economic Research.

Di, W., Y. Haiqing, F. Shuijuan, C. Xiaojing and H. Yong (2008). Short-wave near-infrared spectroscopy technique for fast determination of carbohydrate content in milk powder. 2008 International Conference on Microwave and Millimeter Wave Technology, Nanjing, China, IEEE.

Diezma, B., L. Lleó, J. M. Roger, A. Herrero-Langreo, L. Lunadei and M. Ruiz-Altisent (2013). "Examination of the quality of spinach leaves using hyperspectral imaging." Postharvest Biology and Technology **85**: 8-17.

Dowell, F. E., J. E. Throne and J. E. Baker (1998). "Automated nondestructive detection of internal insect infestation of wheat kernels by using near-infrared reflectance spectroscopy." Journal of Economic Entomology **91**(4): 899-904.

Downey, G., E. Sheehan, C. Delahunty, D. O'Callaghan, T. Guinee and V. Howard (2005). "Prediction of maturity and sensory attributes of Cheddar cheese using near-infrared spectroscopy." International Dairy Journal **15**(6-9): 701-709.

Dufour, É. (2011). "Recent advances in the analysis of dairy product quality using methods based on the interactions of light with matter." International Journal of Dairy Technology **64**(2): 153-165.

El Jabri, M., M. P. Sanchez, P. Trossat, C. Laithier, V. Wolf, P. Grosperrin, E. Beuvier, O. Rolet-Répécaud, S. Gavoye, Y. Gaüzère, O. Belysheva, E. Notz, D. Boichard and A. Delacroix-Buchet (2019). "Comparison of Bayesian and partial least squares regression methods for mid-infrared prediction of cheese-making properties in Montbeliarde cows." Journal of Dairy Science **102**(8): 6943-6958.

ElMasry, G., A. Iqbal, D.-W. Sun, P. Allen and P. Ward (2011). "Quality classification of cooked, sliced turkey hams using NIR hyperspectral imaging system." Journal of Food Engineering **103**(3): 333-344.

ElMasry, G., D.-W. Sun and P. Allen (2012). "Near-infrared hyperspectral imaging for predicting colour, pH and tenderness of fresh beef." Journal of Food Engineering **110**(1): 127-140.

ElMasry, G., N. Wang, A. ElSayed and M. Ngadi (2007). "Hyperspectral imaging for nondestructive determination of some quality attributes for strawberry." Journal of Food Engineering **81**(1): 98-107.

ElMasry, G., N. Wang and C. Vigneault (2009). "Detecting chilling injury in Red Delicious apple using hyperspectral imaging and neural networks." Postharvest Biology and Technology **52**(1): 1-8.

EMA, E. M. A. (2009). Guideline on the use of near infrared spectroscopy by the pharmaceutical industry and the data requirements for new submissions and variations, Committee for human medicinal products.

Eriksson, L., E. Johansson and C. Wikström (1998). "Mixture design—design generation, PLS analysis, and model usage." Chemometrics and Intelligent Laboratory Systems **43**(1): 1-24.

Erkinbaev, C., K. Derksen and J. Paliwal (2019). "Single kernel wheat hardness estimation using near infrared hyperspectral imaging." Infrared Physics & Technology **98**: 250-255.

Esbensen, K. H., D. Guyot, F. Westad and L. P. Houmoller (2002). Multivariate data analysis: in practice: an introduction to multivariate data analysis and experimental design, Multivariate Data Analysis.

FDA (2004). PAT — A framework for innovative pharmaceutical development, manufacturing, and quality assurance. Rockville, MD, U.S. Department of Health and Human Services. Food and Drug Administration Center for Biologics Evaluation and Research.

Feng, C.-H., Y. Makino, S. Oshita and J. F. García Martín (2018). "Hyperspectral imaging and multispectral imaging as the novel techniques for detecting defects in raw and processed meat products: Current state-of-the-art research advances." Food Control **84**: 165-176.

Feng, Y.-Z., G. ElMasry, D.-W. Sun, A. G. M. Scannell, D. Walsh and N. Morcy (2013). "Near-infrared hyperspectral imaging and partial least squares regression for rapid and reagentless determination of Enterobacteriaceae on chicken fillets." Food Chemistry **138**(2): 1829-1836.

Feng, Y.-Z. and D.-W. Sun (2012). "Application of Hyperspectral Imaging in Food Safety Inspection and Control: A Review." Critical Reviews in Food Science and Nutrition **52**(11): 1039-1058.

Feuerstein, D., K. H. Parker and M. G. Boutelle (2009). "Practical methods for noise removal: applications to spikes, nonstationary quasi-periodic noise, and baseline drift." Analytical chemistry **81**(12): 4987-4994.

Forchetti, D. A. P. and R. J. Poppi (2017). "Use of NIR hyperspectral imaging and multivariate curve resolution (MCR) for detection and quantification of adulterants in milk powder." LWT - Food Science and Technology **76**: 337-343.

Fu, X. and J. Chen (2019). "A Review of Hyperspectral Imaging for Chicken Meat Safety and Quality Evaluation: Application, Hardware, and Software." Comprehensive Reviews in Food Science and Food Safety **18**(2): 535-547.

Fu, X., M. S. Kim, K. Chao, J. Qin, J. Lim, H. Lee, A. Garrido-Varo, D. Pérez-Marín and Y. Ying (2014). "Detection of melamine in milk powders based on NIR hyperspectral imaging and spectral similarity analyses." Journal of Food Engineering **124**: 97-104.

Fu, X., M. S. Kim, K. Chao, J. Qin, J. Lim, H. Lee, A. Garrido-Varo, D. Pérez-Marín and Y. Ying (2014). "Detection of melamine in milk powders based on NIR hyperspectral imaging and spectral similarity analyses." Journal of Food Engineering **124**: 97-104.

García-Cañas, V., C. Simó, M. Herrero, E. Ibáñez and A. Cifuentes (2012). "Present and Future Challenges in Food Analysis: Foodomics." Analytical chemistry **84**(23): 10150-10159.

Garcia, D. (2010). "Robust smoothing of gridded data in one and higher dimensions with missing values." Computational Statistics & Data Analysis **54**(4): 1167-1178.

Geladi, P. and M. Manley (2010). Near-Infrared Hyperspectral Imaging in Food Research. Raman, Infrared, and Near-Infrared Chemical Imaging, John Wiley & Sons, Inc.**:** 243-260.

Gholizadeh, A., L. Borůvka, M. Saberioon and R. Vašát (2013). "Visible, near-infrared, and mid-infrared spectroscopy applications for soil assessment with emphasis on soil organic matter content and quality: State-of-the-art and key issues." Applied Spectroscopy **67**(12): 1349-1362.

Giovenzana, V., R. Beghi, R. Civelli and R. Guidetti (2015). "Optical techniques for rapid quality monitoring along minimally processed fruit and vegetable chain." Trends in Food Science & Technology **46**(2, Part B): 331-338.

Gowen, A., C. O'Donnell, P. Cullen, G. Downey and J. Frias (2007). "Hyperspectral imaging–an emerging process analytical tool for food quality and safety control." Trends in Food Science & Technology **18**(12): 590-598.

Gowen, A., C. O'Donnell, P. Cullen, G. Downey and J. Frias (2007). "Hyperspectral imaging–an emerging process analytical tool for food quality and safety control." Trends in Food Science & Technology **18**(12): 590-598.

Gowen, A. A., C. P. O'Donnell, J. Burger and D. J. O'Callaghan (2011). Analytical Methods | Hyperspectral Imaging for Dairy Products A2 - Fuquay, John W. Encyclopedia of Dairy Sciences (Second Edition). San Diego, Academic Press**:** 125-132.

Gupta, A., G. E. Peck, R. W. Miller and K. R. Morris (2004). "Nondestructive measurements of the compact strength and the particle-size distribution after milling of roller compacted powders by near-infrared spectroscopy." Journal of Pharmaceutical Sciences **93**(4): 1047-1053.

Haralick, R. M., K. Shanmugam and I. H. Dinstein (1973). "Textural features for image classification." IEEE Transactions on systems, man, and cybernetics(6): 610-621.

Heigl, N., C. Petter, M. Rainer, M. Najam-ul-Haq, R. Vallant, R. Bakry, G. Bonn and C. Huck (2007). "Near infrared spectroscopy for polymer research, quality control and reaction monitoring." Journal of Near Infrared Spectroscopy **15**(5): 269-282.

Holroyd, S. E., B. Prescott and A. McClean (2013). "The use of in-and on-line near infrared spectroscopy for milk powder measurement." Journal of Near Infrared Spectroscopy **21**(5): 441-443.

Huang, H., L. Liu and M. Ngadi (2014). "Recent Developments in Hyperspectral Imaging for Assessment of Food Quality and Safety." Sensors **14**(4): 7248.

Huang, M., M. Kim, K. Chao, J. Qin, C. Mo, C. Esquerre, S. Delwiche and Q. Zhu (2016a). "Penetration Depth Measurement of Near-Infrared Hyperspectral Imaging Light for Milk Powder." Sensors **16**(4): 441.

Huang, M., M. S. Kim, S. R. Delwiche, K. Chao, J. Qin, C. Mo, C. Esquerre and Q. Zhu (2016b). "Quantitative analysis of melamine in milk powders using near-infrared hyperspectral imaging and band ratio." Journal of Food Engineering **181**: 10-19.

Huang, M., Q. Wang, M. Zhang and Q. Zhu (2014a). "Prediction of color and moisture content for vegetable soybean during drying using hyperspectral imaging technology." Journal of Food Engineering **128**: 24-30.

Huang, Y., S. Min, J. Duan, L. Wu and Q. Li (2014b). "Identification of additive components in powdered milk by NIR imaging methods." Food Chemistry **145**: 278-283.

Huang, Y., K. Tian, S. Min, Y. Xiong and G. Du (2015). "Distribution assessment and quantification of counterfeit melamine in powdered milk by NIR imaging methods." Food Chemistry **177**: 174-181.

Hussain, A., H. Pu and D.-W. Sun (2018). "Innovative nondestructive imaging techniques for ripening and maturity of fruits–a review of recent applications." Trends in Food Science & Technology **72**: 144-152.

Hussain, R., C. Gaiani, C. Jeandel, J. Ghanbaja and J. Scher (2012). "Combined effect of heat treatment and ionic strength on the functionality of whey proteins." Journal of Dairy Science **95**(11): 6260-6273.

IDF (2005). Dried milk and dried milk products. Determination of bulk density. Milk and processed milk products. Netherlands, International Dairy Federation. **IDF 134:2005:** 6.

Isaksson, T. and T. Næs (1988). "The Effect of Multiplicative Scatter Correction (MSC) and Linearity Improvement in NIR Spectroscopy." Applied Spectroscopy **42**(7): 1273-1284.

Islam, T. (2019). Overseas goods trade – 2018 in review. Wellington, New Zealand.

ISO, I. O. f. S. (2014). Instant dried milk -- Determination of the dispersibility and wettability ISO/TS 17758|IDF/RM 87:2014. Milk and processed milk products, International Organization for Standardization.

Itoh, H., S. Kanda, H. Matsuura, N. Shiraishi, K. Sakai and A. Sasao (2010). "Measurement of nitrate concentration distribution in vegetables by near-infrared hyperspectral imaging." Environmental Control in Biology **48**(2): 37-49.

Jain, A. K., M. N. Murty and P. J. Flynn (1999). "Data clustering: a review." ACM Comput. Surv. **31**(3): 264-323.

Jawaid, S., F. N. Talpur, S. Sherazi, S. M. Nizamani and A. A. Khaskheli (2013). "Rapid detection of melamine adulteration in dairy milk by SB-ATR–Fourier transform infrared spectroscopy." Food Chemistry **141**(3): 3066-3071.

Jha, P. K., E. Xanthakis, S. Chevallier, V. Jury and A. Le-Bail (2019). "Assessment of freeze damage in fruits and vegetables." Food Research International **121**: 479-496.

Ji, J., J. Fitzpatrick, K. Cronin, P. Maguire, H. Zhang and S. Miao (2016). "Rehydration behaviours of high protein dairy powders: The influence of agglomeration on wettability, dispersibility and solubility." Food Hydrocolloids **58**: 194-203.

Jin, L. Q. and Q. H. Xu (2011). Application of near infrared spectroscopy and multivariate analysis in the forest products industry. Advanced Materials Research, Trans Tech Publ.

John Ballingall and D. Pambudi (2017). Dairy trade's economic contribution to New Zealand. Wellington, New Zealand, NZ Institute of Economic Research (NZIER).

Jolliffe, I. (2002). Principal component analysis, Wiley Online Library.

Kaddour, A. A. and B. Cuq (2009). "In line monitoring of wet agglomeration of wheat flour using near infrared spectroscopy." Powder Technology **190**(1-2): 10-18.

Kamruzzaman, M., G. ElMasry, D.-W. Sun and P. Allen (2011). "Application of NIR hyperspectral imaging for discrimination of lamb muscles." Journal of Food Engineering **104**(3): 332-340.

Kamruzzaman, M., G. ElMasry, D.-W. Sun and P. Allen (2012). "Prediction of some quality attributes of lamb meat using near-infrared hyperspectral imaging and multivariate analysis." Analytica Chimica Acta **714**: 57-67.

Kamruzzaman, M., Y. Makino and S. Oshita (2016). "Online monitoring of red meat color using hyperspectral imaging." Meat Science **116**: 110-117.

Kandelbauer, A., M. Rahe and R. W. Kessler (2012). "Industrial perspectives." Handbook of Biophotonics.

Kandpal, L. M., J. Tewari, N. Gopinathan, J. Stolee, R. Strong, P. Boulas and B.-K. Cho (2017). "Quality assessment of pharmaceutical tablet samples using Fourier transform near infrared spectroscopy and multivariate analysis." Infrared Physics & Technology **85**: 300-306.

Karoui, R. (2017). Methodologies for the Characterization of the Quality of Dairy Products. Advances in food and nutrition research, Elsevier. **82:** 237-275.

Karoui, R., G. Downey and C. Blecker (2010). "Mid-Infrared Spectroscopy Coupled with Chemometrics: A Tool for the Analysis of Intact Food Systems and the Exploration of

Their Molecular Structure−Quality Relationships − A Review." Chemical Reviews **110**(10): 6144-6168.

Kelly, A. L., J. E. O'Connell and P. F. Fox (2003). Manufacture and Properties of Milk Powders. Advanced Dairy Chemistry—1 Proteins: Part A / Part B. P. F. Fox and P. L. H. McSweeney. Boston, MA, Springer US**:** 1027-1061.

Kelly, J., P. M. Kelly and D. Harrington (2002). "Influence of processing variables on the physicochemical properties of spray dried fat-based milk powders." Le Lait **82**(4): 401-412.

Kelly, P. M. (2006). "Innovation in milk powder technology." International Journal of Dairy Technology **59**(2): 70-75.

Kim, E. H.-J., X. Dong Chen and D. Pearce (2003). "On the mechanisms of surface formation and the surface compositions of industrial milk powders." Drying Technology **21**(2): 265-278.

Kim, E. H. J., X. D. Chen and D. Pearce (2002). "Surface characterization of four industrial spray-dried dairy powders in relation to chemical composition, structure and wetting property." Colloids and Surfaces B: Biointerfaces **26**(3): 197-212.

Kim, E. H. J., X. D. Chen and D. Pearce (2009). "Surface composition of industrial spray-dried milk powders. 2. Effects of spray drying conditions on the surface composition." Journal of Food Engineering **94**(2): 169-181.

Kong, W., C. Zhang, F. Liu, P. Nie and Y. He (2013). "Rice seed cultivar identification using near-infrared hyperspectral imaging and multivariate data analysis." Sensors **13**(7): 8916-8927.

Kulmyrzaev, A., D. Bertrand and É. Dufour (2008). "Characterization of different blue cheeses using a custom-design multispectral imager." Dairy Science and Technology **88**(4-5): 537-548.

Lachenmeier, D. W. and W. Kessler (2008). "Multivariate curve resolution of spectrophotometric data for the determination of artificial food colors." Journal of Agricultural and Food Chemistry **56**(14): 5463-5468.

Lammers, W., H. Van Der Stege and P. Walstra (1987). "Determination of the particle size distribution of non-agglomerated milk powders." Netherlands Milk and Dairy Journal **41**: 147-160.

Lee, J., C. Chai, D. J. Park, K. Lim and J.-Y. Imm (2014). "Novel Convenient Method to Determine Wettability and Dispersibility of Dairy Powders." Korean journal for food science of animal resources **34**(6): 852-857.

Li-Chan, E., J. M. Chalmers and P. R. Griffiths (2010). Applications of vibrational spectroscopy in food science, John Wiley & Sons.

Li, B., M. Cobo-Medina, J. Lecourt, N. Harrison, R. J. Harrison and J. V. Cross (2018). "Application of hyperspectral imaging for nondestructive measurement of plum quality attributes." Postharvest Biology and Technology **141**: 8-15.

Li, H.-D., Y.-Z. Liang, Q. Xu and D.-S. Cao (2009). Key wavelength screening using competitive adaptive reweighted sampling method for multivariate calibration.

Li, J.-L., D.-W. Sun and J.-H. Cheng (2016). "Recent Advances in Nondestructive Analytical Techniques for Determining the Total Soluble Solids in Fruits: A Review." Comprehensive Reviews in Food Science and Food Safety **15**(5): 897-911.

Li, J., J. M. Bioucas-Dias and A. Plaza (2012). "Spectral&Spatial Hyperspectral Image Segmentation Using Subspace Multinomial Logistic Regression and Markov Random Fields." IEEE Transactions on Geoscience and Remote Sensing **50**(3): 809-823.

Liu, D., D.-W. Sun and X.-A. Zeng (2014). "Recent Advances in Wavelength Selection Techniques for Hyperspectral Image Processing in the Food Industry." Food and Bioprocess Technology **7**(2): 307-323.

Liu, Y., H. Pu and D.-W. Sun (2017). "Hyperspectral imaging technique for evaluating food quality and safety during various processes: A review of recent applications." Trends in Food Science & Technology **69**: 25-35.

Lohumi, S., S. Lee, H. Lee and B.-K. Cho (2015). "A review of vibrational spectroscopic techniques for the detection of food authenticity and adulteration." Trends in Food Science & Technology **46**(1): 85-98.

López-Maestresalas, A., J. C. Keresztes, M. Goodarzi, S. Arazuri, C. Jarén and W. Saeys (2016). "Non-destructive detection of blackspot in potatoes by Vis-NIR and SWIR hyperspectral imaging." Food Control **70**: 229-241.

Lü, Q. and M. Tang (2012). "Detection of hidden bruise on kiwi fruit using hyperspectral imaging and parallelepiped classification." Procedia Environmental Sciences **12**: 1172-1179.

M. ElMasry, G. and S. Nakauchi (2016). "Image analysis operations applied to hyperspectral images for non-invasive sensing of food quality – A comprehensive review." Biosystems Engineering **142**: 53-82.

Ma, F., H. Qin, K. Shi, C. Zhou, C. Chen, X. Hu and L. Zheng (2016). "Feasibility of combining spectra with texture data of multispectral imaging to predict heme and non-heme iron contents in pork sausages." Food Chemistry **190**: 142-149.

Ma, J., D.-W. Sun, H. Pu, Q. Wei and X. Wang (2019). "Protein content evaluation of processed pork meats based on a novel single shot (snapshot) hyperspectral imaging sensor." Journal of Food Engineering **240**: 207-213.

Mahesh, S., D. Jayas, J. Paliwal and N. White (2015). "Comparison of partial least squares regression (PLSR) and principal components regression (PCR) methods for protein and hardness predictions using the near-infrared (NIR) hyperspectral images of bulk samples of Canadian wheat." Food and Bioprocess Technology **8**(1): 31-40.

Manley, M. (2014). "Near-infrared spectroscopy and hyperspectral imaging: non-destructive analysis of biological materials." Chemical Society Reviews **43**(24): 8200-8214.

Manley, M., G. Downey and V. Baeten (2008). "Spectroscopic technique: near-infrared (NIR) spectroscopy." Modern Techniques for Food Authentication **1**.

Märk, J., M. Andre, M. Karner and C. W. Huck (2010). "Prospects for multivariate classification of a pharmaceutical intermediate with near-infrared spectroscopy as a process analytical technology (PAT) production control supplement." European Journal of Pharmaceutics and Biopharmaceutics **76**(2): 320-327.

Mattila, M., K. Saloheimo and K. Koskinen (2007). "Improving the Robustness of Particle Size Analysis by Multivariate Statistical Process Control." Particle & Particle Systems Characterization **24**(3): 173-183.

McGoverin, C. M., P. Engelbrecht, P. Geladi and M. Manley (2011). "Characterisation of non-viable whole barley, wheat and sorghum grains using near-infrared hyperspectral data and chemometrics." Analytical and bioanalytical chemistry **401**(7): 2283.

Mehmood, T., K. H. Liland, L. Snipen and S. Sæbø (2012). "A review of variable selection methods in Partial Least Squares Regression." Chemometrics and Intelligent Laboratory Systems **118**: 62-69.

Melfsen, A., E. Hartung and A. Haeussermann (2012). "Accuracy of milk composition analysis with near infrared spectroscopy in diffuse reflection mode." Biosystems Engineering **112**(3): 210-217.

Moore, J. C., A. Ganguly, J. Smeller, L. Botros, M. Mossoba and M. M. Bergana (2012). "Standardisation of non-targeted screening tools to detect adulterations in skim milk powder using NIR spectroscopy and chemometrics." NIR news **23**(5): 9-11.

Moros, J., S. Garrigues and M. de la Guardia (2010). "Vibrational spectroscopy provides a green tool for multi-component analysis." TrAC Trends in Analytical Chemistry **29**(7): 578-591.

Munera, S., J. Blasco, J. M. Amigo, S. Cubero, P. Talens and N. Aleixos (2019). "Use of hyperspectral transmittance imaging to evaluate the internal quality of nectarines." Biosystems Engineering **182**: 54-64.

Munir, M. T., D. I. Wilson, N. Depree, I. Boiarkina, A. Prince-Pike and B. R. Young (2017). "Real-time product release and process control challenges in the dairy milk powder industry." Current Opinion in Food Science **17**: 25-29.

Munir, M. T., D. I. Wilson, W. Yu and B. R. Young (2018). "An evaluation of hyperspectral imaging for characterising milk powders." Journal of Food Engineering **221**: 1-10.

Munir, M. T., W. Yu, B. R. Young and D. I. Wilson (2015). "The current status of process analytical technologies in the dairy industry." Trends in Food Science & Technology **43**(2): 205-218.

Naganathan, G. K., L. M. Grimes, J. Subbiah, C. R. Calkins, A. Samal and G. E. Meyer (2008). "Visible/near-infrared hyperspectral imaging for beef tenderness prediction." Computers and Electronics in Agriculture **64**(2): 225-233.

Nakakimura, Y., M. Vassileva, T. Stoyanchev, K. Nakai, R. Osawa, J. Kawano and R. Tsenkova (2012). "Extracellular metabolites play a dominant role in near-infrared spectroscopic quantification of bacteria at food-safety level concentrations." Analytical Methods **4**(5): 1389-1394.

Nakariyakul, S. and D. P. Casasent (2011). "Classification of internally damaged almond nuts using hyperspectral imagery." Journal of Food Engineering **103**(1): 62-67.

Nansen, C., K. Singh, A. Mian, B. J. Allison and C. W. Simmons (2016). "Using hyperspectral imaging to characterize consistency of coffee brands and their respective roasting classes." Journal of Food Engineering **190**: 34-39.

Nanyam, Y., R. Choudhary, L. Gupta and J. Paliwal (2012). "A decision-fusion strategy for fruit quality inspection using hyperspectral imaging." Biosystems Engineering **111**(1): 118-125.

Nguyen-Do-Trong, N., J. C. Dusabumuremyi and W. Saeys (2018). "Cross-polarized VNIR hyperspectral reflectance imaging for non-destructive quality evaluation of dried banana slices, drying process monitoring and control." Journal of Food Engineering **238**: 85-94.

Niamh Burke, K. A. Z., Mark Southern, Paul Hogan, Michael P. Ryan, Catherine C. Adley (2018). The Dairy Industry: Process, Monitoring, Standards, and Quality. Descriptive Food Science. A. V. D. a. R. M. García-Gimeno. UK, IntechOpen Limited.

Norris, K. H. (1996). "History of NIR." Journal of Near Infrared Spectroscopy **4**(1): 31-37.

Núñez-Sánchez, N., A. Martínez-Marín, O. Polvillo, V. Fernández-Cabanás, J. Carrizosa, B. Urrutia and J. Serradilla (2016). "Near Infrared Spectroscopy (NIRS) for the determination of the milk fat fatty acid profile of goats." Food Chemistry **190**: 244-252.

OECD (2019). OECD-FAO Agricultural Outlook 2019-2028. USA, Organisation for Economic Co-operation and Development.

Oldfield, D. and H. Singh (2005). Functional Properties of Milk Powders. Encapsulated and Powdered Foods. USA, CRC Press**:** 365-386.

Osborne, D. S., R. Künnemeyer and R. B. Jordan (1997). "Method of Wavelength Selection for Partial Least Squares." Analyst **122**(12): 1531-1537.

Ozaki, Y., W. F. McClure and A. A. Christy (2006). Near-infrared spectroscopy in food science and technology, John Wiley & Sons.

Özkan, N., N. Walisinghe and X. D. Chen (2002). "Characterization of stickiness and cake formation in whole and skim milk powders." Journal of Food Engineering **55**(4): 293-303.

Pan, T. T., D. W. Sun, J. H. Cheng and H. Pu (2016). "Regression algorithms in hyperspectral data analysis for meat quality detection and evaluation." Comprehensive Reviews in Food Science and Food Safety **15**(3): 529-541.

Pasikatan, M. C., J. L. Steele, C. K. Spillman and E. Haque (2001). "Near infrared reflectance spectroscopy for online particle size analysis of powders and ground materials." Journal of Near Infrared Spectroscopy **9**(3): 153-164.

Pasquini, C. (2018). "Near infrared spectroscopy: A mature analytical technique with new perspectives – A review." Analytica Chimica Acta **1026**: 8-36.

Pavia, D. L., G. M. Lampman, G. S. Kriz and J. A. Vyvyan (2008). Introduction to spectroscopy, Cengage Learning.

Pérez-Santaescolástica, C., I. Fraeye, F. J. Barba, B. Gómez, I. Tomasevic, A. Romero, A. Moreno, F. Toldrá and J. M. Lorenzo (2019). "Application of non-invasive technologies in dry-cured ham: An overview." Trends in Food Science & Technology **86**: 360-374.

Pierna, J. F., V. Baeten, A. M. Renier, R. Cogdill and P. Dardenne (2004). "Combination of support vector machines (SVM) and near-infrared (NIR) imaging spectroscopy for the detection of meat and bone meal (MBM) in compound feeds." Journal of Chemometrics: A Journal of the Chemometrics Society **18**(7-8): 341-349.

Písecký, J. (2012). Handbook of milk powder manufacture. Copenhagen, Denmark, GEA Process Engineering A/S.

Poonia, A., A. Jha, R. Sharma, H. B. Singh, A. K. Rai and N. Sharma (2017). "Detection of adulteration in milk: A review." International Journal of Dairy Technology **70**(1): 23-42.

Prieto, N., O. Pawluczyk, M. E. R. Dugan and J. L. Aalhus (2017). "A review of the principles and applications of near-infrared spectroscopy to characterize meat, fat, and meat products." Applied Spectroscopy **71**(7): 1403-1426.

Priyashantha, H., A. Höjer, K. H. Saedén, Å. Lundh, M. Johansson, G. Bernes, P. Geladi and M. Hetta (2020). "Use of near-infrared hyperspectral (NIR-HS) imaging to visualize and model the maturity of long-ripening hard cheeses." Journal of Food Engineering **264**: 109687.

Qiao, T., J. Ren, C. Craigie, J. Zabalza, C. Maltin and S. Marshall (2015). "Singular spectrum analysis for improving hyperspectral imaging based beef eating quality evaluation." Computers and Electronics in Agriculture **115**: 21-25.

Rady, A. M., D. E. Guyer, W. Kirk and I. R. Donis-González (2014). "The potential use of visible/near infrared spectroscopy and hyperspectral imaging to predict processing-related constituents of potatoes." Journal of Food Engineering **135**: 11-25.

Rajalahti, T. and O. M. Kvalheim (2011). "Multivariate data analysis in pharmaceutics: A tutorial review." International Journal of Pharmaceutics **417**(1): 280-290.

Rajkumar, P., N. Wang, G. Eimasry, G. S. V. Raghavan and Y. Gariepy (2012). "Studies on banana fruit quality and maturity stages using hyperspectral imaging." Journal of Food Engineering **108**(1): 194-200.

Ravikanth, L., D. S. Jayas, N. D. G. White, P. G. Fields and D.-W. Sun (2017). "Extraction of Spectral Information from Hyperspectral Data and Application of Hyperspectral Imaging for Food and Agricultural Products." Food and Bioprocess Technology **10**(1): 1-33.

Reinsch, C. H. (1967). "Smoothing by spline functions." Numerische mathematik **10**(3): 177-183.

Reis, M. M., R. Van Beers, M. Al-Sarayreh, P. Shorten, W. Q. Yan, W. Saeys, R. Klette and C. Craigie (2018). "Chemometrics and hyperspectral imaging applied to assessment of chemical, textural and structural characteristics of meat." Meat Science **144**: 100-109.

Renzullo, L. J., A. L. Blanchfield and K. S. Powell (2006). "A method of wavelength selection and spectral discrimination of hyperspectral reflectance spectrometry." IEEE Transactions on Geoscience and Remote Sensing **44**(7): 1986-1994.

Resch, J. J. and C. R. Daubert (2002). "RHEOLOGICAL AND PHYSICOCHEMICAL PROPERTIES OF DERIVATIZED WHEY PROTEIN CONCENTRATE POWDERS." International Journal of Food Properties **5**(2): 419-434.

Ribeiro, J., M. Ferreira and T. Salva (2011). "Chemometric models for the quantitative descriptive sensory analysis of Arabica coffee beverages using near infrared spectroscopy." Talanta **83**(5): 1352-1358.

Rimpiläinen, V., J. P. Kaipio, N. Depree, B. R. Young and D. I. Wilson (2015). "Predicting functional properties of milk powder based on manufacturing data in an industrial-scale powder plant." Journal of Food Engineering **153**(Supplement C): 12-19.

Rinnan, Å., F. v. d. Berg and S. B. Engelsen (2009). "Review of the most common pre-processing techniques for near-infrared spectra." TrAC Trends in Analytical Chemistry **28**(10): 1201-1222.

Rivera, N. V., J. Gómez-Sanchis, J. Chanona-Pérez, J. J. Carrasco, M. Millán-Giraldo, D. Lorente, S. Cubero and J. Blasco (2014). "Early detection of mechanical damage in mango using NIR hyperspectral images and machine learning." Biosystems Engineering **122**: 91-98.

Rutlidge, H. T. and B. J. Reedy (2009). "Classification of Heterogeneous Solids Using Infrared Hyperspectral Imaging." Applied Spectroscopy **63**(2): 172-179.

Sanahuja, S., M. Fédou and H. Briesen (2018). "Classification of puffed snacks freshness based on crispiness-related mechanical and acoustical properties." Journal of Food Engineering **226**: 53-64.

Sanz, J. A., A. M. Fernandes, E. Barrenechea, S. Silva, V. Santos, N. Gonçalves, D. Paternain, A. Jurio and P. Melo-Pinto (2016). "Lamb muscle discrimination using hyperspectral imaging: Comparison of various machine learning algorithms." Journal of Food Engineering **174**: 92-100.

Savitzky, A. and M. J. Golay (1964). "Smoothing and differentiation of data by simplified least squares procedures." Analytical chemistry **36**(8): 1627-1639.

Schuck, P. (2011). Milk powder: physical and functional properties of milk powders.

Sendin, K., P. J. Williams and M. Manley (2018). "Near infrared hyperspectral imaging in quality and safety evaluation of cereals." Critical Reviews in Food Science and Nutrition **58**(4): 575-590.

Sharma, A., A. H. Jana and R. S. Chavan (2012). "Functionality of Milk Powders and Milk-Based Powders for End Use Applications—A Review." Comprehensive Reviews in Food Science and Food Safety **11**(5): 518-528.

Shi, T., Y. Chen, Y. Liu and G. Wu (2014). "Visible and near-infrared reflectance spectroscopy—An alternative for monitoring soil contamination by heavy metals." Journal of hazardous materials **265**: 166-176.

Shikata, F., S. Kimura, Y. Hattori and M. Otsuka (2017). "Real-time monitoring of granule properties during high shear wet granulation by near-infrared spectroscopy with a chemometrics approach." RSC Advances **7**(61): 38307-38317.

Silva, J. V. C. and J. A. O'Mahony (2016). "Flowability and wetting behaviour of milk protein ingredients as influenced by powder composition, particle size and microstructure." International Journal of Dairy Technology **70**(2): 277-286.

Singh, H. (2007). "Interactions of milk proteins during the manufacture of milk powders." Le Lait **87**(4-5): 413-423.

Siripatrawan, U. and Y. Makino (2015). "Monitoring fungal growth on brown rice grains using rapid and non-destructive hyperspectral imaging." International Journal of Food Microbiology **199**: 93-100.

Skanderby, M., V. Westergaard, A. Partridge and D. D. Muir (2009). Dried Milk Products. Dairy Powders and Concentrated Products, Wiley-Blackwell**:** 180-234.

Soriano-Disla, J. M., L. J. Janik, R. A. Viscarra Rossel, L. M. Macdonald and M. J. McLaughlin (2014). "The performance of visible, near-, and mid-infrared reflectance spectroscopy for prediction of soil physical, chemical, and biological properties." Applied Spectroscopy Reviews **49**(2): 139-186.

Spyros, A. and P. Dais (2009). "31P NMR spectroscopy in food analysis." Progress in Nuclear Magnetic Resonance Spectroscopy **54**(3-4): 195-207.

Su, W.-H. and D.-W. Sun (2017). "Evaluation of spectral imaging for inspection of adulterants in terms of common wheat flour, cassava flour and corn flour in organic Avatar wheat (Triticum spp.) flour." Journal of Food Engineering **200**: 59-69.

Subramanian, A., V. Prabhakar and L. Rodriguez-Saona (2016). Analytical Methods: Infrared Spectroscopy in Dairy Analysis. Reference Module in Food Science, Elsevier.

Sun, D.-W. (2008). Modern techniques for food authentication, Academic Press.

Sun, D.-W. (2009). Infrared spectroscopy for food quality analysis and control, Academic Press.

Sun, M., D. Zhang, L. Liu and Z. Wang (2017). "How to predict the sugariness and hardness of melons: A near-infrared hyperspectral imaging method." Food Chemistry **218**: 413-421.

Swarbrick, B. (2014). "Advances in instrumental technology, industry guidance and data management systems enabling the widespread use of near infrared spectroscopy in the

pharmaceutical/biopharmaceutical sector." Journal of Near Infrared Spectroscopy **22**(3): 157-168.

Tatzer, P., M. Wolf and T. Panner (2005). "Industrial application for inline material sorting using hyperspectral imaging in the NIR range." Real-Time Imaging **11**(2): 99-107.

TEC (2012). Virtual Dairy Plant, Milkpowder, Tertiary Education Commission, New Zealand.

Trung, T., G. Downes, R. Meder and B. Allison (2015). "Pulp mill and chemical recovery control with advanced analysers-from trees to final product." Appita: Technology, Innovation, Manufacturing, Environment **68**(1): 39.

Tung, K.-C., C.-Y. Tsai, H.-C. Hsu, Y.-H. Chang, C.-H. Chang and S. Chen (2018). "Evaluation of Water Potentials of Leafy Vegetables Using Hyperspectral Imaging." IFAC-PapersOnLine **51**(17): 5-9.

Tuohy, J. J. (1989). "Some Physical Properties of Milk Powders." Irish Journal of Food Science and Technology **13**(2): 141-152.

Van Beers, R., M. Kokawa, B. Aernouts, R. Watté, S. De Smet and W. Saeys (2018). "Evolution of the bulk optical properties of bovine muscles during wet aging." Meat Science **136**: 50-58.

Vermeulen, P., M. Suman, J. A. Fernández Pierna and V. Baeten (2018). "Discrimination between durum and common wheat kernels using near infrared hyperspectral imaging." Journal of Cereal Science **84**: 74-82.

Vidal, M. and J. M. Amigo (2012). "Pre-processing of hyperspectral images. Essential steps before image analysis." Chemometrics and Intelligent Laboratory Systems **117**: 138-148.

Vignolles, M. L., C. Lopez, M. N. Madec, J. J. Ehrhardt, S. Méjean, P. Schuck and R. Jeantet (2009). "Fat properties during homogenization, spray-drying, and storage affect the physical properties of dairy powders." Journal of Dairy Science **92**(1): 58-70.

Vivó-Truyols, G. and P. J. Schoenmakers (2006). "Automatic Selection of Optimal Savitzky−Golay Smoothing." Analytical chemistry **78**(13): 4598-4608.

Vote, D., K. Belk, J. Tatum, J. Scanga and G. Smith (2003). "Online prediction of beef tenderness using a computer vision system equipped with a BeefCam module." Journal of animal science **81**(2): 457-465.

Wang, L., D. Liu, H. Pu, D.-W. Sun, W. Gao and Z. Xiong (2015). "Use of Hyperspectral Imaging to Discriminate the Variety and Quality of Rice." Food Analytical Methods **8**(2): 515-523.

Wang, L., D.-W. Sun, H. Pu and J.-H. Cheng (2017). "Quality analysis, classification, and authentication of liquid foods by near-infrared spectroscopy: A review of recent research developments." Critical Reviews in Food Science and Nutrition **57**(7): 1524-1538.

Wang, L., D.-W. Sun, H. Pu and Z. Zhu (2016). "Application of hyperspectral imaging to discriminate the variety of maize seeds." Food Analytical Methods **9**(1): 225-234.

Wang, Y. (2011). Smoothing splines: methods and applications, Chapman and Hall/CRC.

Watari, M. (2014). "A review of online real-time process analyses of melt-state polymer using the near-infrared spectroscopy and chemometrics." Applied Spectroscopy Reviews **49**(6): 462-491.

Whittaker, E. T. (1922). "On a new method of graduation." Proceedings of the Edinburgh Mathematical Society **41**: 63-75.

Williams, A. M. (2017). Instant milk powder production: Determining the extent of agglomeration Department of chemical technology. Palmestron North, New Zealand, Massey university. **Ph.D.:** 251.

Williams, P. and K. Norris (1987). Near-infrared technology in the agricultural and food industries, American Association of Cereal Chemists, Inc.

Williams, P. J., P. Geladi, T. J. Britz and M. Manley (2012). "Investigation of fungal development in maize kernels using NIR hyperspectral imaging and multivariate data analysis." Journal of Cereal Science **55**(3): 272-278.

Wold, H. (1966). Estimation of principal components and related models by iterative least squares. Multivariate Analysis. Edited by: Krishnaiaah PR. 1966, New York: Academic Press.

Wold, S., M. Sjöström and L. Eriksson (2001). "PLS-regression: A basic tool of chemometrics." Chemometrics and Intelligent Laboratory Systems **58**(2): 109-130.

Wolf, I. V., C. V. Bergamini, M. C. Perotti and E. R. Hynes (2013). Sensory and Flavor Characteristics of Milk. Milk and Dairy Products in Human Nutrition, John Wiley & Sons**:** 310-337.

Woodcock, T., C. C. Fagan, C. P. O'Donnell and G. Downey (2008). "Application of near and mid-infrared spectroscopy to determine cheese quality and authenticity." Food and Bioprocess Technology **1**(2): 117-129.

Wu, D., S. Feng and Y. He (2007). "Infrared Spectroscopy Technique for the Nondestructive Measurement of Fat Content in Milk Powder." Journal of Dairy Science **90**(8): 3613-3619.

Wu, D., S. Feng and Y. He (2008). "Short-Wave Near-Infrared Spectroscopy of Milk Powder for Brand Identification and Component Analysis." Journal of Dairy Science **91**(3): 939-949.

Wu, D. and D.-W. Sun (2013). "Advanced applications of hyperspectral imaging technology for food quality and safety analysis and assessment: A review — Part I: Fundamentals." Innovative Food Science & Emerging Technologies **19**: 1-14.

Wu, X., X. Song, Z. Qiu and Y. He (2016). "Mapping of TBARS distribution in frozen–thawed pork using NIR hyperspectral imaging." Meat Science **113**: 92-96.

Xie, L., A. Wang, H. Xu, X. Fu and Y. Ying (2016). "Applications of near-infrared systems for quality evaluation of fruits: A review." Transactions of the ASABE **59**(2): 399-419.

Xing, J. and J. De Baerdemaeker (2005). "Bruise detection on 'Jonagold'apples using hyperspectral imaging." Postharvest Biology and Technology **37**(2): 152-162.

Xiong, Z., D.-W. Sun, H. Pu, A. Xie, Z. Han and M. Luo (2015). "Non-destructive prediction of thiobarbituricacid reactive substances (TBARS) value for freshness evaluation of chicken meat using hyperspectral imaging." Food Chemistry **179**: 175-181.

Xu, J.-L., C. Riccioli and D.-W. Sun (2017). "Comparison of hyperspectral imaging and computer vision for automatic differentiation of organically and conventionally farmed salmon." Journal of Food Engineering **196**: 170-182.

Yang, C., W. S. Lee and J. G. Williamson (2012). Classification of blueberry fruit and leaves based on spectral signatures.

Yang, D. and Y. Ying (2011). "Applications of Raman spectroscopy in agricultural products and food analysis: A review." Applied Spectroscopy Reviews **46**(7): 539-560.

Ye, A., H. Singh, M. Taylor and S. Anema (2005). "Disruption of fat globules during concentration of whole milk in a pilot scale multiple-effect evaporator." International Journal of Dairy Technology **58**(3): 143-149.

Yoon, S. C., B. Park, K. C. Lawrence, W. R. Windham and G. W. Heitschmidt (2010). Development of real-time line-scan hyperspectral imaging system for online agricultural and food product inspection.

Yu, X., Q. Lu, H. Gao and Z. Peng (2013). "Current status and prospects of portable NIR spectrometer." Guang pu xue yu guang pu fen xi= Guang pu **33**(11): 2983-2988.

Zábrodská, B. and L. Vorlová (2015). "Adulteration of honey and available methods for detection–a review." Acta Veterinaria Brno **83**(10): 85-102.

Zhang, C., H. Jiang, F. Liu and Y. He (2017). "Application of Near-Infrared Hyperspectral Imaging with Variable Selection Methods to Determine and Visualize Caffeine Content of Coffee Beans." Food and Bioprocess Technology **10**(1): 213-221.

Zhang, H., X. Qiao, Z. Li and D. Li (2015). Effective Wavelengths Selection of Hyperspectral Images of Plastic Films in Cotton. International Conference on Computer and Computing Technologies in Agriculture, Springer.

Zhang, L. and M. J. Henson (2007). "A Practical Algorithm to Remove Cosmic Spikes in Raman Imaging Data for Pharmaceutical Applications." Applied Spectroscopy **61**(9): 1015-1020.

Zheng, X., Y. Li, W. Wei and Y. Peng (2019). "Detection of adulteration with duck meat in minced lamb meat by using visible near-infrared hyperspectral imaging." Meat Science **149**: 55-62.

Appendix

A-1 Hyperspectral imaging for the discrimination of milk powder

A-1.1 Preface

This section is based upon the preliminary experimentation done in the provisional year of this Ph.D. research. Hyperspectral imaging (HSI) data of milk powder produced in this phase enabled us to understand and develop the pre-processing treatments that were suitable for further analysis.

A-1.2 Abstract

High-quality milk powders have attractive functional and physical properties and perform well when re-dissolved. The performance of milk powders can be tested and quantified using post-manufacturing quality testing. However, these quality tests are off-line, time-consuming, after the fact, and awkward to implement on-line. As a result, it can be advantageous to imitate existing quality tests to test and quantify milk powder functional and physical properties in-situ and in real-time to reduce the production of off-spec milk powder and downgrade costs. For this objective, a hyperspectral imaging (HSI) process analyser and multivariate data analysis by principal component analysis (PCA) was performed. Milk powder of various qualities (‘good’ and ‘poor’) were scanned using HSI; PCA was used to discriminate between milk powders having different post-manufacturing quality attributes. The PCA results showed that the HSI can distinguish

between milk powders of different qualities and the most obvious differences were in the second and third principal components.

Keywords: Milk powder, hyperspectral imaging, principal component analysis

A-1.3 Introduction

Liquid milk is converted into powder form to increase its shelf life while not compromising the quality and benefits of its ingredients. This conversion makes the handling and storage of milk easy. The production of milk powder is vital for the New Zealand economy. According to the United States Department of Agriculture (USDA), 2013 report on world markets and trade, New Zealand is producing around 1700 k MT/year of various types of milk powder such as whole, skim, and infant formula. One-third of international dairy trade is done by New Zealand every year, accounting for more than 25 % of NZ's export earnings (John Ballingall and Pambudi 2017). Other large producers of milk powder include China (1665 k MT/year) and the EU–27 (1665 k MT/year).

Milk powder is not only reconstituted to liquid but also used as a "key ingredient" in various "value-added-products" such as in bakery products, confectionery and certain meat products. The physical and functional properties of milk powder play a key role in the functionality of milk powder in various products (Kelly et al. 2003). In other words, attractive physical and functional properties of milk powder are required for various applications.

Milk powder quality refers to its physical, chemical, and biological nature; nutritional value; and consumer acceptance (Caric 2004). Determining and maintaining milk powder quality is usually a complicated task due to the multi-array nature of quality. In the case

of dairy powders, one aspect of the quality term also refers to how easily it rehydrates. Milk powder rehydration performance is believed to depend on various physical and functional properties of the milk powder. Functional properties (e.g. dispersibility) of milk powder are supposed to depend on physical properties (e.g. particle size distribution) of milk powder which can be dependent on various processes (e.g. operational conditions) and design parameters (e.g. dryer type). Milk powder functional performance attributes are mainly influenced by powder physical characteristics (Özkan et al. 2002).

Another challenge affecting milk powder quality is its off-line quality testing. Traditionally, milk powder quality is tested using off-line quality tests after the production of milk powder. For example, milk powder dispersibility is tested using the IDF 134 (2005) test (ISO 2014). The challenge with post-manufacturing quality testing is that if the product is characterised as off-specification, then it is difficult to improve or modify its quality. Therefore, alternative milk powder quality testing techniques are desirable which can predict quality close to real-time.

Hyperspectral imaging (HSI) is an emerging technology that combines imaging and spectroscopy techniques in a way that generates a spatial map of spectral variation. It measures both spectral (λ) and spatial (x - y) information from the sample. Hyperspectral images, known as hypercubes, can be represented as three-dimensional blocks of data, comprised of two spatial and one wavelength dimensions. A wide array of applications for HSI has been suggested previously, such as remote sensing, astronomy, agriculture, biomedical, mineralogy and food applications. Particularly, the scope of HSI has been widely explored for food inspection and quality monitoring in the last decade (Baiano 2017). However, in most food quality applications, the hyperspectral images exhibited

clearly defined areas of different absorbances whereas in this milk powder application, the visible differences in the images are far more subtle and not immediately apparent.

This paper outlines a novel quality estimation route for milk powder using HSI analysis. Multivariate data analysis (mainly PCA) of hyperspectral data was employed to detect milk powder discrimination.

A-1.4 Material and Methods

A-1.4.1 Milk powder samples

Milk powder samples were provided by a local manufacturing plant. A total of 24 milk powder samples from three separate batches were used in these experiments. These milk powder samples were manually tested for quality at the production plant. These quality tests cannot be explained in detail due to the manufacturer's confidentiality requirements. However, the manufacturer assigned either 'Good' or 'Poor' grades to all milk powder samples provided. Batch-1 had four milk powder samples and all were of a good grade. There were eight samples of batch-2 milk powder which were also of a good grade. However, batch-3 was a mixture of good and poor grade milk powder i.e., eight samples were good and four samples were of bad/poor grade.

A-1.4.2 Hyperspectral imaging

A Headwall Photonics Hyperspec^{TM} - VNIR, C series with 400 – 1000 nm wavelength range, HSI instrument was used in this work, as shown in Figure A.1. The HSI instrument consists of four major components: a spectrograph, camera (Schneider Kreuznach Xenoplan), lamp and transition stage as shown in Figure A-1.1. The spectrograph generates a spectrum for each pixel in the picture taken by the camera. The lamp acts as a lighting source and the transition stage is used to place a sample for

analysis. The milk powder sample was placed in a glass container and placed on the transition stage for analysis. This transition stage can be moved across the horizontal axis to position the sample for HSI data acquisition.

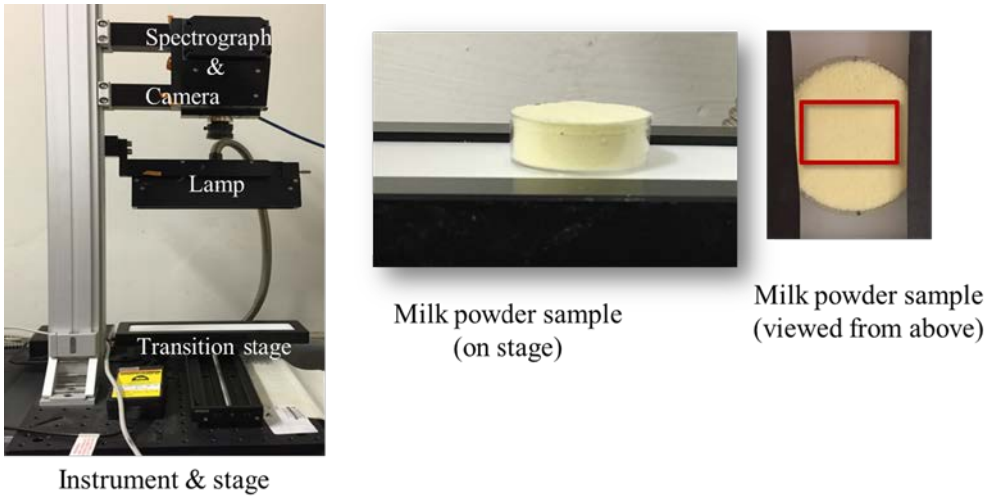

Figure A-1.1. Hyperspectral imaging experimental setup

The hyperspectral data of the milk powder samples was recorded using the HSI instrument. The data cube was stored in a Matlab data structure. A standard data format was used consisting of row vectors (representing pixels or spatial data) and column vectors (represented wavelength or spectral data) in a data matrix.

A-1.4.3 Pre-processing and data analysis

Pre-processing of HSI data is an important step prior to performing any data analysis on HSI information. The data cube produced by HSI systems contains a mass of information with large dimensionality. The main purpose of hyperspectral data analysis was to reduce the dimensionality and to retain the useful data for discrimination or qualitative analysis.

Reflectance calibration was performed by recording the dark response. This is the background response of the camera caused by a dark current of the instrument in the

absence of any light. The bright response, representing the total reflected light intensity from the illumination was obtained from a uniform high reflectance tile, which reflects 99 % of light. Corrected hyperspectral images were obtained from the data obtained.

After the reflectance calibration, the region of interest (ROI) was specified. A similar set of pixel coordinates (100 by 150 pixels) was extracted for all the samples. Spectral normalisation was performed by standard normal variance (SNV) on each hyperspectral image of milk powder sample. Spectral smoothing and derivation are normal practices to enhance spectral variations (Gowen et al. 2007). For spectral smoothing, various smoothing techniques including LOESS (Cleveland et al. 1988), spline (Wang 2011), Savitzky - Golay (SG) (Savitzky and Golay 1964), Whittaker (Whittaker 1922), and multi-dimensional smoother (Garcia 2010) have been employed on milk powder hyperspectral data. All of these smoothing alternatives have tuning factors that adjust the degree of smoothing, but multi-dimensional smoother is preferable for HSI data for milk powder samples. This method was used for data smoothing in this study. Furthermore, the effect of first and second order spectral derivatives was also trialled on principal component-based discrimination of milk powder samples.

Principal component analysis (PCA) is an unsupervised classification technique widely used in various applications of multivariate data analysis (Abdi and Williams 2010). Principal component analysis is equally popular in spectroscopy to discriminate the spectral variation within different food products (Sun 2008). If the data cube (I) consists of $x * y * \lambda$ pixels, the first step in PCA is to unfold the cube in two dimensions and represent it as matrix I ($x * y, \lambda$). PCA can be applied, decomposing the matrix into a score T ($x*y, \lambda$) and a loading $P_T(\lambda,y)$ matrix, depending on the number of principal components (PCs), λ. The scores retain the variability of the pixels density, whereas the loadings

contain the spectral variability (Jolliffe 2002). In this research, we used the PCA routines from the Statistics toolbox for Matlab 2016.

A-1.5 Preliminary experimentation results

A-1.5.1 Spectral plots from hyperspectral imaging data of milk powder

HSI normally generates a large volume of data so, a sub-sampled image of approximately 100 by 150 pixels (ROI) giving 15,000 pixels or observations measured at 933 equally spaced wavelengths from 400 to 1000 nm was selected. Reflectance calibration of the HSI equipment was done with white and dark references using the software package installed in the computer component of the HSI equipment, provided by manufacturer Headwall photonics.

The spectra of the milk powder samples when plotted as HSI data as a function of wavelength is shown in Figure A-1.2. The zoomed portion of Figure A.2 refers to the baseline noise thus, it was required to perform pre-treatment on this spectral information. Data smoothing was a mandatory step to carry out multivariate data analysis.

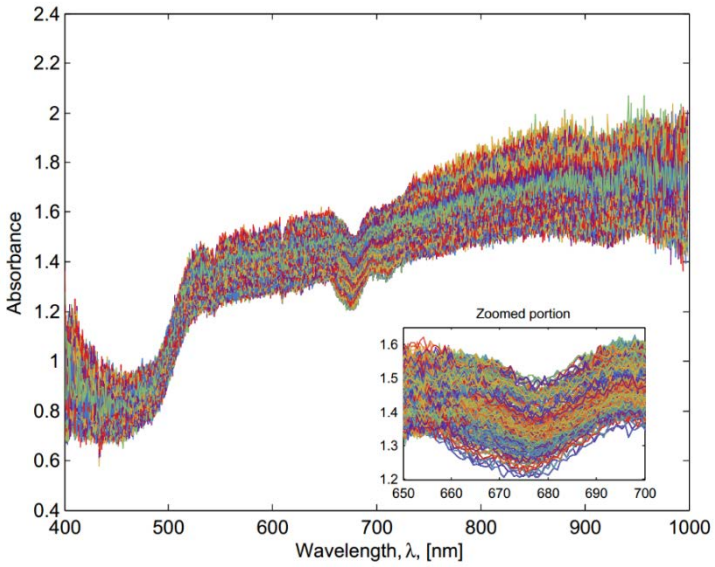

Figure A-1.2 Raw spectra of a selected number of observations. A zoomed inset shows all spectra centred around 680nm.

A-1.5.2 Principal component analysis and spectral smoothing

Spectral smoothing is one of the main design choices required for milk powder quality testing using HSI. Figure A-1.3 shows a comparison of spectrum smoothing by various smoothing techniques such as LOESS, spline, SG, and Whittaker filtering. The outcome of each smoothing technique is a unique smooth spectrum, and therefore, can significantly affect subsequent multivariate data analysis results. Spline method performed the most denoising of spectra and a Matlab function `smoothn` by Garcia (2010) was used. It was based on the Spline smoothing technique and was able to handle multi-dimensional data.

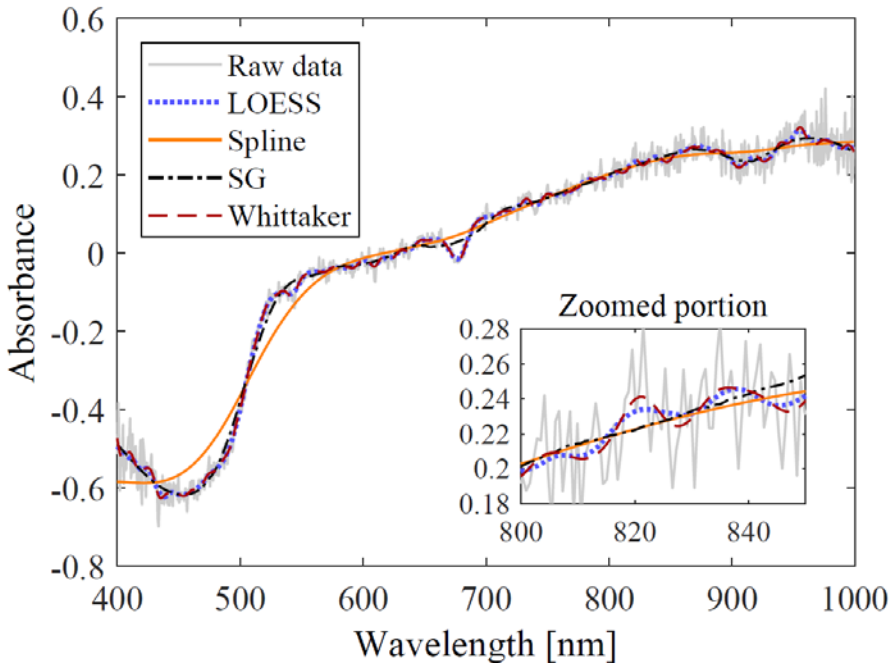

Figure A-1.3. Effect of different smoothing techniques on HSI spectra

Figure A-1.4 shows PCA with the first three PCs for milk powder samples of three different batches. In this figure, the columns of the subplot are at a given smoothing level, and rows show the three combinations of the first three PCs. Furthermore, plots show the 95 % probability ellipses because plotting individual points adds limited information and hides overlapping data.

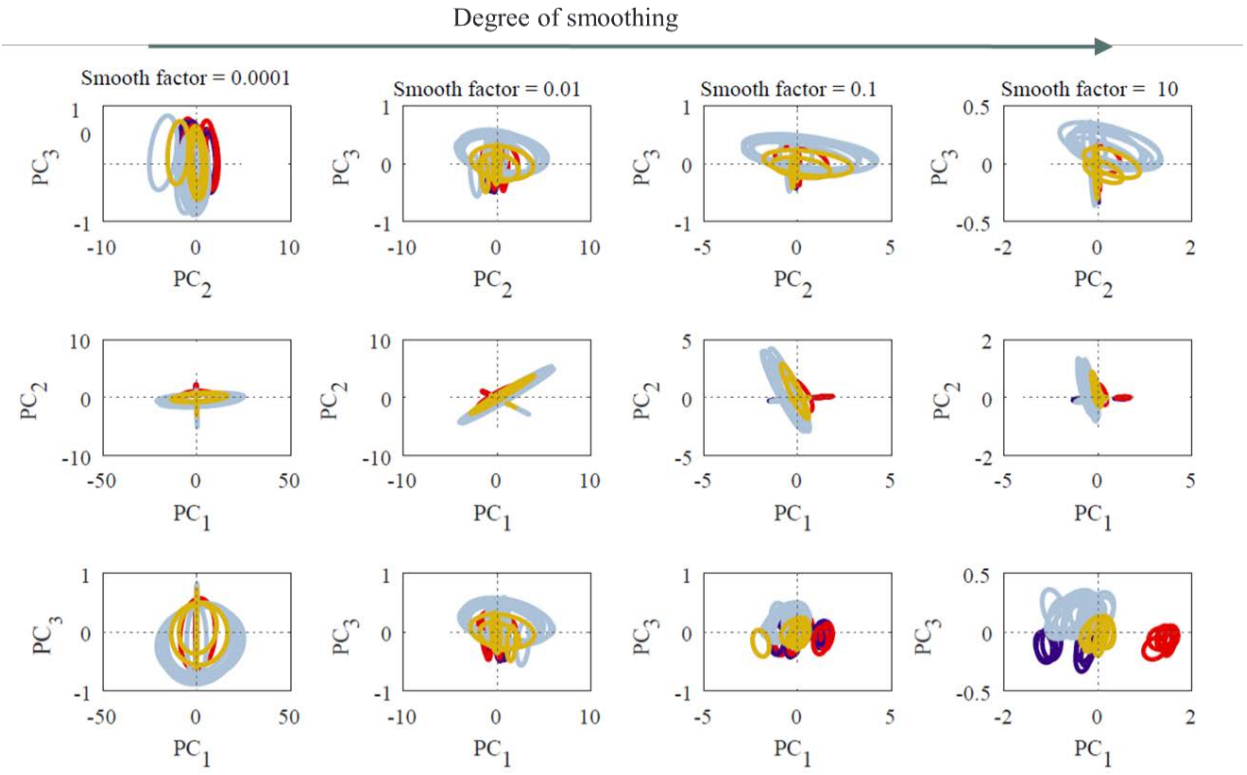

Figure A-1.4. First three PCs of 2000 spectra of each milk powder sample at different smoothing levels and ellipses[2] containing 95 % of the score plot data.

The first component PC_1 accounted for ~ 62 % variation, with PC_2 and PC_3 accounting for ~8% and ~2% respectively of the total variation in the spectra. As the smoothing factor was increased, discrimination between all the batches was observed. The poor grade samples, represented in red, could be seen separately from the rest of the samples. Since this segregation is pronounced at smoothing factor 10, we will use this value for further data analysis.

A-1.5.3 Principal component analysis and spectral derivatives

Similar score plots representing the projections of the 3D ellipsoid of the first three principal components for first and second order derivative were plotted and represented in Figure A-1.5.

[2] Whereas colour reference is the following: Gold; batch-1(good quality), Sky blue; batch-2 (good quality), Indigo; batch-3 (good quality) and Red; batch-3 (poor quality).

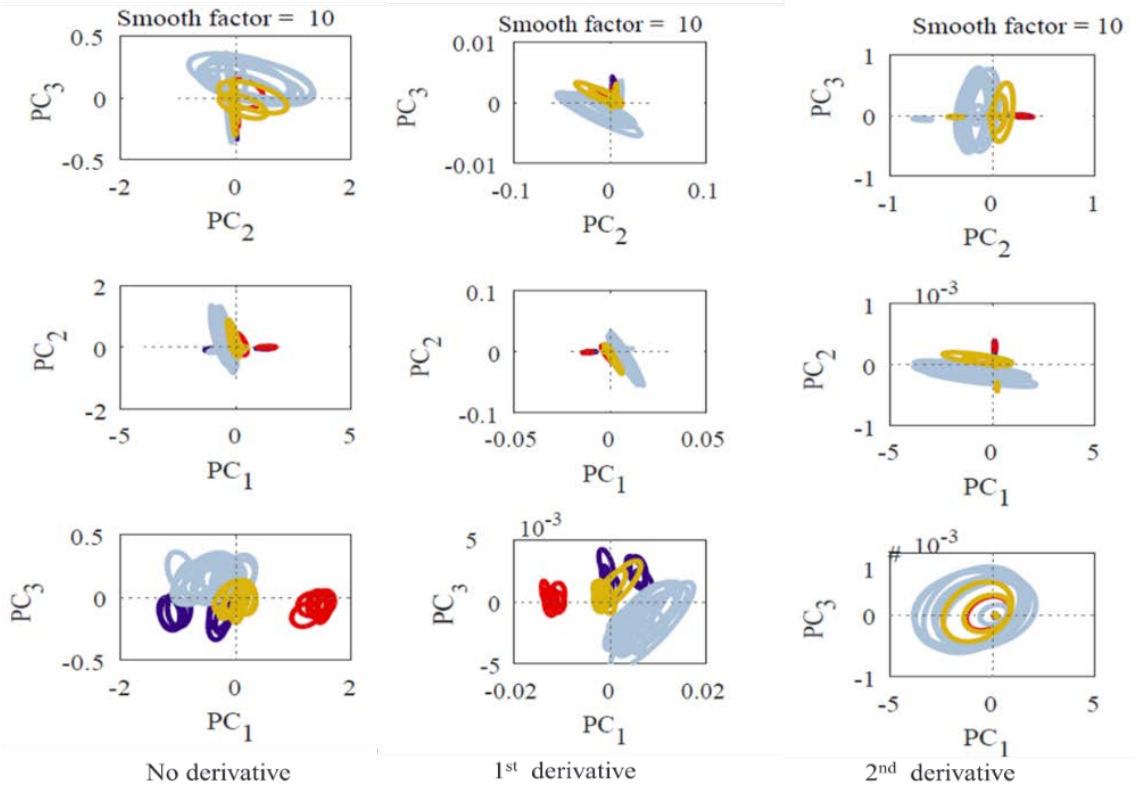

Figure A-1.5. First three PCs of 2000 spectra with and without derivatives at a given smoothing level and ellipses[3] containing 95 % of the score plot data.

The zero and first order derivative score plots differentiate the two quality grades and the three different batches for PC_1 vs PC_3 plot somewhat. But in the second derivative plots, all the ellipsoids overlap one another. The reason may be that higher order derivatives are applied to magnify/maximise the various trend lines. But in this case, the milk powder samples were of a homogeneous nature and various properties of samples were not distinctive; the higher order of derivatives may deal with the distribution maps similarly for different grades of milk powder samples.

A-1.6 Conclusions

This paper demonstrates the worth of HSI applied to milk powder quality prediction. The analysis of milk powder from three different batches of milk powder showed differences

[3] Whereas colour reference is following: Gold; batch-1(good quality), Sky blue; batch-2 (good quality), Indigo; batch-3 (good quality) and Red; batch-3 (poor quality).

primarily in PC_2 and PC_3 with very little difference in PC_1. Furthermore, different smoothing techniques had a prominent impact on milk powder spectra and an appropriate level of smoothing was also required to discriminate two quality grades of milk powder. However, higher order spectral derivatives deteriorated the discrimination.

The analysis given in sections A-1.5 indicated that the HSI technique has the potential to become a non-invasive and real-time quality monitoring technique for large scale milk powder plants. Notwithstanding, we acknowledge that a robust strategy to distinguish different milk powders using HSI has not fully been developed yet. Pairing correlations to functional properties or quality attributes also need to be addressed to close the loop of real-time milk powder quality estimation.

A-1.7 Summary

Production of poor grade milk powder is always attempted to be avoided at a commercial manufacturing unit. Therefore, the ‘poor’ grade samples were lesser in number than that of ‘good’ grade samples. In order to address this issue, milk powder samples were planned to be manually tempered by adding more fine particles opposed to coarse particles because it was supported from the literature evidence that a higher fraction of fine particles was responsible for ‘poor’ rehydration performance (Kelly 2006). This study also helped to choose a suitable stepwise pre-processing strategy that was used in spectral data analysis of milk powder at different stages of this Ph.D. research.

A-2: Principal component analysis

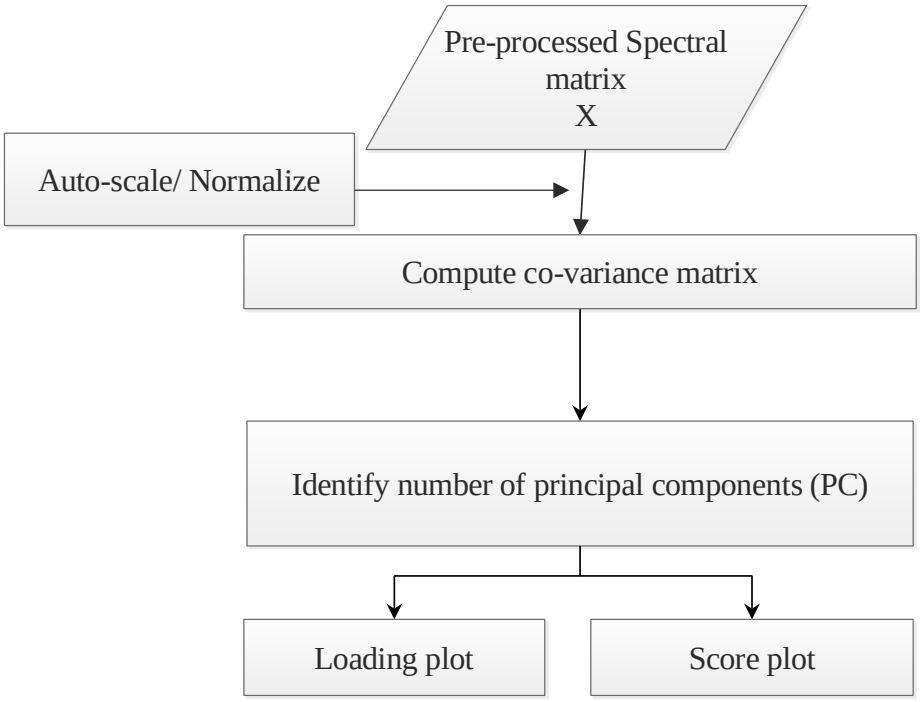

Figure A-2.1 Flow chart to perform principal component analysis

1. The pre-processed HSI data cube was normalized to be prepare for further analysis.

```
%HSI data cube = X
Xc = detrend (X,'constant ');
 Xn = Xc ./ repmat (std (X), size (X ,1) ,1); % mean of columns = 0; std = 1.4
```

2. The number of principal components were selected by their contribution to total variance of the HSI data.

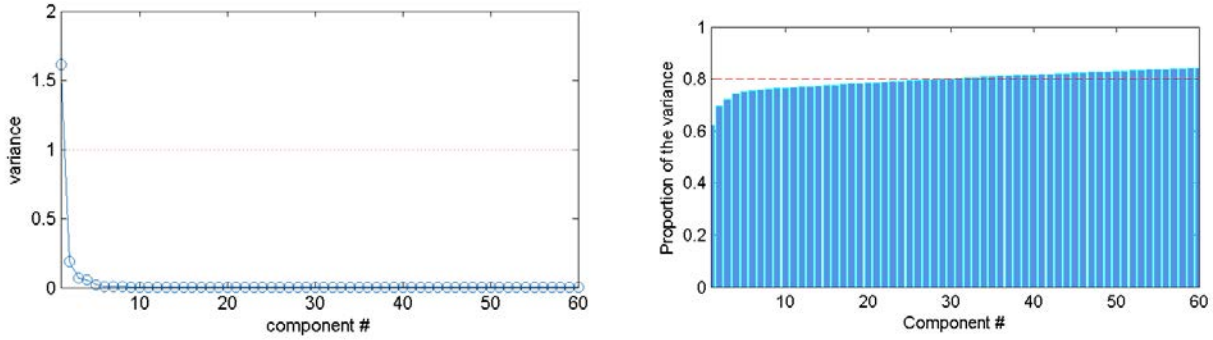

Figure A-2.2. The actual variance, and the proportional of the total variance for the 60 components to the overall variance.

3. The PCA routine was applied.

```
[P, T, compVar , T_2 , EXPLAINED ] = pca(X,' NumComponents ' ,3);
```

4. The confidence interval of spectral information was analysed to estimate the spread of spectral data.

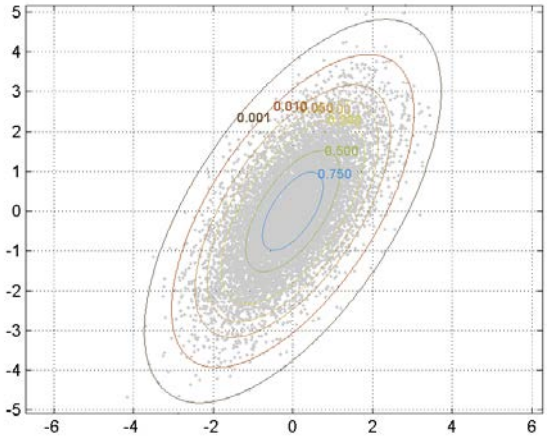

Figure A-2.3. Elliptical confidence regions at various probability levels

5. Sub-sampling was performed in range of 500 -10000 spectra to verify the robustness of the model.

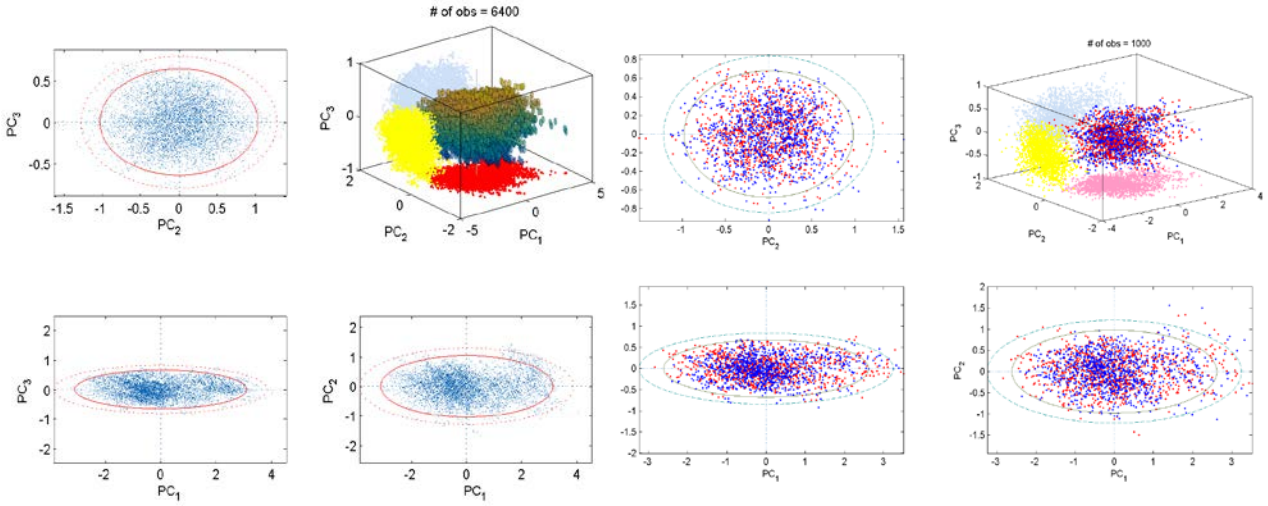

Figure A-2.4. The first 3 principle components of 6500 and 1000 spectra observations

6. Loading and score plots of PCA were produced.

A-3: Partial least squares (PLS) model

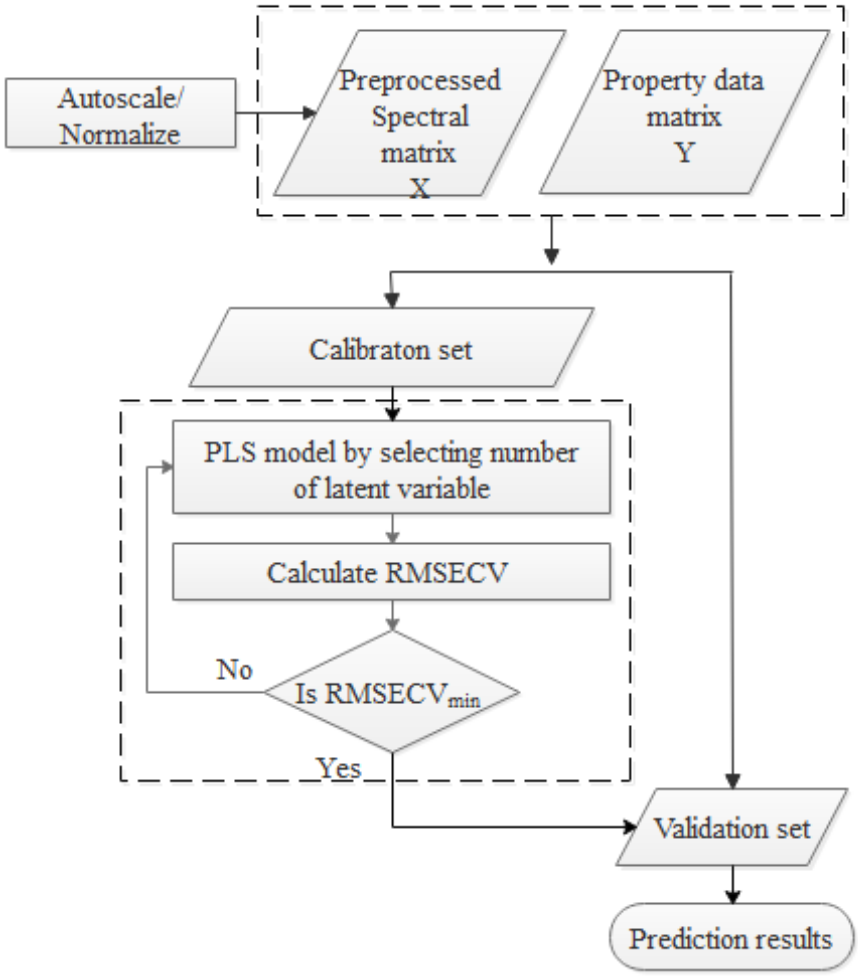

Figure A-3.1. Flow chart to perform partial least square analysis

Input and outputs for the partial least square (PLS) analysis are mentioned below:

```
%Nomenclature
%# of sample in experiment = N
%# of measurements (wavelengths) = K
%# of quality variables (responses) = M
%# of components retained = A
%Predictor matrix = X (N x K)
%Response matrix = Y (N x M)
%X scores = T (N x A)
%Y scores = U (N x A)
%X loadings = P (K x A)
%Y loadings = Q (M x A)
%B model coefficients = B (K x M)
%component variances  = (N x 1)
```

To perform PLS, the following steps were adopted:

1. The pre-processed spectral data matrix was labelled as X, while the sample's properties were listed in matrix Y. X and Y matrices were auto-scaled.

Here auto-scaling refers to centring and scaling. The mean of each variable becomes zero by subtracting the mean of each variable from the variable in centring. The standard deviation of each variable becomes one by dividing by the standard deviation of each variable from the variable in scaling.

```
function [T,P,W,U,Q,B,ssq,Ro,Rv,Lo,Lv] = pls(X,Y,nF,options)
```

2. Estimated Y with cross-validation (CV), changing the number of components from 1 to m.

Leave-one-out CV is very popular, but it causes over-fitting when the number of training samples is high. So, *n*-fold CV is better, where *n* is often either 2 or 5. First, training samples are divided into *n* groups. Second, one group is handled as the test samples and a model is built with the other group(s). This is repeated *n* times until every group is handled as the test samples. Then, not calculated Y, but estimated Y can be obtained.

3. The Root-Mean-Squared Errors (RMSE) between actual Y and estimated Y for each number of components were calculated.

Better PLS models have higher R^2_{CV} values and lower RMSECV values. A large difference between R^2_c and R^2_{CV} and between RMSEC and RMSECV mean PLS model

overfitting to training samples. However, R^2_{CV} and RMSECV cannot represent true predictability of the PLS model since it is CV, not external validation.

4. The optimal number of components were decided with the minimum RMSECV value.

```
% cross validation of PLS to select the best PLS component
CV=pls-fold(Xtrain,Ytrain,A_max,fold,method);
```

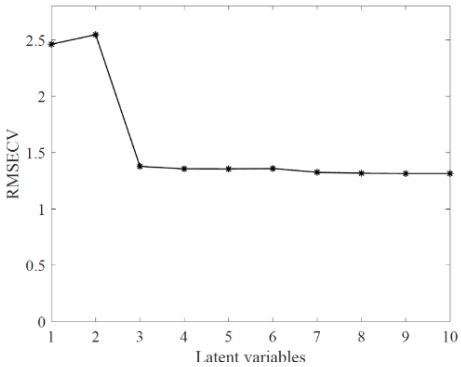

Figure A-3.2. Optimal latent variable selection

5. The PLS model with the optimal number of components was constructed and standard regression coefficient R^2_p was calculated.

7. Plots between actual property Y and calculates property $Y_{prediction}$ were developed.

A-4. Euclidian distance calculation and spectral correlation

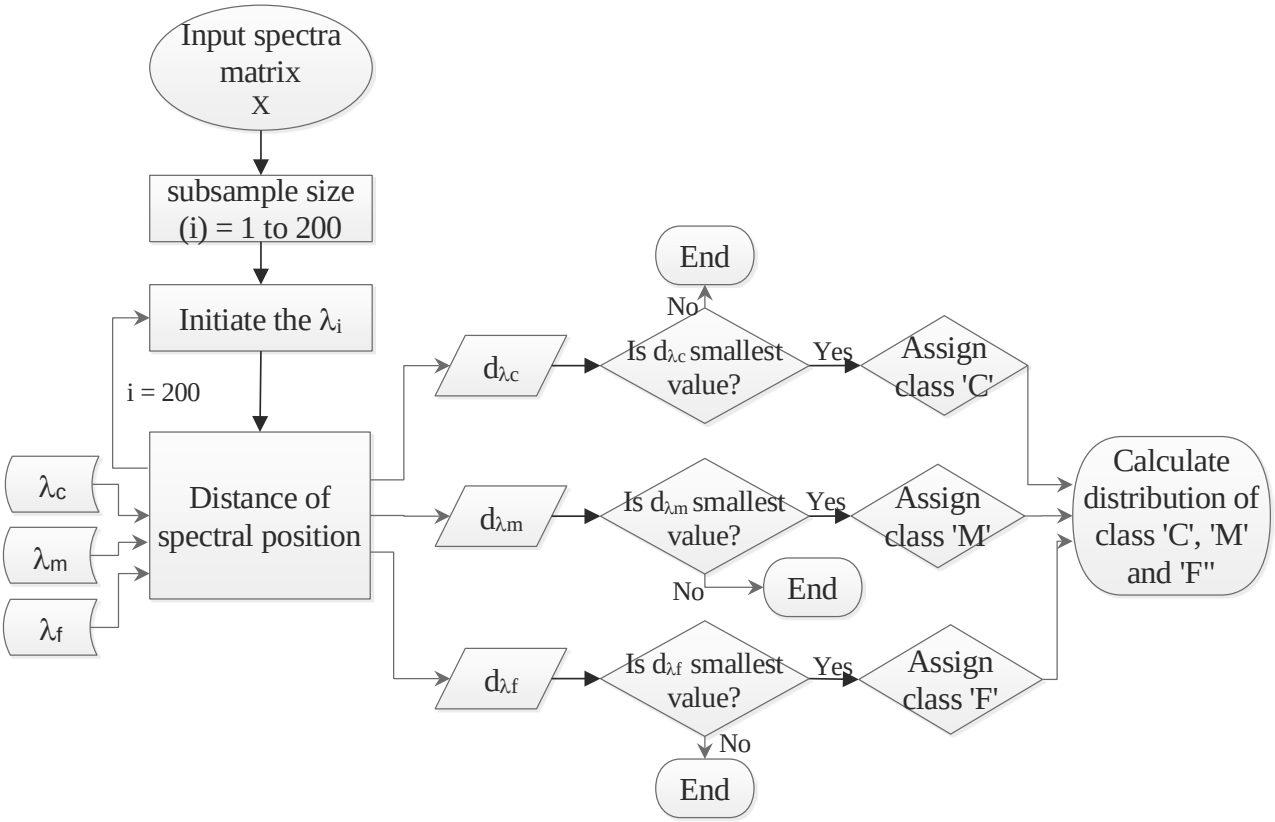

Figure A-4.1. Flow chart for Euclidean distance based spectral distribution of recombined samples

The following steps were followed to calculate spectral distribution:

1. A suitable subsampling range (1-200) was selected from pre-processed spectral data matrix X with 2000 spectra.

2. Spectral distances from reference spectra of the three classes were calculated and shortest distance was retained.

```
% Preprocessed spectral data matrix X
% Reference spectral matrix R
% Smallest distance vector D
[D,I] = pdist2(X,R,'seuclidean','Smallest',1)
```

3. Each spectrum was assigned a particle size class based upon the shortest distance to the reference spectra for the coarse, medium and fine fractions.

4. The spectral distribution among the three particle size classes was calculated.

5. The spectral correlation coefficient was calculated by the following equation for measuring the spectral similarity between the test spectrum and reference spectrum.

$$r_m = \frac{n\sum \lambda_f \lambda_r - \sum \lambda_f \sum \lambda_r}{\sqrt{\left[n\sum \lambda_f^2 - \left(\sum \lambda_f\right)^2\right]\left[n\sum \lambda_r^2 - (\sum \lambda_r)^2\right]}} \quad \textbf{A-4.1}$$

Where

λ_f = Reference spectrum of individual particle size fraction
λ_r = Spectrum from recombined sample
r_m = Correlation of matching position of spectra
n = Total number of spectra from recombined sample